construction
engineering
research
laboratory

TECHNICAL REPORT M-94
January 1976

STUDY OF ARTICULATED CONCRETE REVETMENT MATTRESS: TEST AND ANALYSIS—RESULTS OF FY 1974 PROGRAM

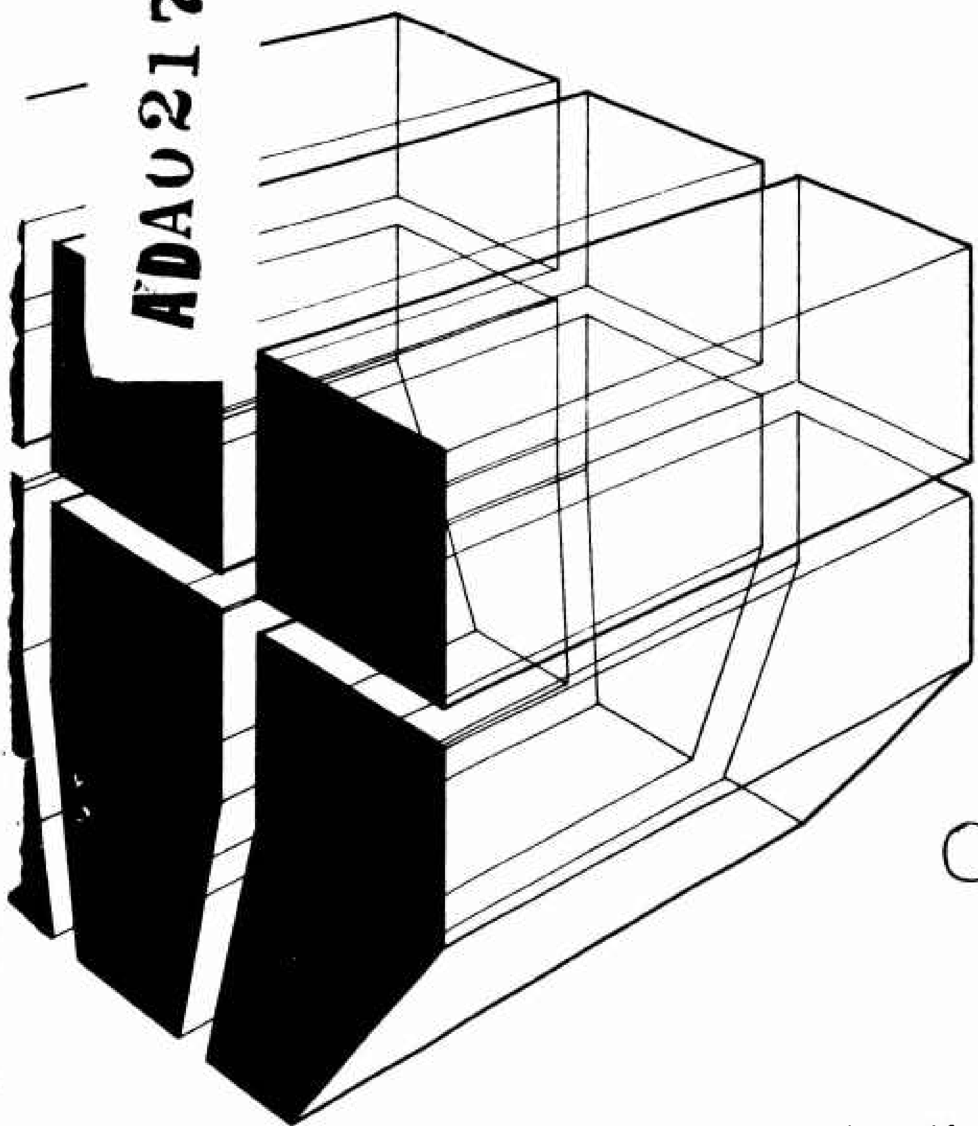

by
F. Kearney
J. Prendergast

Approved for public release; distribution unlimited.

The contents of this report are not to be used for advertising, publication, or promotional purposes. Citation of trade names does not constitute an official indorsement or approval of the use of such commercial products. The findings of this report are not to be construed as an official Department of the Army position, unless so designated by other authorized documents.

DESTROY THIS REPORT WHEN IT IS NO LONGER NEEDED
DO NOT RETURN IT TO THE ORIGINATOR

UNCLASSIFIED

SECURITY CLASSIFICATION OF THIS PAGE (When Data Entered)

14

REPORT DOCUMENTATION PAGE

READ INSTRUCTIONS BEFORE COMPLETING FORM

1. REPORT NUMBER CERL-TR-M-94	2. GOVT ACCESSION NO.	3. RECIPIENT'S CATALOG NUMBER
4. TITLE (and Subtitle) 6 STUDY OF ARTICULATED CONCRETE REVETMENT MATTRESS: TEST AND ANALYSIS — RESULTS OF FY 1974 PROGRAM.		5. TYPE OF REPORT & PERIOD COVERED 9 FINAL t [illegible] Rept. 6. PERFORMING ORG. REPORT NUMBER
7. AUTHOR(s) 10 F. Kearney J. Prendergast		8. CONTRACT OR GRANT NUMBER(s) IAO LMMDC FA 75-2
9. PERFORMING ORGANIZATION NAME AND ADDRESS CONSTRUCTION ENGINEERING RESEARCH LABORATORY P.O. Box 4005 Champaign, IL 61820		10. PROGRAM ELEMENT, PROJECT, TASK AREA & WORK UNIT NUMBERS
11. CONTROLLING OFFICE NAME AND ADDRESS 11		12. REPORT DATE Jan[redacted]976 13. NUMBER OF PAGES 67
14. MONITORING AGENCY NAME & ADDRESS (if different from Controlling Office) 12 70p.		15. SECURITY CLASS. (of this report) Unclassified 15a. DECLASSIFICATION/DOWNGRADING SCHEDULE

16. DISTRIBUTION STATEMENT (of this Report)

Approved for public release; distribution unlimited.

17. DISTRIBUTION STATEMENT (of the abstract entered in Block 20, if different from Report)

18. SUPPLEMENTARY NOTES

Copies are obtainable from National Technical Information Service
Springfield, VA 22151

19. KEY WORDS (Continue on reverse side if necessary and identify by block number)

revetment mattress
structural analysis

20. ABSTRACT (Continue on reverse side if necessary and identify by block number)

This report presents (1) results of field and laboratory test measurements of the force levels in an articulated concrete revetment mattress (mat) during the placement process, and (2) a structural analysis of the mat.

The purpose of this test and analysis program was to determine the feasibility of redesigning the wire fabric used in the mat. over

DD FORM 1473 1 JAN 73 EDITION OF 1 NOV 65 IS OBSOLETE

UNCLASSIFIED

SECURITY CLASSIFICATION OF THIS PAGE (When Data Entered)

405 279

Block 20 continued.

Study results show that a mattress with two (rather than three) 4000-lb longitudinal wires is structurally feasible. Further, it appears that testing may confirm that a two-wire, 3000-lb fabric would be adequate.

FOREWORD

This study is sponsored by the Memphis Engineering District, Lower Mississippi Valley Division (LMVD), U.S. Army Corps of Engineers. Mr. B. D. Gray is project coordinator. Personnel most closely associated with the project were Messrs. J. Graham and H. Harz (LMVD); Messrs. R. B. Deason, C. L. Curry, J. Creed (Memphis District); and Messrs. J. Harrison and R. Campbell (Vicksburg District). Professor V. J. McDonald of the Civil Engineering Department, University of Illinois at Urbana-Champaign, was Consultant to the U.S. Army Construction Engineering Research Laboratory (CERL) for this project.

The study was performed by the Metallurgy Branch and the Structural Mechanics Branch, Materials Systems and Science Division, CERL. CERL personnel conducting this investigation included Dr. J. Prendergast and Messrs. F. Kearney, H. Stringfellow, R. Neu, and A. Jones.

Dr. R. Quattrone is Chief, Materials Systems and Science Division; A. Kumar is Acting Chief, Metallurgy Branch; and Dr. W. Fisher is Chief, Structural Mechanics Branch.

COL M. D. Remus is Commander and Director of CERL and Dr. L. R. Shaffer is Deputy Director.

CONTENTS

FIGURES

FIGURES (Cont.)

TABLES

STUDY OF ARTICULATED CONCRETE REVETMENT MATTRESS: TEST AND ANALYSIS–RESULTS OF FY 1974 PROGRAM

1 INTRODUCTION

Background

The Lower Mississippi Valley Division of the Corps of Engineers uses some 600,000 articulated concrete mattresses (mats) every year as revetments in the Mississippi River to stop the water from eroding its banks and to maintain navigation channels. The 4 ft x 25 ft mats are composed of 20 concrete blocks connected and reinforced with stainless steel or copper-coated steel wire. (See Appendix A for a detailed description of the mats.)

A value engineering study has indicated that substantial economic benefits could be achieved by changing the design of these mats. In March 1972, the U.S. Army Construction Engineering Research Laboratory (CERL) was asked to determine the magnitude and distribution of forces developed during launching of the mats. An analytical study was also requested in order to provide guidance for design changes in the mat structure.

CERL conducted field tests during the launch season August through December 1972. The analytical study and laboratory tests began at the same time and continued until June 1973. The results of that program were reported in CERL Interim Report M-84.[1]

The major observations of the initial study were: (1) that the bracket wires and longitudinal wires had much more than adequate strength, and (2) that the highest forces in the longitudinal wires were occurring on the launch plant as the mat went over the side. It was recommended that the possibility of using two, rather than three, 4000-pound breaking strength longitudinal wires be investigated.

Objective

The primary objective of this study was to investigate the structural feasibility of a two-longitudinal-wire mat. A secondary objective was to confirm the experimental results contained in the previous report and to demonstrate the validity of the conclusions when applied to the Corps of Engineers Vicksburg District sinking unit. This unit had not been tested in the FY73 study, and differs in some possibly significant aspects from the Memphis District sinking unit which had been tested.

Approach

This program consisted of two principal efforts: (1) expansion of the previous analysis to describe the structural behavior and force distributions in fabrics of various wire configurations, and (2) extensive field testing to provide sufficient data to compare loading characteristics of two- and three-wire fabrics.

Laboratory tests were conducted as needed to measure parameters required for the analytical model, and to determine properties of materials not previously tested. Mechanical/electrical force gages developed for the FY73 study were used for the field tests. (The principle of this gage is described in the previous report and is discussed in more detail in Appendix B of this report.)

Specifically, the following were included in the program:

1. Determine why the stresses in the longitudinal wires drop to very low levels when the mattress enters the water.

2. Perform slippage tests on the bracket wire/launch cable connections.

3. Expand the analysis of stress distribution among the longitudinal wires.

4. Conduct laboratory tests to measure stiffness changes in the bracket wire/launch cable connection as the exposure of bracket wire in the scarf box is increased in 1/2-in. increments.

5. Measure the stress developed in the longitudinal wires between internal blocks of a square by electronic strain gages as the mattress is launched.

2 FIELD TESTS AND RESULTS

General

Force levels measured on the Memphis District and Vicksburg District sinking units during the FY74

[1] F. Kearney and F. Plummer, *Study of Articulated Concrete Revetment Mattress: Test and Analysis*, Interim Report M-84 (Construction Engineering Research Laboratory [CERL], 1974).

launching season appear in Appendix C. Figure 1 is a histogram summarizing the field data in 500-lb intervals. The histogram for the FY73 field tests is included in Figure 2 for comparison.*

Since the distribution of hydrodynamic forces on the mat (Figure 3) shows that the maximum pressure force occurs close to the mat's upstream edge, most of the gages were installed in square three. It was usually not possible to gage squares one and two because of double layering of mattress squares.

Table 1 lists the river velocity measurements at representative revetments. These measurements were made on the off-shore end of the mooring barge with a current meter. Bracket wires were instrumented at Burnside, Plaquemine, and Allendale, LA all deep-water locations with some mats having 17 to 18 launches. The purpose of these tests was to determine if the bracket wires had substantial load levels in multiple-launch situations; the data show this did not occur. (See Appendix C for raw field test results.)

Tests to Determine Effect of Finger Apron on Longitudinal Wires

The FY73 tests indicated that the largest stress levels were being induced in the longitudinal wire as the launch passed over the edge of the plant, particularly over the finger apron used to place the first launch. Figure 4 shows these sharp-radius (i.e. 1 ft, 7 3/4 in.) fingers and the arrow in Figure 5 indicates this radius on the launch plant. When the blocks traverse this curve, large tensile forces occur. Chapter 4 details the geometry and force-time histories of the mat at this point on the plant.

To further study the effect of these large tensile forces, two tests were conducted 7 November 1973 on mats five and six at Baleshed, MS. Three longitudinal gages were installed on mat five between launches eight and nine. The three longitudinal wires were cut at the end blocks as shown in Figure 6; with this condition, the only force that constrained the two end blocks to follow the sharp curve of the fingers was the torsional force of the bracket wires and the weight of the blocks. As can be seen in Figure 6, gage 108 (upstream wire) indicated 0.4 kips, gage 123 (center wire) indicated 0 kip, and gage 312 (downstream wire) indicated 0.25

*Since the objective of the FY73 testing was to study the feasibility of a 16-block square, there is a preponderance of bracket wire data in Figure 2, because it was thought that this element would be the weakest link for the 16-block array.

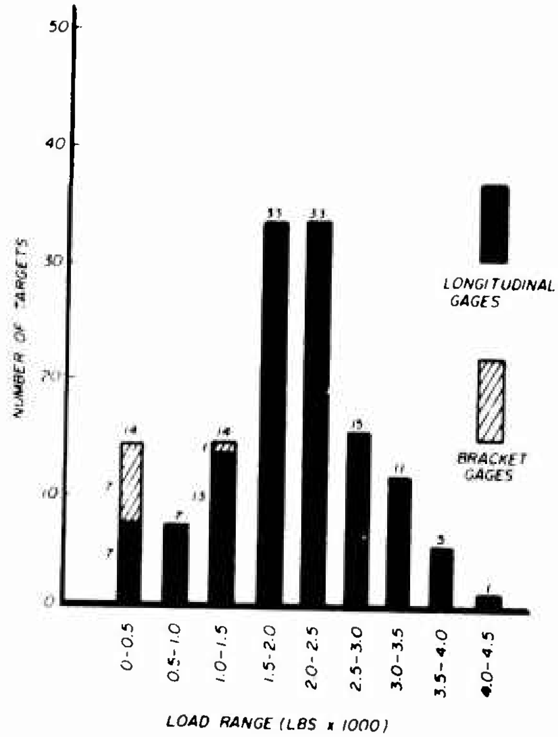

Figure 1. Summary of FY74 tests distribution of measured forces.

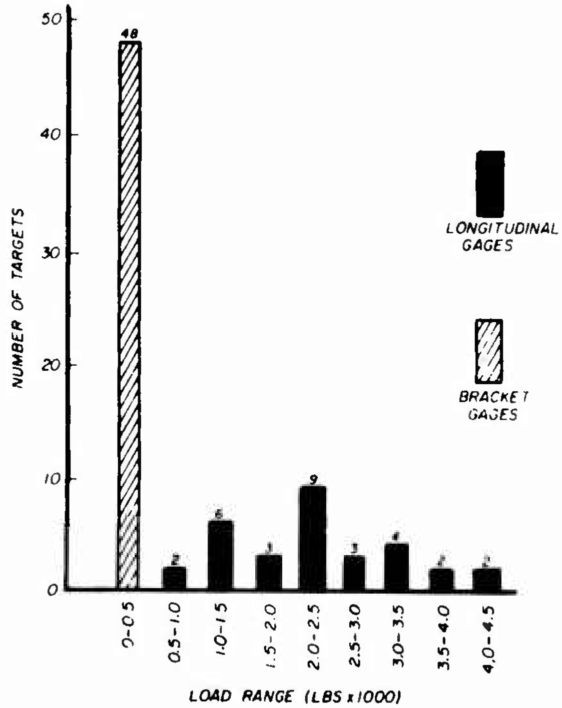

Figure 2. Summary of FY73 tests distribution of measured forces.

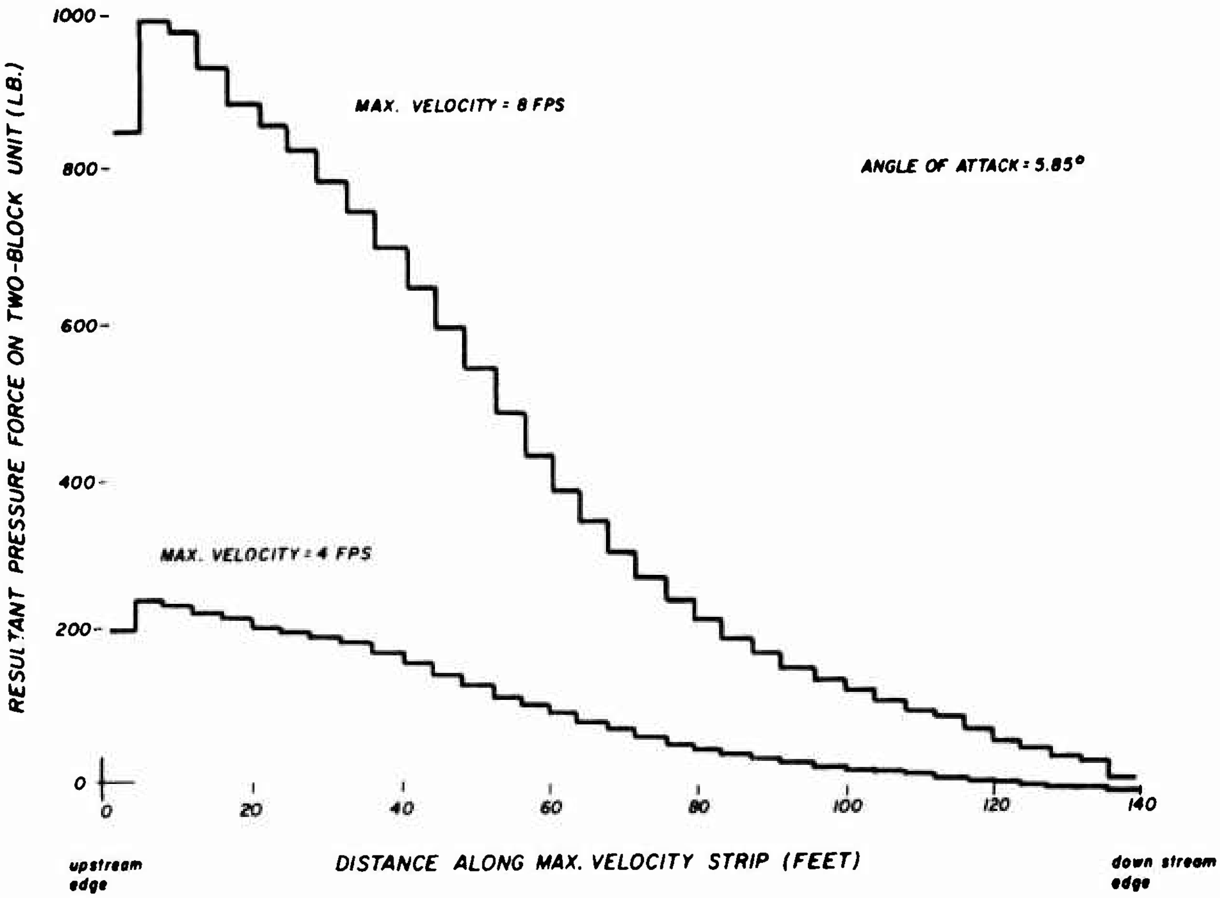

Figure 3. Pressure forces on two-block units along the strip of maximum velocity.

kip. Three gages were installed on the same mat between the tenth and eleventh launches, with only the center longitudinal wire cut at the end blocks as shown in Figure 7. With this condition, the end blocks were constrained by the outer wires and thus followed the curve. The center longitudinal wire could not carry any load from the mat since the cut ends prevented it from being a continuous member. However, gage 103 on the center wire indicated a load of 2.9 kip which can only be attributed to the load induced by the blocks being "forced" around the finger radius.

A repeat of this test on mat six showed a load of 2.1 kip (gage 139) in the center wire, again due to the geometry.

Electrical instrumentation used at Marchant, Allendale, and Point Breeze, LA consisted of strain gages bonded directly to the longitudinal wires between blocks in the mid-section of squares, and mechanical gages modified to produce an output signal proportional to force (Figure 8). This instrumentation provided a continuous force-time history. These tests confirmed results of the electrical gage tests conducted at Burnside, LA in December 1972, which showed that the peak force occurred at the finger apron.

3 LAB TESTS

Tests to Determine Effect of Changing Scarf Box

One recommendation resulting from the FY73 work was to investigate the change in the stiffness of the bracket wire/launch cable connection as more bracket wire is exposed in the scarf box. A reduction in this stiffness would allow the connection to accommodate larger deflections during abnormal launch conditions.

Table 1

Velocity Summary

Location (Date)	Distance from Shore (ft)	Depth (ft)	Velocity (ft/sec)
Baleshed, MS (7 Nov)	135	5	2.25
		10	2.75
		15	2.6
	300	10	3.9
		15	3.13
		20	2.75
		25	3.2
Coochie, LA (12 Nov)	360	5	3.47
		10	3.26
		25	2.98
" (13 Nov)		5	5.31
		10	5.06
		15	5.06
		20	5.06
		25	4.95
Pt. Breeze, LA (14 Nov)	360	5	4.5
		10	4.35
		15	4.5
		20	4.15
" (15 Nov)	360	5	3.89
		10	3.8
		15	3.84
		20	4.42
Pt. Pleasant, LA (4 Dec)	300	10	4.85
		20	4.73
	300	10	4.25
		20	4.28
	300	10	4.1
		20	4.3
Burnside, LA*			5
Marchant, LA*			5
Plaquemine, LA*			5
Allendale, LA*			5

*Velocity measurements were not actually made at these locations, but the estimated velocities were 5 ft/sec.

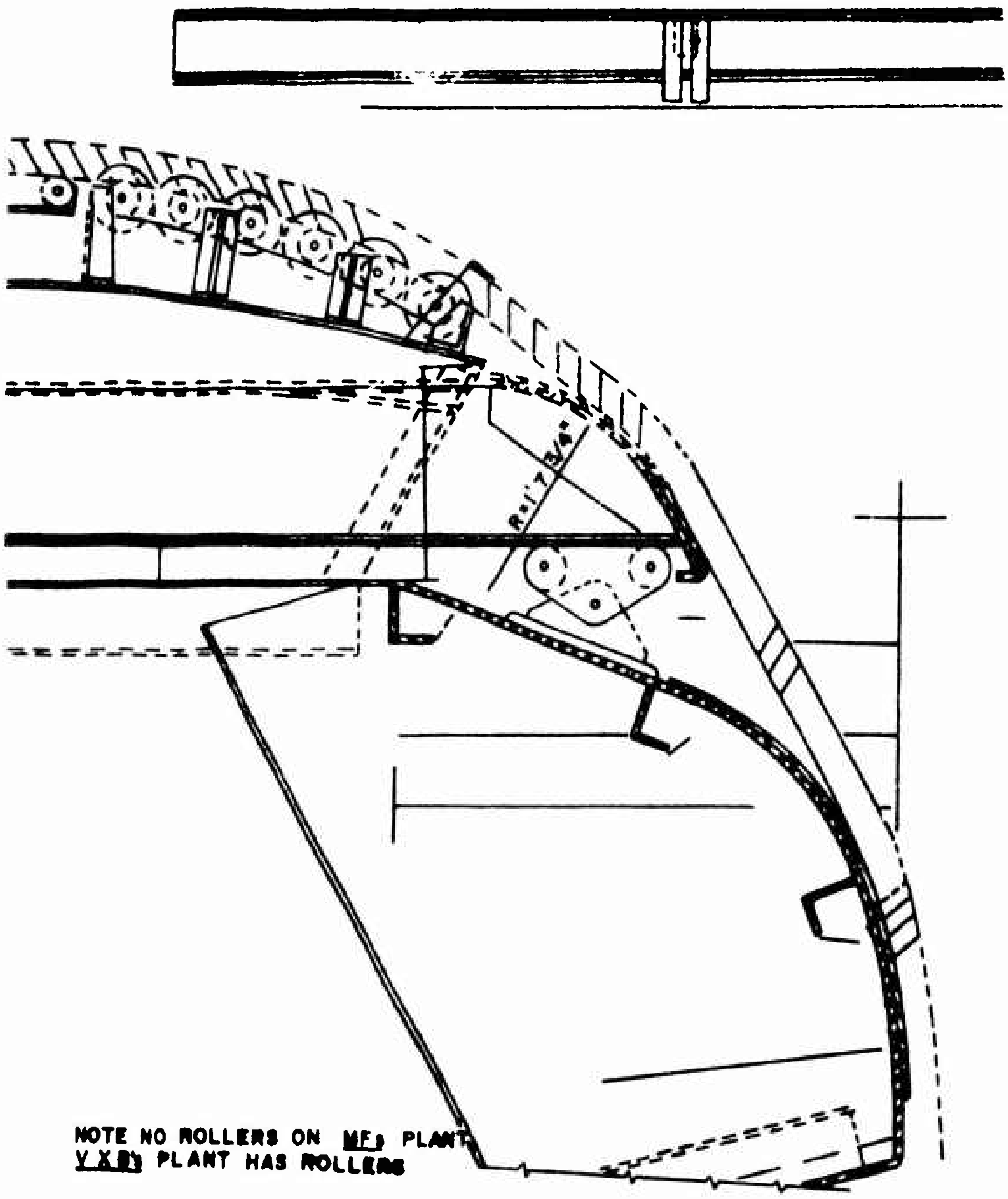

Figure 4. Section of launch plant showing launch fingers and curved bearing surfaces.

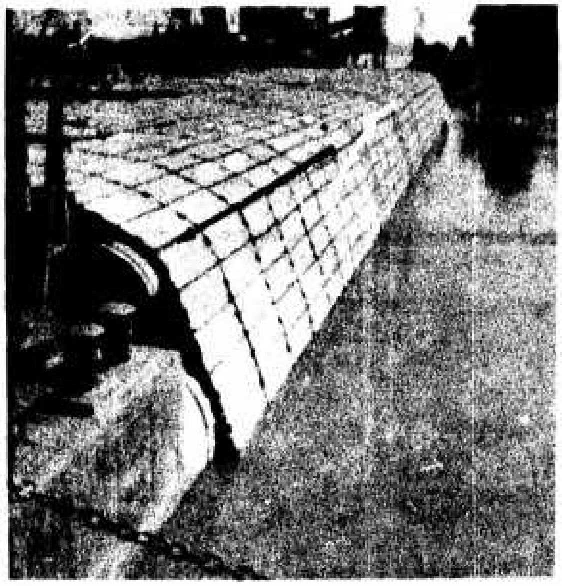

Figure 5. Mattress on launch fingers.

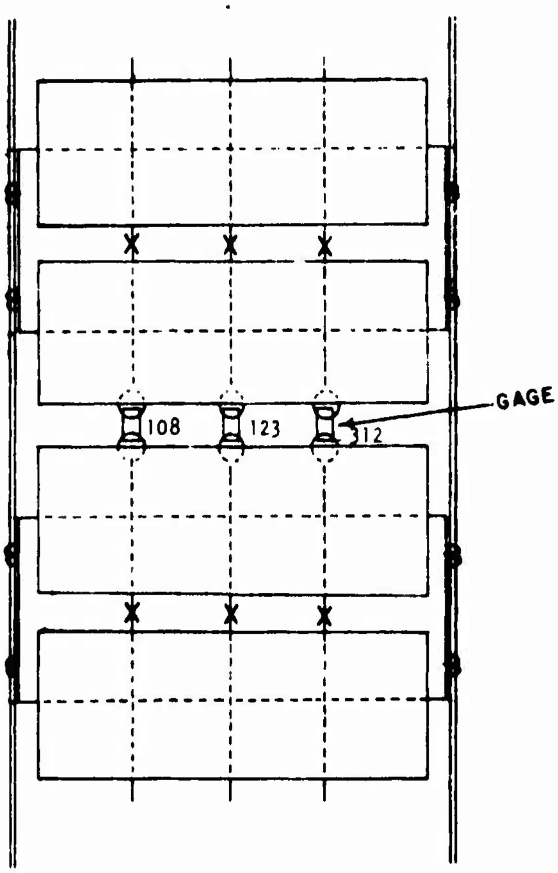

Figure 6. Three longitudinal wires cut at end blocks.

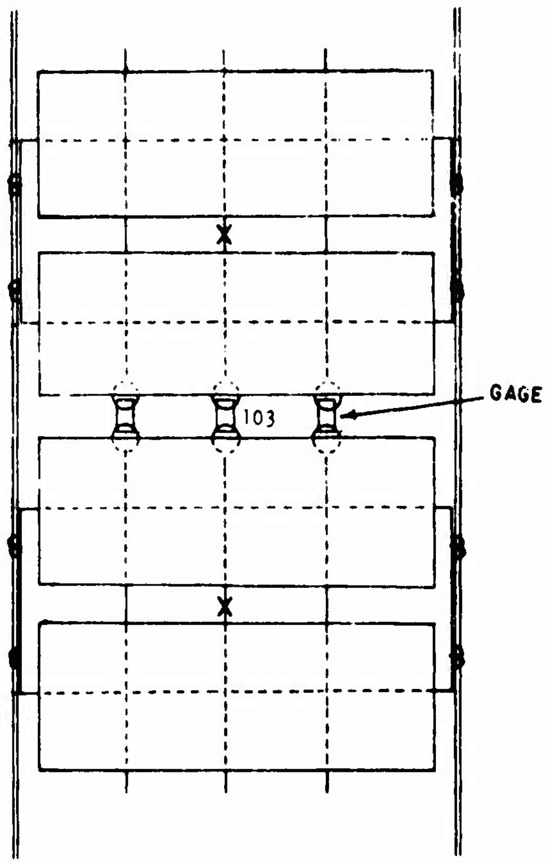

Figure 7. Center longitudinal wire cut.

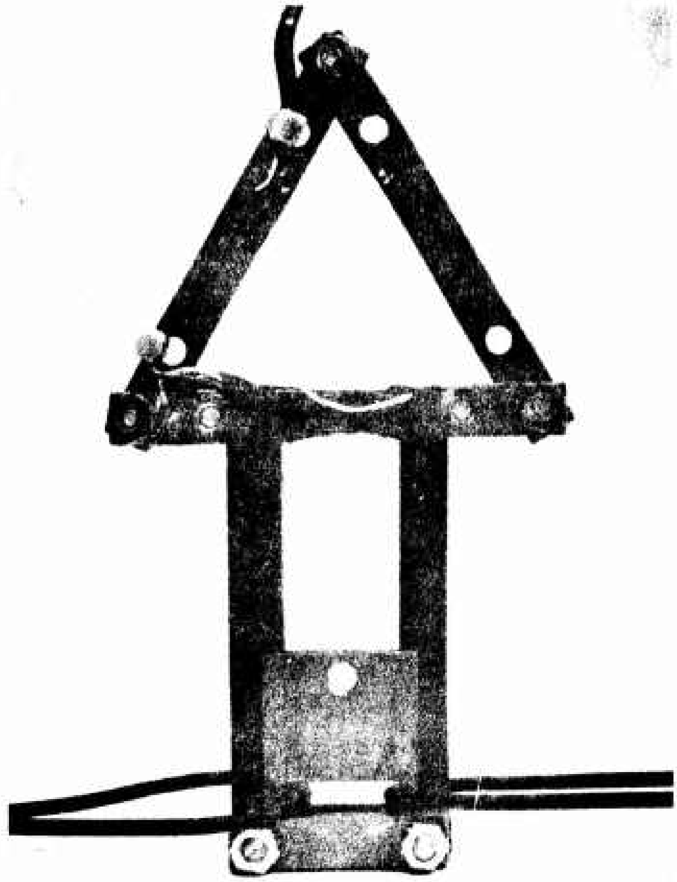

Figure 8. Mechanical gage modified to produce an electrical signal proportional to force.

A series of out-of-plane load/deflection tests was performed with the wire exposure increased 1/8 in. for each succeeding test. The first test was run with the exposure or protrusion that existed in the unmodified mats—7/8 in.—and the last test at 2 1/8 in.

The magnitude of the deflection at 4000 lbs was noted for each protrusion and plotted (Figure 9). This deflection did not change significantly until the protrusion approached 2 in.

Slippage Tests on Bracket Wire/Launch Cable Connections

Tests conducted in FY73 indicated an average slippage resistant force of 1600 lbs for copper-clad bracket wires and 350 lbs for stainless steel; copper-clad wraps were used in both cases. When these tests were repeated in FY74, however, the average slippage force for both stainless steel and copper clad was 350 lbs. For the copper-clad wire, the most probable cause of this reduced force could be the presence of oil which impaired the binding effect.

4 ANALYTICAL ANALYSES AND RECONCILIATION WITH FIELD DATA

Basis for Analyses

The first phase of the test program was conducted September-December 1973. Electrical/mechanical gages were used to determine the location and nature of the maximum longitudinal wire force. The time history recorded from these gages revealed that: (1) the gages were not loaded simultaneously nor to the same level, and the loading was very erratic; (2) the maximum forces occurred as the mat began its descent over the edge of the launch barge; and (3) by the time the gages

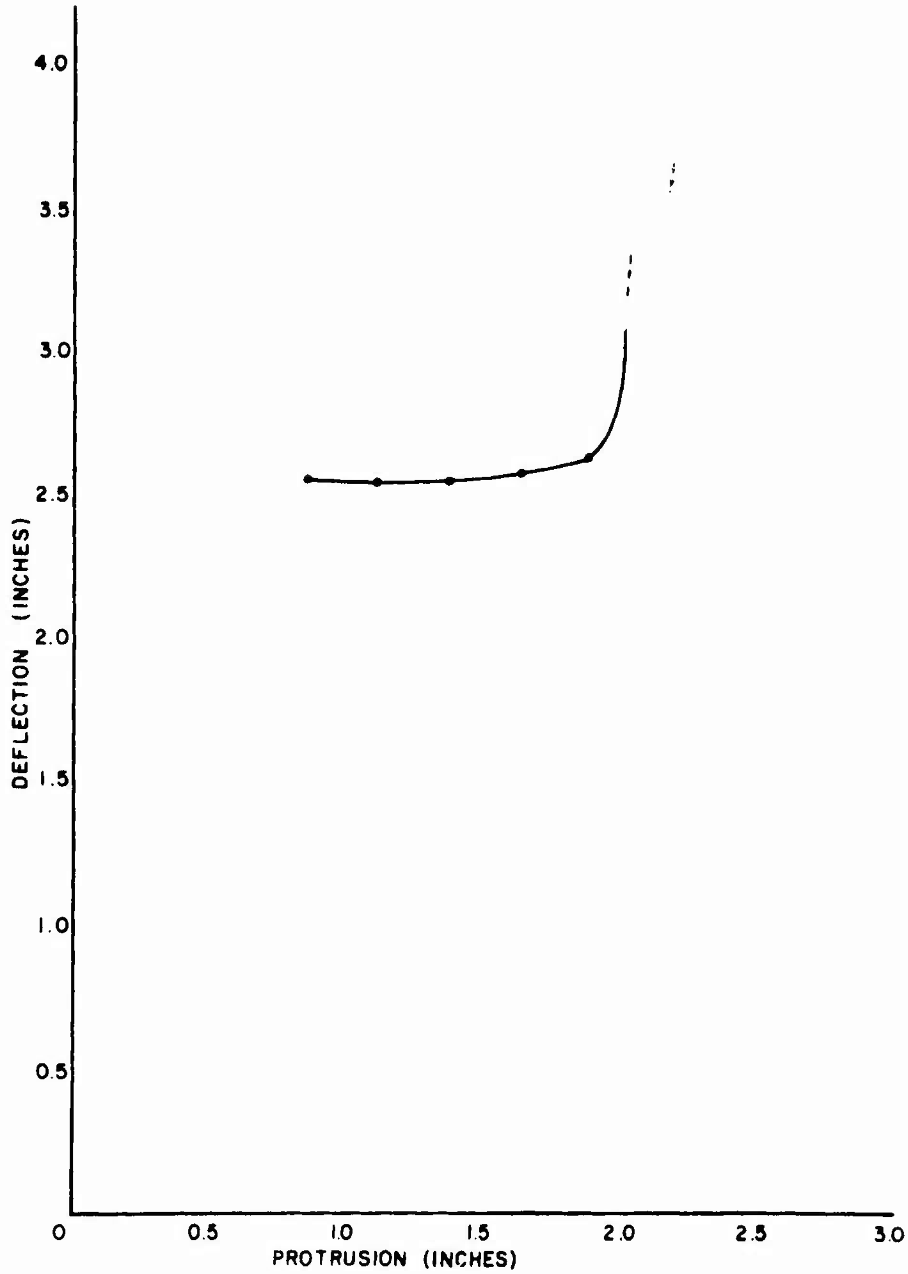

Figure 9. Out-of-plane deflection at 4000 lbs vs. bracket wire protrusion.

entered the water and left the influence of the launch barge, the forces had diminished significantly and appeared to be redistributed among the longitudinal wires. To explain these phenomena, the second phase of the test program in October-December 1973 was structured to include special tests to:

1. Determine why the forces in the longitudinal wires decrease when the mat enters the water

2. Investigate force distribution among the three longitudinal wires.

Scope of Analyses

An elaborate simulation model of the behavior of an articulated concrete mattress was not undertaken, because a mat is a complicated structural assemblage and is subjected to a series of dynamic forces of undetermined magnitude during the launching process. Instead, the analyses were restricted to simple static calculations and analytical models which could provide insight into the general behavior of the mattress and could be correlated with the field data.

Analyses

During the launch process several factors induce forces in the longitudinal wires. Included among these are:

1. Static friction between the mat and the rollers
2. Rolling friction between the mat and the rollers
3. Sliding friction between the mat and the launching barge edge
4. The sharp curvature occurring as the mat traverses the launch finger apron
5. Fluid forces on the submerged mat
6. The weight of the submerged mat
7. Inertial effects.

However, time-history records from the electrical/mechanical gages used in the field tests indicated that the peak longitudinal forces were, in general, associated with the mat's progress over the edge of the launch plant. At this stage in the launch operation, forces produced by the angle change associated with the mat traversing the launch finger apron would be most likely to cause the peak forces.

The basic cross-sectional dimensions and spacings of a typical concrete end block of a square are shown in Figure 10. A typical block is 3 in. thick and 14 3/8 in. in length at the bottom. The interstitial spacing between the blocks is 1 in. at the top and tapers to 5/8 in. at the bottom. The end block spacing is a constant 1/2 in. End-twist-tie connections are installed at the end block which has the constant spacing of 1/2 in.; however, because the amount of slack associated with the end-twist connection is unknown, it was decided to use the interstitial spacings to determine the angle change of the mat as it follows the curvature of the launch finger apron.

The launch finger apron (Figure 4) has a radius of 1 ft 7 3/4 in. If adjacent blocks in a square are considered to be rigid and are assumed to adopt a configuration where they remain tangent to the radius of the launch finger (Figure 11), lower corners of the adjacent blocks will meet and the longitudinal wire will undergo strain. The angle change associated with this configuration is 39° 59' 43" and change in length of the longitudinal wire is 0.465 in. That change in length corresponds to an average strain of approximately 0.437 in./in. This would produce fracture of the wire since the failure strain of the wire, determined by laboratory testing, was about 0.015 in./in.

Results of this simple calculation prompted further examination of the possible angle change which adjacent blocks could assume without inducing fracture strain in the longitudinal wires. For these calculations, the three configurations shown in Figure 12 were assumed to represent conditions that might exist in the field. In the first and second configurations the

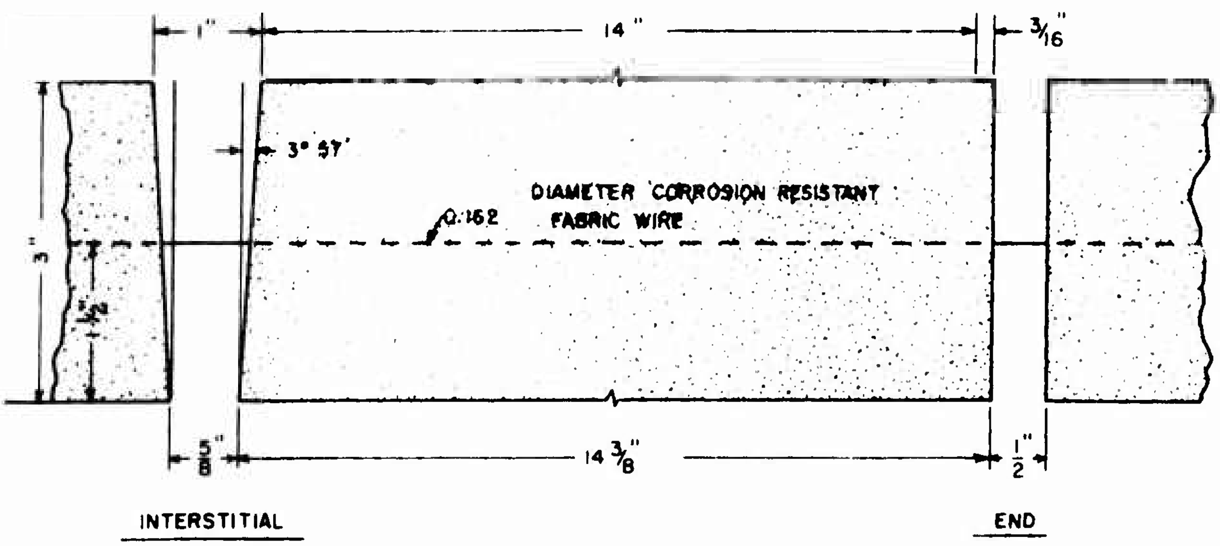

Figure 10. Block dimensions and spacings.

blocks were assumed to lock at their lower corners, while in the third configuration one block was allowed to ride up on the other. In the first configuration the longitudinal wire was assumed to adopt a curvature that produced an angle change of 23° 52' 28". For the second configuration, the longitudinal wire was assumed to remain straight and the angle change was computed to be 24° 33' 25". In the third configuration the angle change was 25° 34' 21".

The angle change that can occur in the blocks without causing failure strain was computed to be only about 60 percent of the maximum angle change the blocks might experience while traversing the launch finger apron. It was anticipated that any force in the longitudinal wires induced by the weight of the mat suspended below the launch finger apron might result in sufficient force for the mat to experience an angle change larger than 23° to 25° and thus produce the peak force in the longitudinal wires.

It was also recognized that several potential effects could be responsible for the 40 percent difference between (1) the angle change the blocks could undergo without breaking the longitudinal wires, and (2) the angle change associated with the launch finger apron. These effects are:

1. Crushing of the concrete at the lower corners of the blocks when the blocks lock up
2. Different spacings between the blocks
3. Different radii for the launch finger aprons
4. The effective angle in the launch finger apron being less than 39° 59' 43".
5. Crushing of the concrete around the points where the longitudinal wires enter and exit the block, caused by high bearing stress imposed by deformation of the longitudinal wires as the blocks traverse the launch finger apron.
6. Placement of the longitudinal wires at other than mid-height of the block.

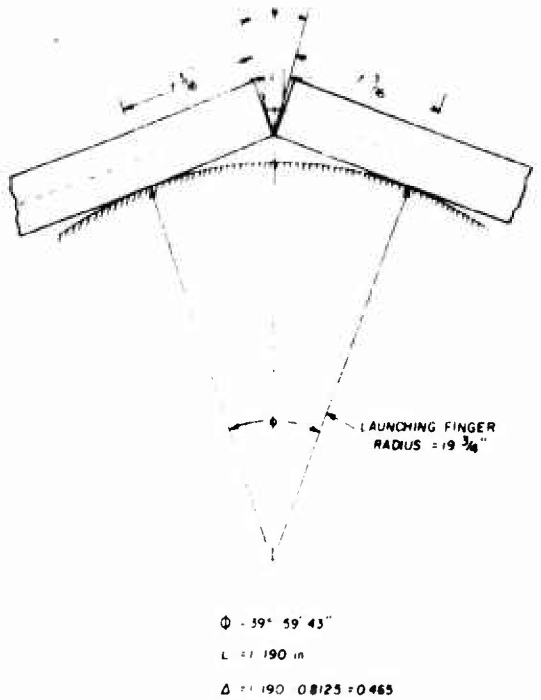

Figure 11. Angle change at launch finger apron.

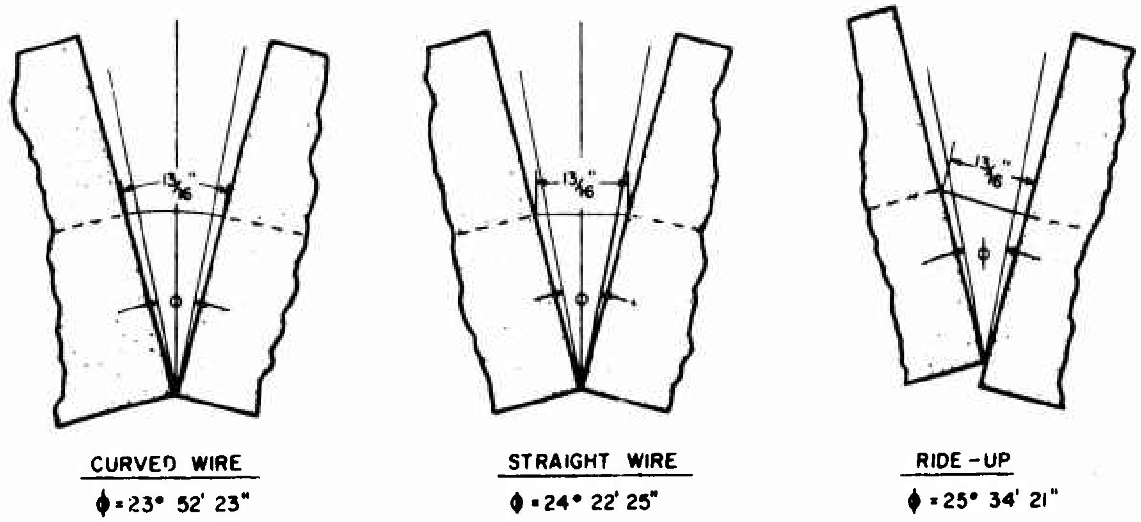

Figure 12. Potential angle change configurations.

Of all these effects, the most logical explanation appeared to be that the effective angle change experienced at the launch finger apron is less than 39° 59' 43". If the launch finger were retracted more than is shown in Figure 4, the angle change experienced by the blocks would decrease. Likewise, if the blocks did not fully conform to the launch finger apron radius i.e., if the lead block were restrained from conforming to the launch finger apron radius by the force in the longitudinal wires an effective angle change less than 39° 59' 43" would also result.

The field data were analyzed to determine if they supported the theory that the maximum forces were occurring as the mat traversed the launch finger apron and that these forces were being induced in the longitudinal wires as a result of an angle or curvature change other than that caused by actual forces being applied to the mat and then transmitted to the longitudinal wires. The first field data which tended to confirm this theory were the results of the special tests conducted at Baleshed, MS, on 7 November 1973 (see Chapter 3 for details). When all the longitudinal wires on either side of the end block were cut, the torsional spring constant of the bracket wires was the only force restraining the blocks against rotation as they traversed the launch finger apron curvature. In this particular test the sum of the three forces recorded by the mechanical gages connecting the two end blocks was 0.65 kip. On a similar test only the outer longitudinal wires on either side of the end block were cut, while the other two outer longitudinal wires were left intact. For this particular test the sum of the three forces recorded by the mechanical gages connecting the two end blocks was 7.90 kips.

Since the results from the special tests performed at Baleshed, MS tended to support the theory that the forces induced in the longitudinal wires were produced by the angle changes associated with the launch finger apron, it was decided to analyze the end connection force data recorded by the mechanical gages in the two- and three-gage configurations. Theoretically, if the peak forces induced in the longitudinal wires were attributable to the angle change at the launch finger apron, the total connection force would be proportional to the number of longitudinal wires; i.e. the total force for the two-gage configuration would be two-thirds of the total force for the three-gage configuration. (Note that for the two-gage configuration the center end-twist-tie connection was not installed; consequently the two mechanical gages installed on the outer longitudinal wires carried all the force transmitted between squares. In the case of the three-gage configuration, however, the three wires do not carry equal loads because of dimensional variations in assembling the mat on the launch plant. One of the gages is likely to carry only a percentage of the average of the force being carried by the two gages which initially define a straight line.

Table 2 summarizes the two-gage connection force measurements and indicates that the average total force for the two-gage configuration was 4.79 kips, with a standard deviation of 1.76 kips. Table 3 summarizes the three-gage connection force measurements and indicates at the average total force for this configuration was 6.55 kips, with a standard deviation of 2.43 kips. Based on these average values, the ratio of the total two-gage connection force to the total three-gage connection force is 0.74 which is about 10 percent higher than the theoretical value of 0.67. This, however, does not include a correction for the fact that one gage of the three-gage configuration is not 100 percent effective. To estimate the effectiveness of that gage for each set of three-gage data, the smallest gage force was divided by the average of the two larger gages; the results of this calculation appear in Table 3. Based on the 20 sets of data, the smallest gage force was an average of 63 percent of the average of the two larger gage forces i.e., one end-twist-tie connection is only 63 percent effective. Consequently, the average force of 6.55 kips for the three-gage configuration must be corrected by the factor

$$\frac{3.0}{2.63} = 1.14$$

to compensate for the fact that on the average only 2.63 gages were fully effective. Applying this correction factor results in an average three-gage force of 7.47 kips. If the mat assembly tolerances were such that the three gages were fully effective, 7.47 kips would be the average total force for the three-gage configuration. The ratio of the average values of the total two-gage connection force to the corrected total three-gage connection force now becomes 0.64. This ratio compares extremely favorably (with 1/2 percent) with the theoretical value of 0.67.

Although the results of this analysis were encouraging, it was necessary to determine the force induced in the longitudinal wire by the submerged mat hanging vertically in the water, to ascertain that the forces recorded by the mechanical gages were not attributable solely to the weight of the hanging mat. To estimate

Table 2

Summary of Two-Gage Connection Force Measurements

Location	Date	Mat Number	Launch Barge	Individual Gage Forces (kips) 1	3	Total Force (kips)
Marchant, LA	22 Oct 73	15	Vicksburg	1.65	1.6	3.25
Marchant, LA	22 Oct 73	15	Vicksburg	2.2	1.9	4.10
Marchant, LA	22 Oct 73	15	Vicksburg	2.4	1.3	3.70
Marchant, LA	22 Oct 73	16	Vicksburg	2.5	1.7	4.20
Marchant, LA	22 Oct 73	16	Vicksburg	2.3	2.0	4.30
Allendale, LA	26 Oct 73	7	Vicksburg	3.15	3.75	6.90
Coochie, LA	12 Nov 73	12	Vicksburg	2.4	2.3	4.70
Coochie, LA	13 Nov 73	19	Vicksburg	2.85	3.2	6.05
Pt. Breeze, LA	15 Nov 73	19	Vicksburg	2.7	2.5	5.20
Pt. Breeze, LA	15 Nov 73	20	Vicksburg	2.9	2.15	5.05
Pt. Breeze, LA	15 Nov 73	21	Vicksburg	2.5	1.4	3.90
Pt. Pleasant, LA	4 Dec 73	4	Memphis	5+	5	10.0
Pt. Pleasant, LA	4 Dec 73	4	Memphis	2.75	1.1	3.85
Pt. Pleasant, LA	4 Dec 73	5	Memphis	2.5	2.7	5.20
Pt. Pleasant, LA	5 Dec 73	11	Memphis	0.9	0.95	1.85
Pt. Pleasant, LA	5 Dec 73	12	Memphis	3.3	2.25	5.55
Pt. Pleasant, LA	5 Dec 73	12	Memphis	3.9	1.4	5.30
Pt. Pleasant, LA	5 Dec 73	13	Memphis	2.05	1.8	3.85
Pt. Pleasant, LA	6 Dec 73	17	Memphis	3.5	2.95	6.45
Pt. Pleasant, LA	6 Dec 73	17	Memphis	1.6	0.75	2.35
					Average:	4.79
					Standard Deviation:	1.76

Table 3

Summary of Three-Gage Connection Force Measurements

Location	Date	Mat Number	Launch Barge	Individual Gage Forces 1	2	3	Total Force	Smallest Force ½ ϵ large forces
Burnside, LA	19 Oct 73	23	Vicksburg	1.25 K	1.4 K	1.6 K	4.25 K	0.83
Marchant, LA	22 Oct 73	14	Vicksburg	3.1	2.0	2.15	7.25	0.75
Allendale, LA	25 Oct 73	1	Vicksburg	2.8	1.8	2.0	6.60	0.75
Allendale, LA	26 Oct 73	7	Vicksburg	2.15	1.65	1.9	5.70	0.81
Baleshed, MS	7 Nov 73	6	Memphis	2.9	2.1	2.2	7.20	0.82
Coochie, LA	12 Nov 73	12	Vicksburg	1.8	1.75	1.65	5.20	0.93
Coochie, LA	13 Nov 73	19	Vicksburg	2.5	2.15	2.5	7.15	0.86
Pt. Breeze, LA	15 Nov 73	18	Vicksburg	1.65	0.5	2.05	4.20	0.27
Pt. Breeze, LA	15 Nov 73	19	Vicksburg	1.9	2.0	1.8	5.70	1.00
Pt. Pleasant, LA	4 Dec 73	4	Memphis	1.3	3.7	0.5	5.50	0.20
Pt. Pleasant, LA	4 Dec 73	4	Memphis	2.95	5+	5	12.95	0.59
Pt. Pleasant, LA	4 Dec 73	5	Memphis	1.9	1.7	2.3	5.90	0.81
Pt. Pleasant, LA	5 Dec 73	11	Memphis	3.6	1.8	4	9.40	0.47
Pt. Pleasant, LA	5 Dec 73	12	Memphis	1.65	0.5	0.75	2.90	0.42
Pt. Pleasant, LA	5 Dec 73	13	Memphis	2.4	2.1	1.3	5.80	0.20
Pt. Pleasant, LA	5 Dec 73	13	Memphis	4.3	1.1	0.55	5.95	0.58
Pt. Pleasant, LA	5 Dec 73	14	Memphis	3.5	5+	3	11.50	0.71
Pt. Pleasant, LA	5 Dec 73	14	Memphis	2.0	.95	2.4	5.35	0.43
Pt. Pleasant, LA	6 Dec 73	17	Memphis	3.2	1.65	1.9	6.75	0.65
Pt. Pleasant, LA	o Dec 73	17	Memphis	2.25	2.1	1.3	5.65	0.60
						Average:	6.55	0.63
						Standard Deviation:	2.43	0.24

the total force at the connection for the case of one square submerged in water, the simple calculation illustrated in Figure 13 was performed, with the following assumptions:

1. A fixed support is representative of the constraint conditions at the river surface
2. A free support is representative of the constraint conditions at the river bottom
3. Fluid pressure and frictional forces are negligible
4. Inertial forces are negligible
5. The launch cable stiffness is many times greater than the bracket wire stiffness
6. The blocks of the square are rigid.

On the basis of these assumptions the solution to the problem was simplified to one equation with one unknown. Laboratory tests indicated that the longitudinal stiffness of an individual end-twist-tie connection was approximately 8869 lb/in and the longitudinal bracket wire stiffness was about 5200 lb/in. Also, field data from the initial phase of the test program indicated that when all three longitudinal wires were connected by mechanical gages at the connection between squares, the third gage recorded only about 50 percent of the average force recorded by the other gages. It was consequently assumed that the total longitudinal wire connection stiffness was about 2 1/2 times the individual stiffness. Using these numerical values, solving the single equation, and back-substituting the result to calculate the forces, it was determined that the total end-twist-tie connection force would be about 571.0 lbs and the total bracket wire force would be about 133.8 lbs. While both these values appeared reasonable because they did not contradict the observed field data, it was realized that:

1. If the launch cable stiffness were included, the forces in the longitudinal wires would increase

2. If more squares were added, the weight of the suspended model would increase and the forces carried in the longitudinal wires would consequently increase

3. To determine how the forces were distributed among the launch cable, bracket wires, longitudinal wires, and longitudinal connection wires (end-twist-tie connection), a more refined model was required that could be used to investigate the impact of changes in number and size of longitudinal wires. Figure 14 illustrates the more refined model that was developed.

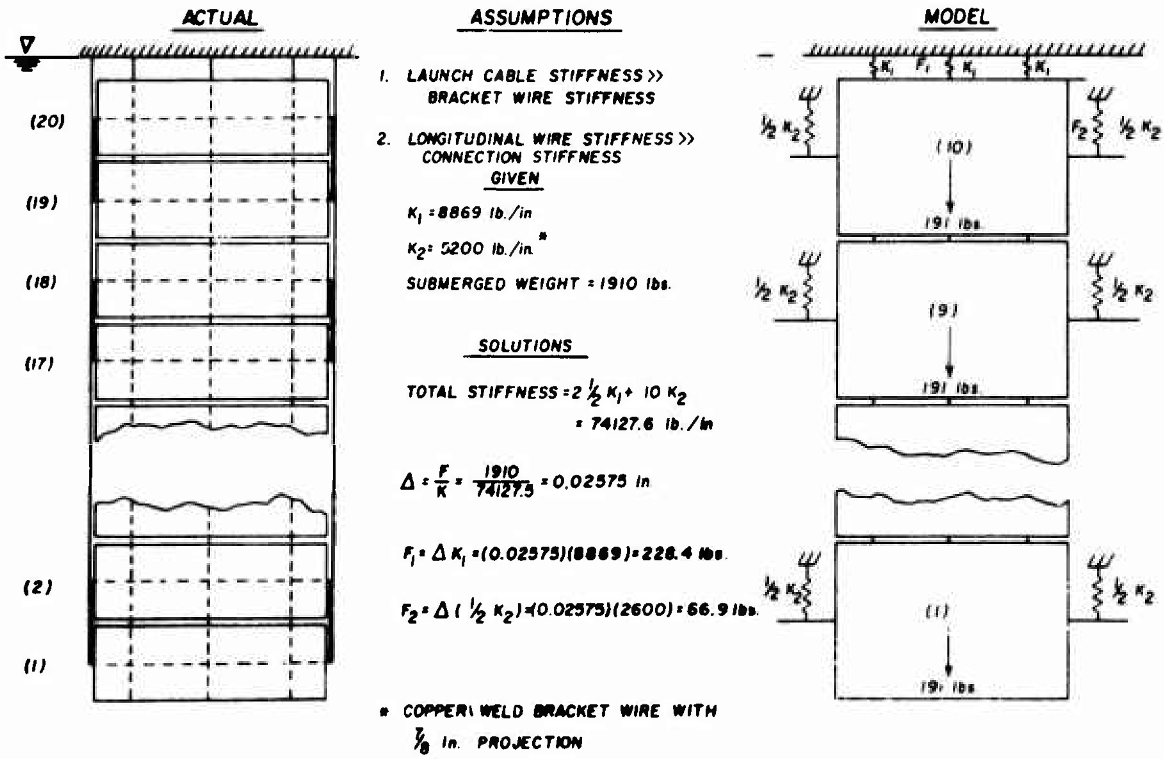

Figure 13. Simple force distribution model.

The model, consisting of 40 block systems, represents the force distribution in four squares of mattress hanging in water at a depth of 100 feet or more. As seen in Figure 14, each system is made up of two rectangular blocks weighing 95.5 lbs. The various springs represent the different wires throughout the mattress. The vertical spring with stiffness K_1 connects each block system and is representative of the launch cable stiffness. The bracket wires, which pass through the concrete blocks latitudinally and are connected to the launch cable longitudinally, are represented by the vertical springs with stiffnesses of K_2 equal to one-half the bracket wire longitudinal stiffness. These springs are mutually connected within each block system, and have the launch cable spring, K_1, at a common point.

After every tenth block system, which represents a square, the following block system is connected by a spring with a stiffness, K_3, equal to the total connection wire stiffness in the actual mattress. The other systems are all connected by a vertical spring, K_4, which joins the center of the upper block of each system to the lower block of the system above it. K_4 represents the total stiffness of the longitudinal wires embedded in the concrete blocks.

The assumptions for this analysis are similar to those for the simple force distribution analysis, except that in this multi-square force distribution model, the launch cable stiffness and the longitudinal wire stiffness are included, and the forces in these wires are determined. In the multi-square force distribution model the submerged weight of the concrete blocks causes each spring to displace, creating a force which is representative of the actual forces induced in the wires of the mattress. A series of simultaneous equilibrium equations was developed based on the displacements of the springs. A computer program was then written which solved the equations by the Gauss Elimination method and then calculated the forces in each spring.

The analysis of the multi-square force distribution model can be divided into three cases. Each case calculated the total forces which would occur in the launch cable, bracket wires, longitudinal wires, and end-twist-tie connections for (1) a three-longitudinal-wire system, (2) a two-longitudinal-wire system, and (3) a one-longitudinal-wire system. The three-longitudinal-wire system represents the mattress in its original configuration with three longitudinal wires; the two-longitudinal-wire system represents deletion of one of the three longitudinal wires; and the one-longitudinal-wire system represents deletion of two of the three longitudinal wires.

The launch cable stiffness and bracket wire stiffness were constant in all three cases. However, in the first case, stiffnesses representative of 0.162-in. diameter wire were used for the longitudinal wire springs, and stiffnesses representative of the end-twist-tie wire were used for the end-twist-tie connection springs. In case two, stiffnesses representative of 0.141 in. diameter wire were used for the longitudinal wire springs and the stiffnesses of the end-twist-tie connection springs remained the same. The final case also used stiffnesses representative of the 0.141-in. diameter wire; however, the stiffnesses of the end-twist-tie connection spring were reduced by 21 percent to simulate the use of smaller diameter end-twist-tie connection wires. The values of the different spring constants for these three cases are presented in Table 4.

The spring constant K_1 is representative of the stiffness of a 30-in. length of 3/8-in. diameter launch cable and was determined from actual test data. K_2 represents the values determined from the longitudinal bracket wire tests on copper-clad wire. The values for K_3 are integer multiples of the number of longitudinal wires used in the system except for the three-wire system, in which K_3 was taken to be 2.63 times the individual end-twist-tie connection wire stiffness, as discussed earlier. The stiffness values of K_4, the longitudinal wire stiffness, were multiples of the number of longitudinal wires in the system times the average stiffness of a 15-in. length of longitudinal wire.

Results from the refined force distribution model are presented in Figures 15 through 20. Figures 15 through 17 are plots of the launch cable forces and the longitudinal wire forces for cases 1, 2, and 3, respectively. These plots show that the forces in the launch cable and longitudinal wires increase approximately linearly with depth. The slight cusping effect is due to the transfer of forces between the launch cable and the longitudinal wire through the bracket wires. (For clarity, the data points between the cusps were deleted.) It should be noted that as the number of longitudinal wires is decreased within a given case, the launch cable takes up more of the load.

Figures 18 through 20 are plots of the forces in the bracket wires for cases 1, 2, and 3, respectively. The forces in the bracket wires are seen to fluctuate within each square of the 10-block system. It can also

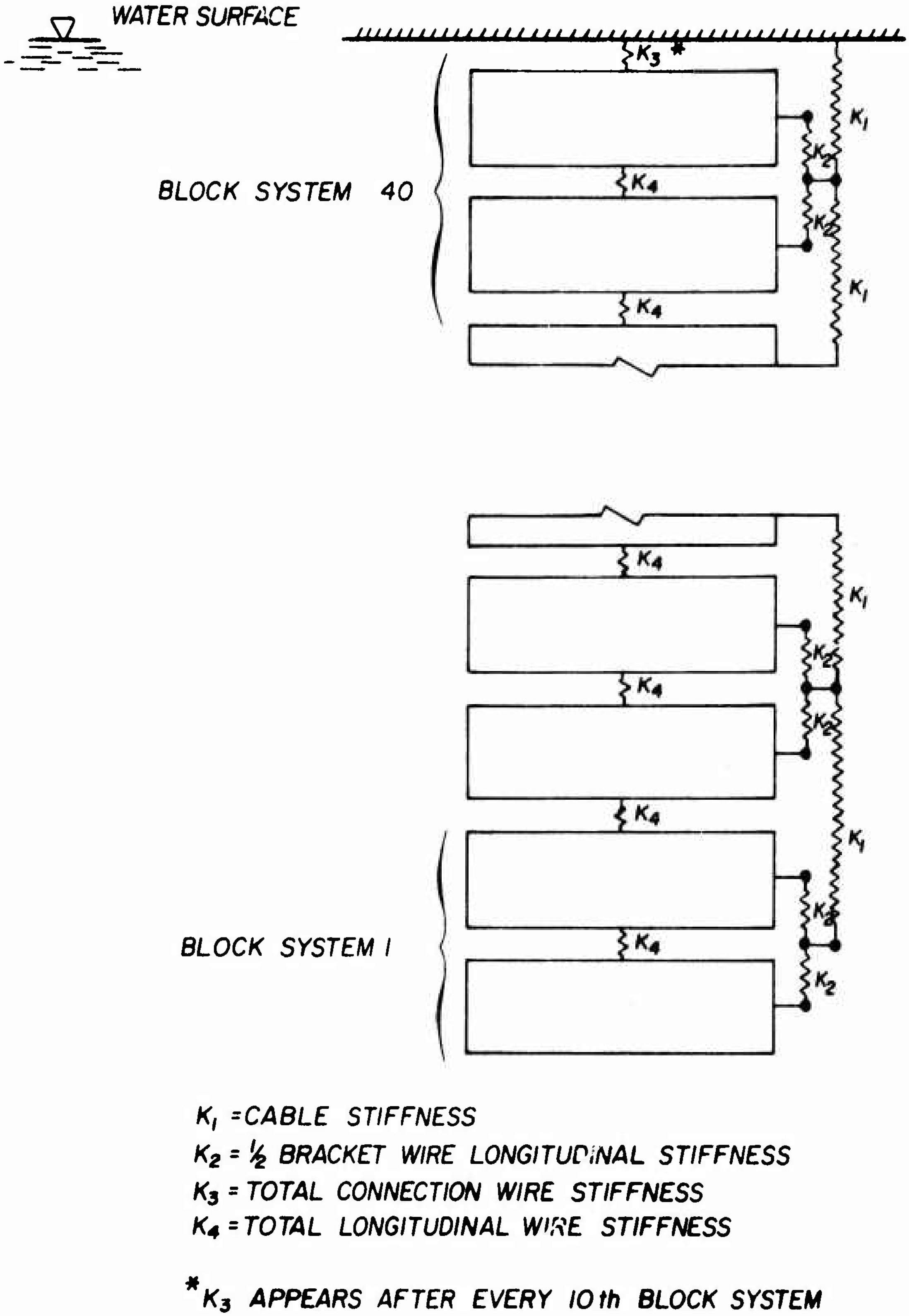

Figure 14. Multi-square force distribution model.

Table 4

Spring Constants for Force Distribution Model

Case	Longitudinal Wires	Spring Constants (lb/in.) K_1	K_2	K_3	K_4
	3	61261.1	2600.0	22172.0	105000.0
1	2	61261.1	2600.0	17737.0	70000.0
	1	61261.1	2600.0	8868.8	35000.0
	3	61261.1	2600.0	22172.0	82960.5
2	2	61261.1	2600.0	17737.0	55307.0
	1	61261.1	2600.0	8868.8	27653.5
	3	61261.1	2600.0	17518.1	82960.5
3	2	61261.1	2600.0	14014.0	55307.0
	1	61261.1	2600.0	7007.2	27653.5

be seen that the bracket wires interact with the launch cable; as the launch cable forces increase and decrease, so do the bracket wire forces.

The total forces in the end-twist-tie connection wire and the bracket wires of the simple free distribution model are slightly less than those in the multi-square force distribution model, although the two models are in reasonable agreement. For the multi-square force distribution model at the tenth block system of case 1 for three wires, the total bracket wire force was 157.76 lbs and the total connection wire force was 725.78 lbs. This compares to 133.8 lbs in the bracket wires and 571.0 lbs in the connection wires for the simple force distribution model.

The plot presented in Figure 21 was developed to check the results of the multi-square distribution model against the observed field data. The water depth at the time of launching of the various two- and three-mechanical-gage configurations used to acquire the data for the initial portion of this analysis was estimated from notes taken during the launching operations and some interpolation. The various data points in Figure 21 were plotted from the sum of the two- and three-wire forces recorded by the mechanical gages, and the estimated water depth. For comparison, Figure 21 also contains the estimated total end-twist-tie connection force predicted by the multi-square force distribution model of the orignial mat design. A comparison of the average total connection force for the two- and three-gage configuration and the result of the multi-square force distribution model indicates the weight of the hanging mattress should not influence the peak connection forces recorded by the mechanical gages, since all the observed field data plot above the force levels predicted by the model. Furthermore, the mats have to have been launched in 156 to 230 ft of water for the weight of the hanging mat to exceed the peak forces induced when the mat traverses the curvature of the launch finger apron.

To evaluate results of the multi-square force distribution model, the maximum forces in the launch cable spring, the two longitudinal wire springs, and the end-twist-tie connection were selected from each system for the three different cases, and stresses and factors of safety were calculated for each wire. Tables 5 and 6 show these results. For these calculations, 20,000 lbs was used as the ultimate load capacity of the cable as determined by laboratory tests, 4200 lbs and 3350 lbs were used as the ultimate load capacity of the 0.162- and 0.141-in. diameter wires, respectively; 3550 lbs was used for the ultimate load capacity of end-twist-tie connection wire. Table 4 shows that for each case, the factor of safety is greater than 2 and tends to decrease as the number of longitudinal wires decreases. A more balanced factor of safety is observed for case 3 with two longitudinal wires; for this combination the average factor of safety is 3.30 and the standard deviation is 0.14. However, in considering the factors of safety, it should be remembered that fluid and inertial forces were considered negligible in the model and that the factor of safety is based on an average launch depth of 100 feet.

Table 6 presents the stress levels associated with the peak force levels predicted by the multi-square force distribution model with the exception of the end-twist-tie wires. Stresses were not calculated for the end-twist-tie wire because the area to be used in the calculation was indeterminate. Results in Table 6 indicate that all stresses are within acceptable levels.

Table 5

Factors of Safety

Number of Longitudinal Wires	Wires	Case 1	Case 2	Case 3
	Interblock	3.47	3.10	3.18
	Cable	4.17	4.00	3.83
	Block-to-Block	3.43	3.04	3.13
3	End-Twist-Tie	3.67	3.97	3.83
	Average F. S.	3.69	3.53	3.49
	Standard Deviation	0.34	0.53	0.39
	Interblock	3.48	3.16	3.25
	Cable	3.74	3.61	3.49
	Block-to-Block	3.41	3.08	3.17
2	End-Twist-Tie	3.09	3.37	3.28
	Average F. S.	3.43	3.31	3.30
	Standard Deviation	0.27	0.24	0.14
	Interblock	2.86	2.70	2.76
	Cable	3.16	3.10	3.04
	Block-to-Block	2.75	2.57	2.62
1	End-Twist-Tie	2.70	2.96	2.96
	Average F. S.	2.87	2.83	2.85
	Standard Deviation	0.21	0.24	0.19

Table 6

Maximum Stress (ksi)

Number of Longitudinal Wires	Wire	Case 1	Case 2	Case 3
	Interblock	48.9	57.7	56.2
1	Cable	59.8	62.5	65.2
	Block-to-Block	49.5	58.8	57.2
	Interblock	58.5	67.8	65.9
2	Cable	66.7	69.2	71.4
	Block-to-Block	59.5	69.5	67.5
	Interblock	71.1	79.4	77.7
3	Cable	79.1	80.5	82.2
	Block-to-Block	74.0	83.4	81.7

Cable	Longitudinal Wires 0.162	Longitudinal Wires 0.141
fpu = 250 ksi		
.8 fpu = 200 ksi	fpu = 204 ksi	fpu = 215 ksi
pu = 20 k	pu = 4.2 k	pu = 3.35 k

The bending stresses within the concrete blocks were also calculated. For each of the three wire systems analyzed, the highest differential between the longitudinal wires at the top and bottom of the concrete block model was chosen. The block was then idealized as a simply supported beam with either three-, two- or one-point loads depending on the number of longitudinal wires. The maximum moment at the center line was then obtained for the given load condition and the bending stress was calculated. The values for the bending stress were very low (less than 15 psi) in each system and were not considered to have much influence on the overall analysis. Therefore, they can be disregarded.

5 CONCLUSIONS

Based on observed field data and analyses, the following conclusions can be drawn:

1. For the condition assumed, it appears structurally feasible to change to a system employing two 0.162-in.-diameter longitudinal wires, with an appropriate reduction in the end-twist-tie and bracket wire diameters.

2. The maximum longitudinal wire forces on either the Memphis or Vicksburg sinking plant are essentially the same and are produced by the angle change associated with the mat traversing the launch finger. The magnitude of this force is about 2.55 kips/wire.

3. One end-twist-tie connection is only about 63 percent as effective as the average of the other two connections.

6 RECOMMENDATIONS

1. Several squares of mat should be placed using only two 0.162-in. diameter longitudinal wires; the existing end-twist-tie wire and the launching operation should be carefully monitored to ascertain if any difficulties are encountered. If no difficulties are encountered, it is recommended that several three-wire squares with 0.141-in. diameter fabric be launched the following season. If this operation is successful, two-wire test squares with 0.141-in. diameter fabric should then be launched.

2. The angle change associated with the launch finger should be reduced to less than about 20° either by changing the radius of the launch finger or retracting the launch finger into the launch plant a greater distance.

3. Further testing and analysis should be performed to achieve a comprehensive understanding of the entire mat system, including launch cables and shore anchors, to determine if materials use and economic benefits can be further optimized.

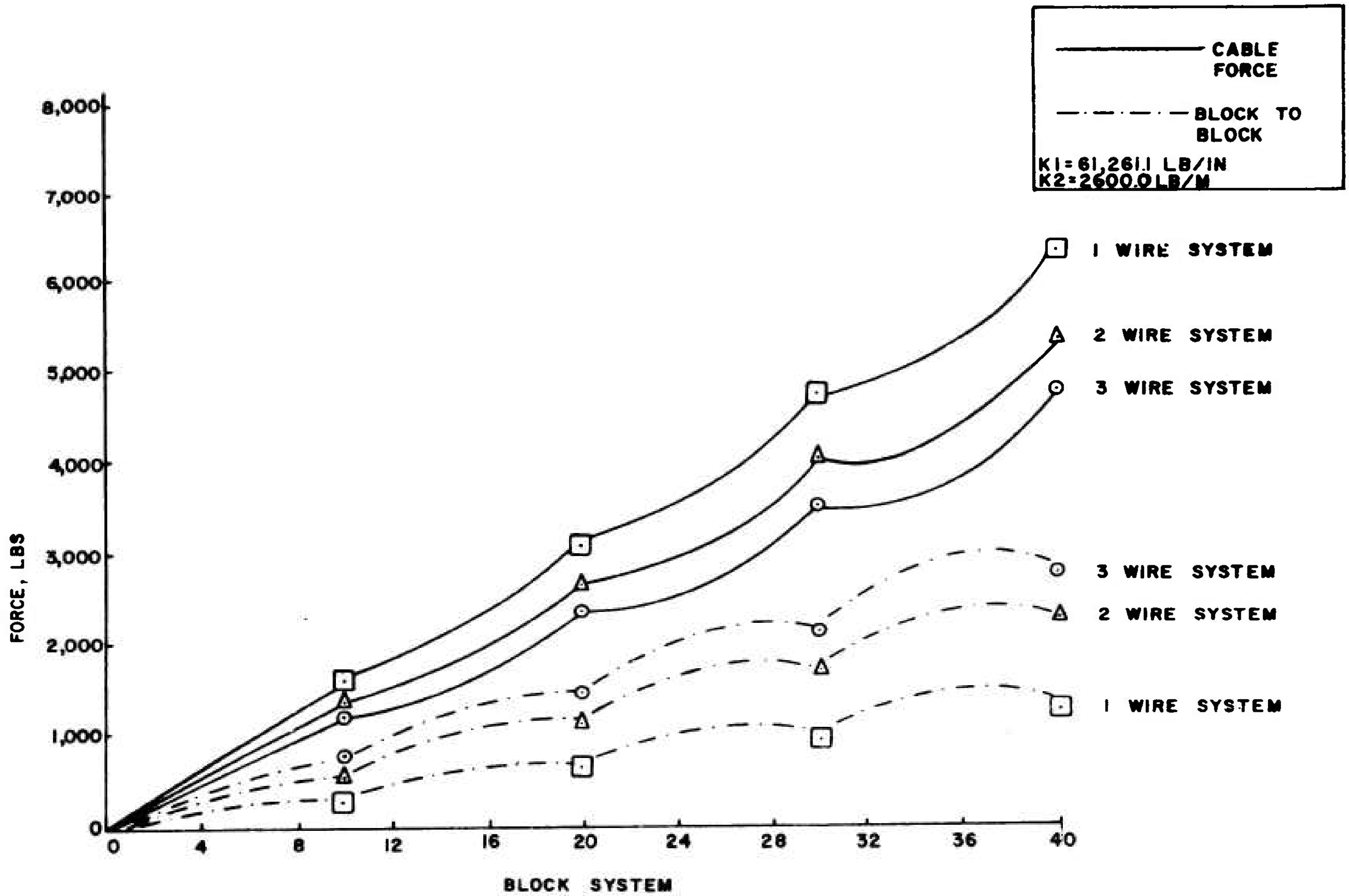

Figure 15. Launch cable, longitudinal wire and end-twist-tie forces for case 1.

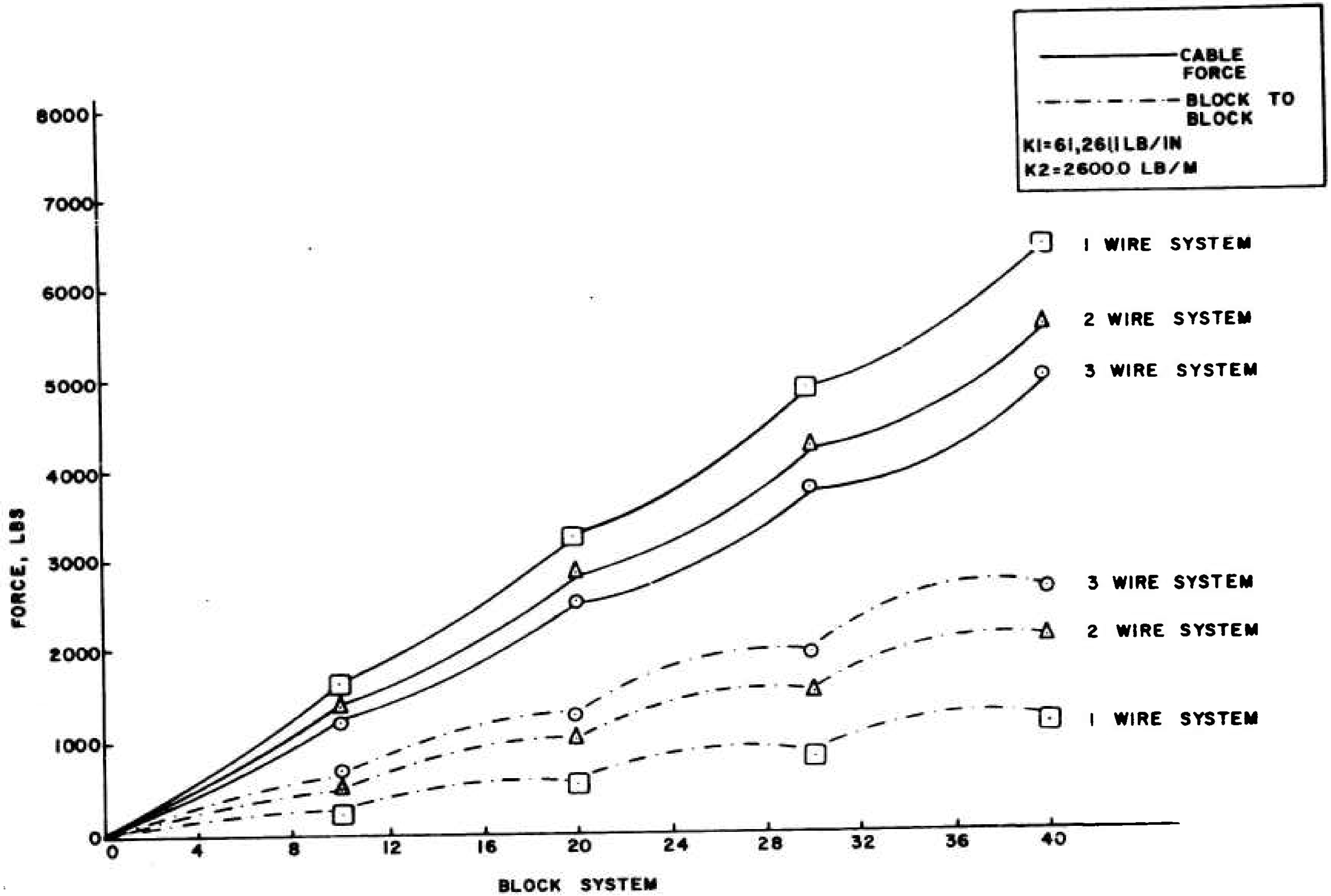

Figure 16. Launch cable, longitudinal wire and end-twist-tie forces for case 2.

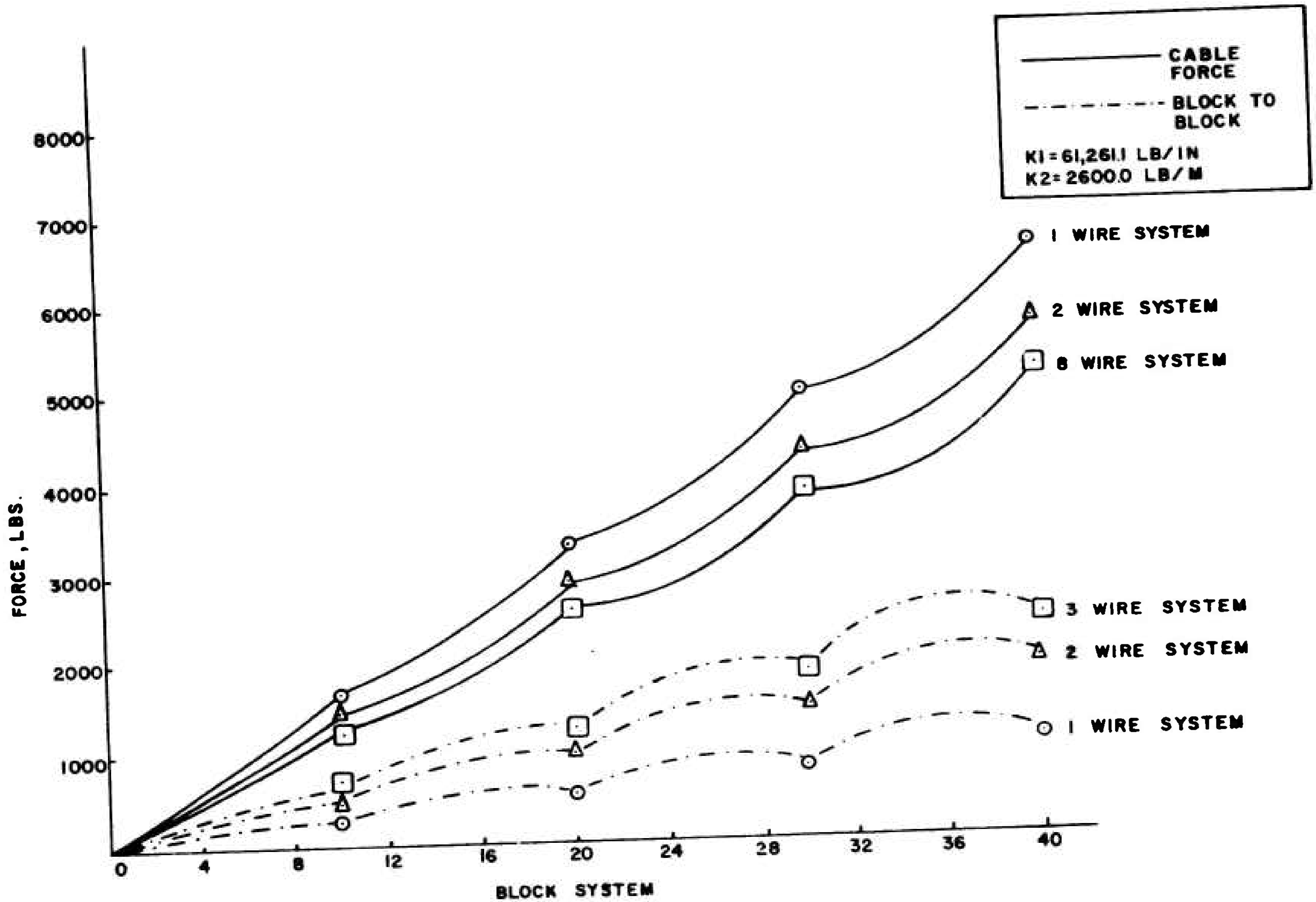

Figure 17. Launch cable, longitudinal wire and end-twist-tie forces for case 3.

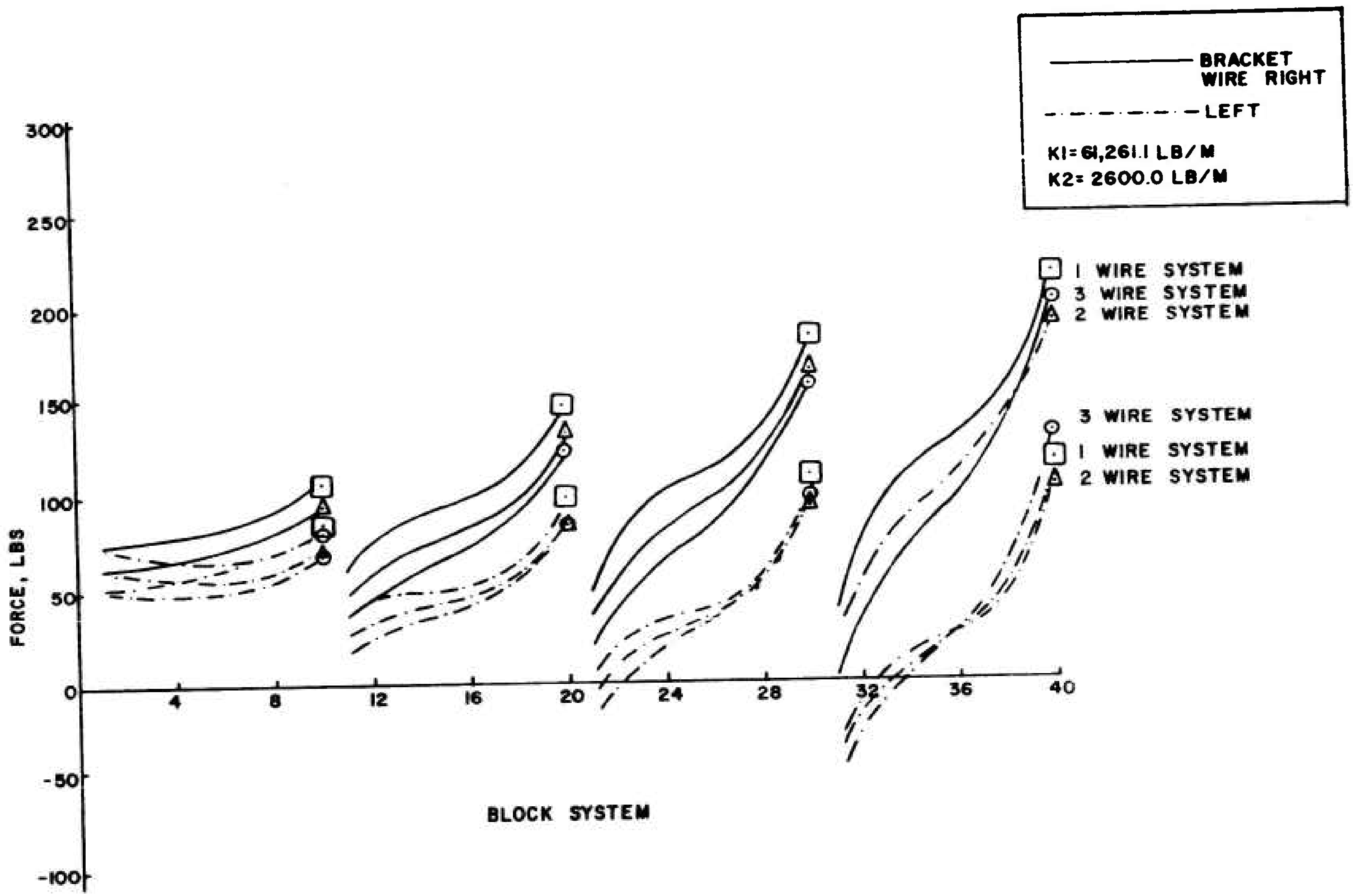

Figure 18. Bracket wire forces for case 1.

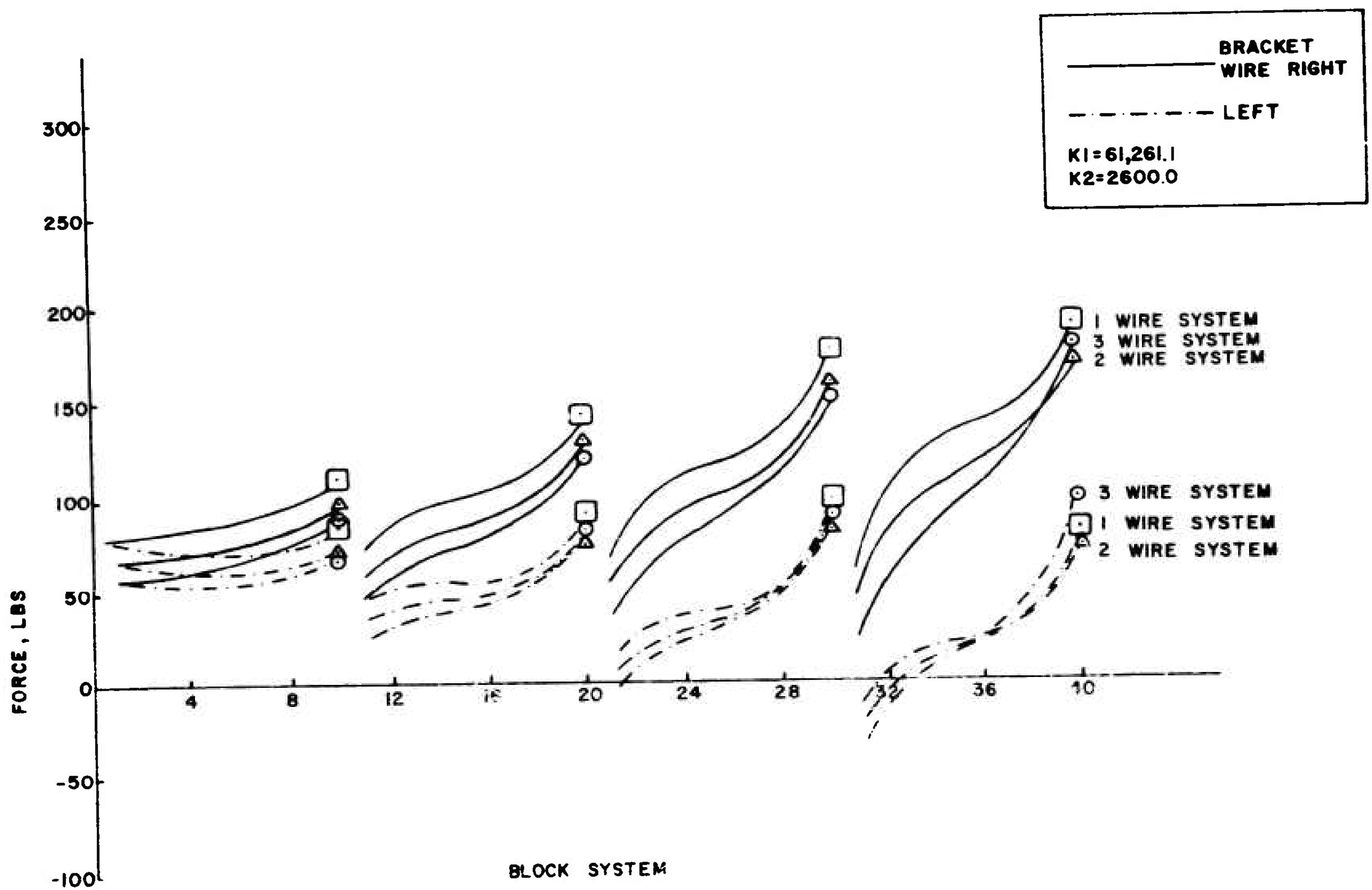

Figure 19. Bracket wire forces for case 2.

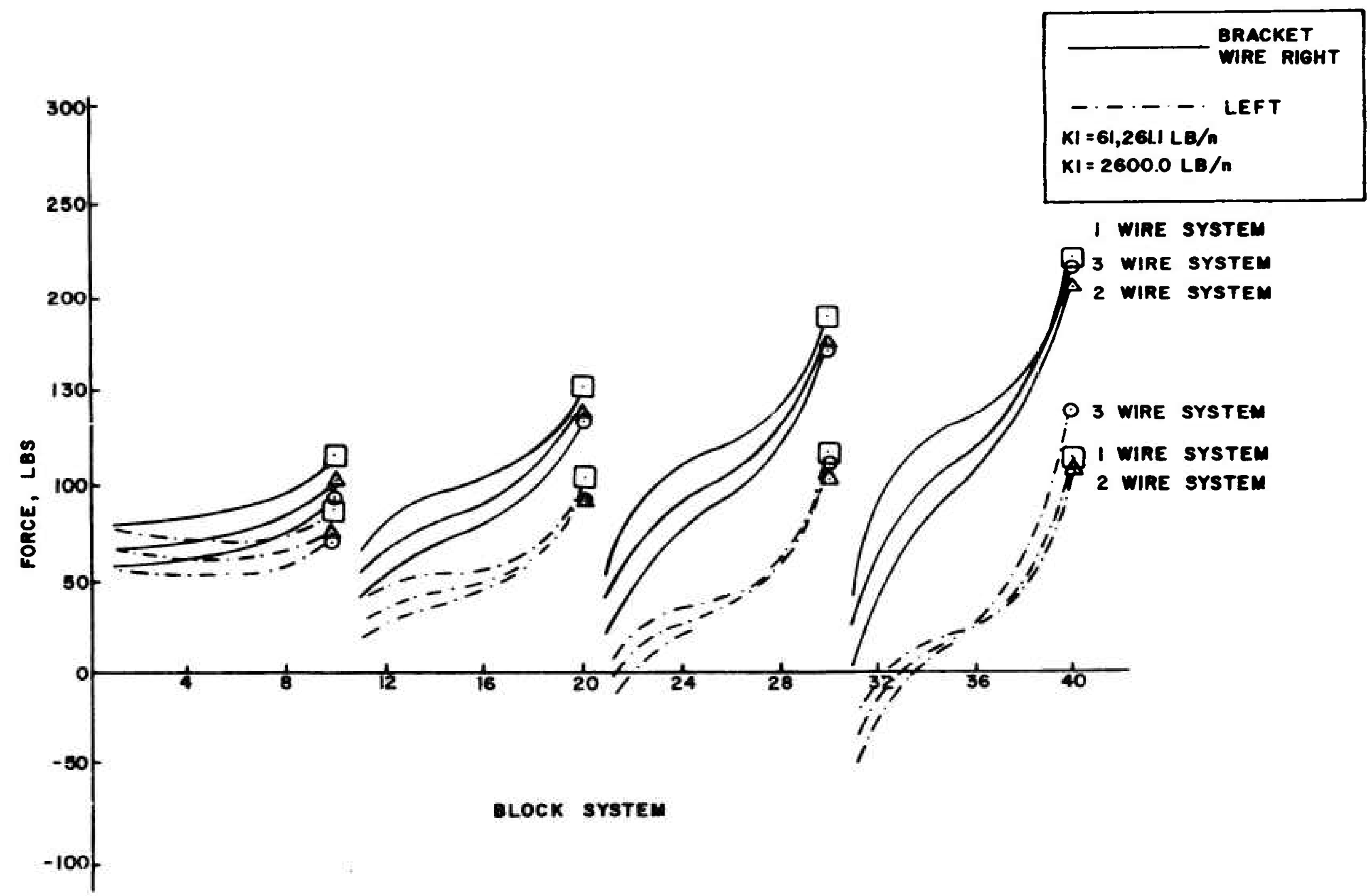

Figure 20. Bracket wire forces for case 3.

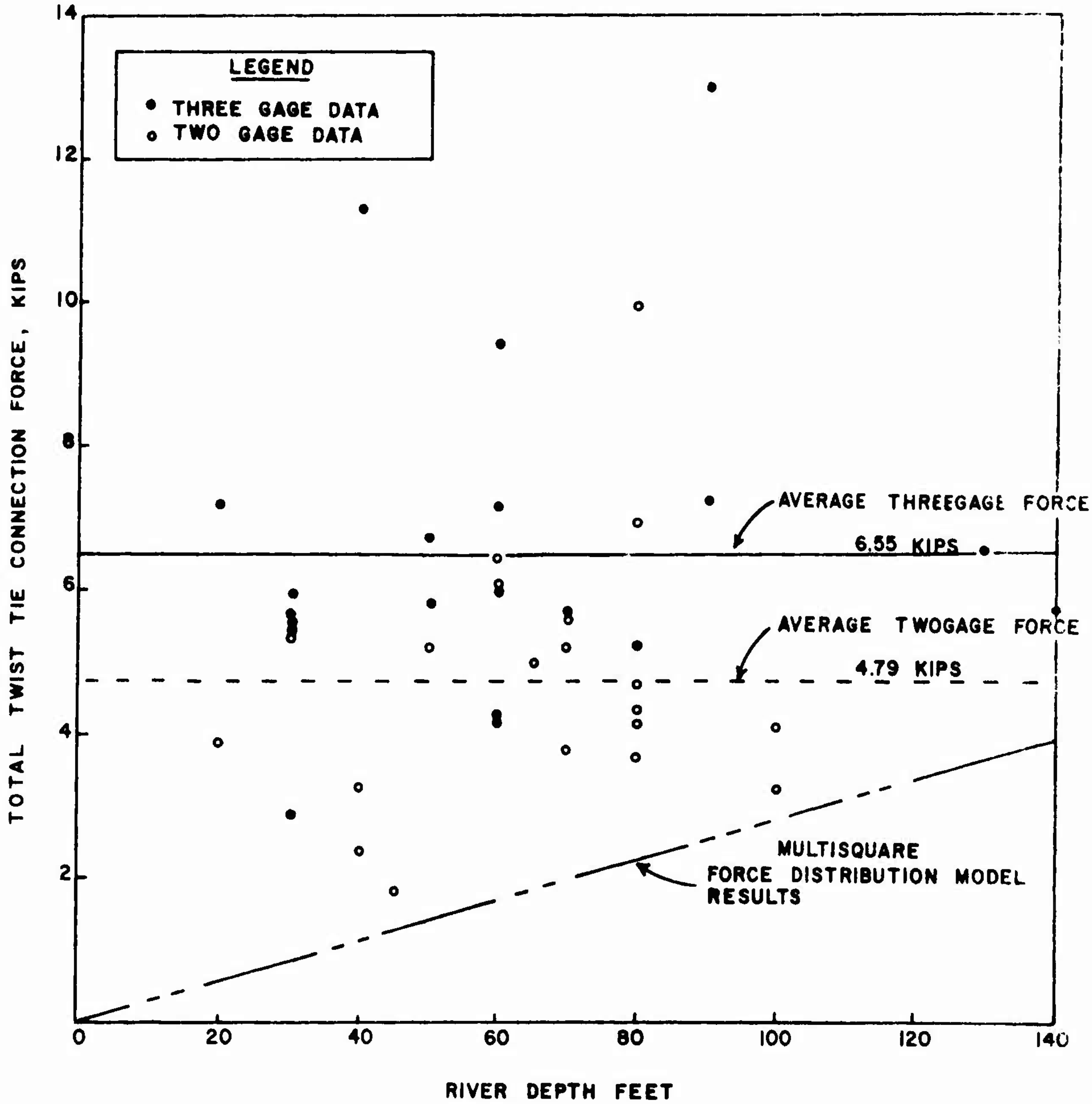

Figure 21. Total end-twist-tie connection vs. river depth.

APPENDIX A: MATTRESS GEOMETRY AND TERMINOLOGY

The mattress configuration used in the field tests is shown in Figures A1 and A2.

The term "square" refers to a basic assembly of twenty 46 1/4 in. x 14 in. concrete blocks cast with corrosion-resistant wire fabric which runs laterally and longitudinally and forms a structure with overall dimensions of 25 ft x 4 ft x 3 in. The lateral wires are referred to as "bracket" wires.

These squares are assembled into an articulated array by connecting the longitudinal end loops (detail B, Fig A2) and the bracket wires (detail S, Fig A1). A pneumatic wrapping tool is used to make the mechanical ties.

The articulated system is assembled on the mat sinking unit to form a mattress which is an array of L x S; L = number of launches (length) and S = number of squares. The term "launch" refers to a row of squares which may be 35 wide.

Figure A3 is an overview of the launch operation, showing the squares connected in the horizontal direction. The water depth and river bottom grade determine the number of launches (length) of a particular mattress.

Launch numbers start at the shore and increase as placement proceeds out into the channel. Square numbers start at the mooring barge (upstream edge extreme left, Figure A3) and increase downstream; square number one is always farthest upstream.

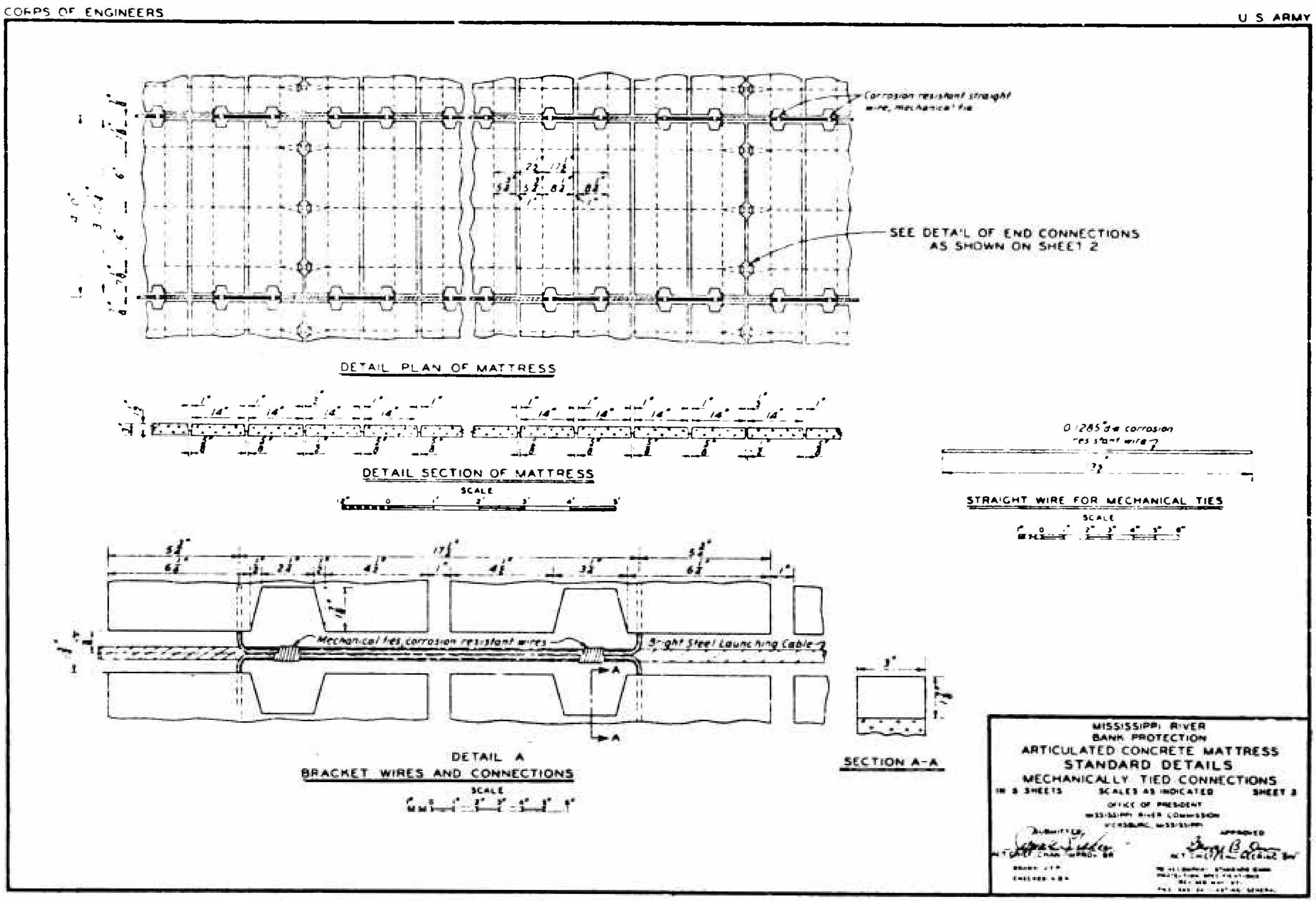

Figure A1. Test mattress and mechanical-manual tie wraps for 20-block square.

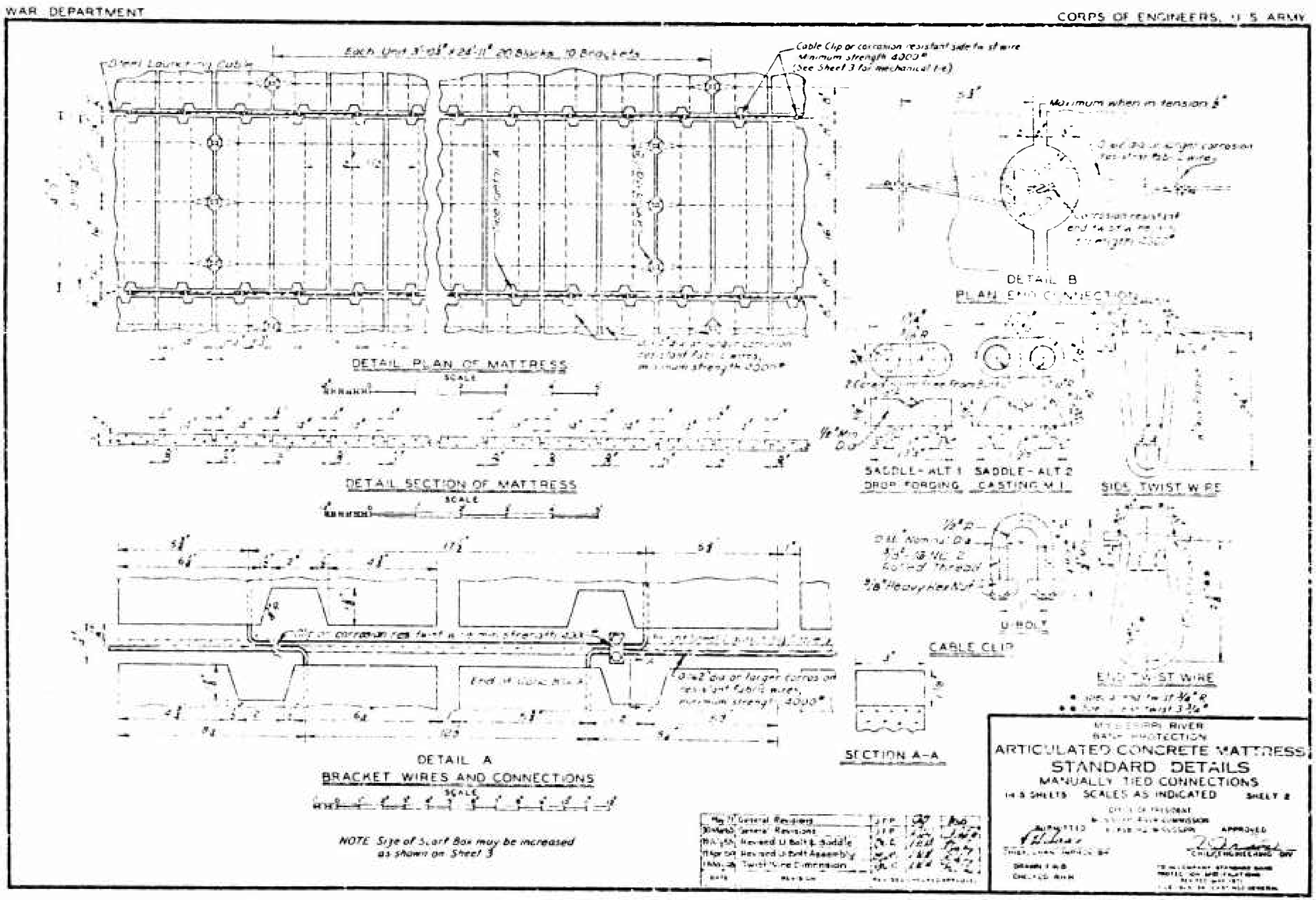

Figure A2. End twist connections for three longitudinal wires.

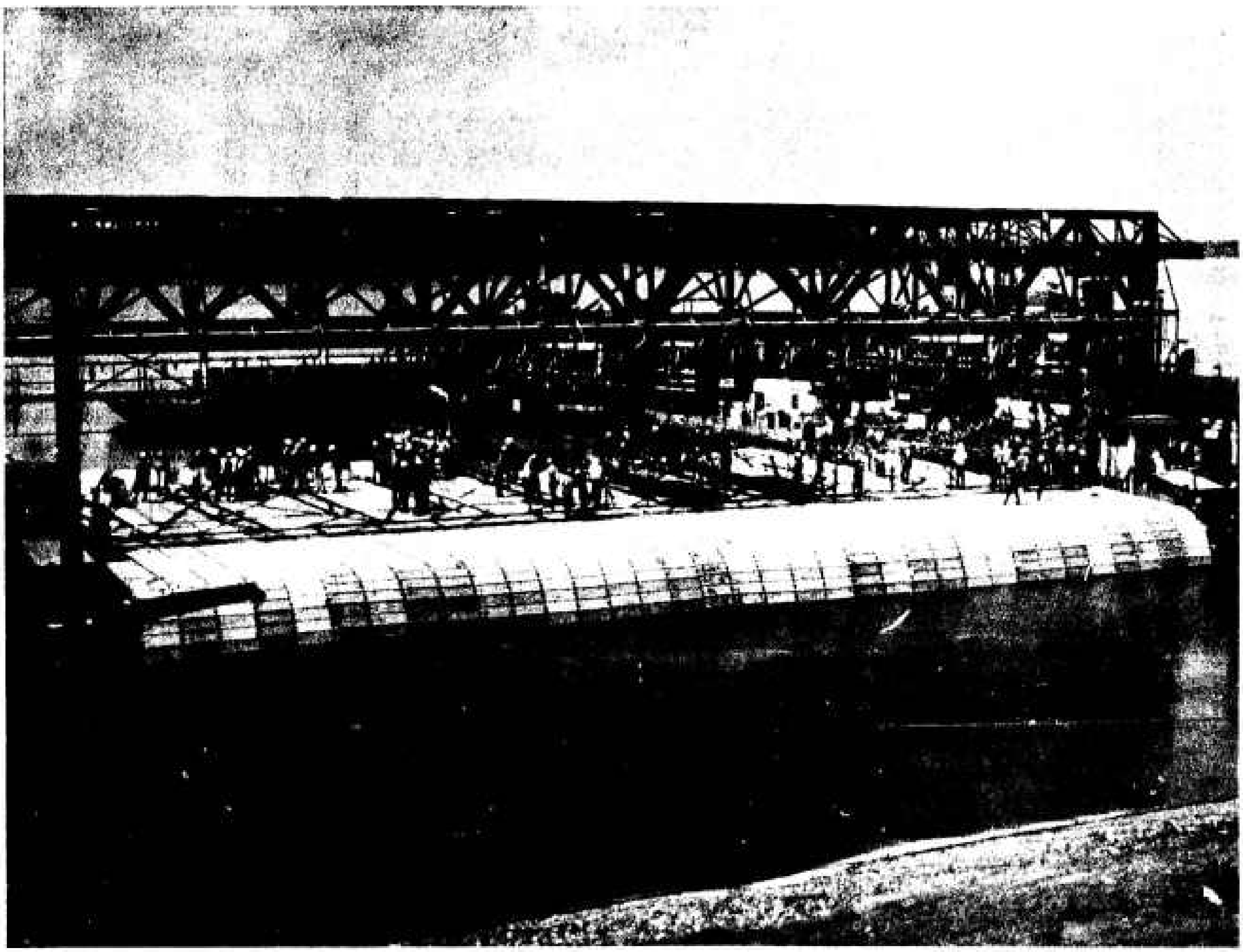

Figure A3. Overview of launch operation.

APPENDIX B: DISCUSSION OF GAGES

CERL began development of the mechanical gage in April 1972, using a nine-square test mat assembled at the laboratory. The prototype gage was tested at Kentucky Point, KY, on 12 September 1972 and was then modified to facilitate field installation.

In operation, the gage is installed in place of the usual mechanical connection at the location on the mat where a force measurement is desired. For bracket wire measurements the wire wrap is replaced with the bracket wire gage; for longitudinal wire measurements the longitudinal gage is installed instead of the longitudinal end-twist-tie link. The wires press against the soft brass beveled-edge "target" as the mat is launched; the depth that the wires penetrate the target is a measure of the maximum force that occurred at that location in the mattress during the launching operation.

Figure B1 shows the gage configuration for longitudinal wire measurements and Figure B2 shows the configuration for bracket wire measurements (the semi-circular notch is to accommodate the launch cable).

The target remains in place until it is retrieved, either while the mat is on the river bottom or at an earlier time. The retrieval mechanism is shown in Figure A3. The assembled gages (Figures B1 and B5) are held together by the "T" link; when this is pulled off by the retrieval line the gage sides swing aside and release the target, which is recovered with the retrieval line.

Gages are calibrated by application of a known force through a wire configuration which reproduces the load geometry occurring on the fabric wire in the mat. The resultant target indentation is optically measured to provide a calibration curve of target indentation versus applied load. The loads are carefully applied to the calibration specimens so that a clear target indentation is obtained.

Indented targets obtained from field tests are measured in the same manner to establish the applied load. The penetration depth is taken as the perpendicular distance of penetration from the undisturbed gage profile line (Figure B4). In the case of light loads, the indentation mark obtained in the field is usually quite clean and appears to be identical to the calibration specimens. Where loads are 3000 lbs or more, however, the targets often have other deformation which results from gage frame distortions as described below.

Accurate measurement with this gage requires a solid supporting frame beneath the target so that the applied forces produce indentation in the knife edges of the target rather than distortion and bending of the target material.

The original gage frame (Figure B5) had a measured load-carrying capability in excess of 3600 lbs for sustained loads. Because of problems installing this gage in the restricted space between squares in the field, the frame was modified in 1972 to permit easier installation. The modification essentially involved changing a bolt hole into a slot so that one side member could be installed after the balance of the frame was in the proper position (Figure B6). This modification weakened the gage frame and consequently reduced the gage capacity for sustained loads. Failure of the gage frame occurred in the slotted section (Figure B7). The results obtained in 1972 and 1973 with both the modified and unmodified gages indicated, however, that the strength of the modified gage was adequate for most of the measurements taken.

It should be stressed, however, that despite the modified gage's reduced load capacity, it provided other valuable information relative to mat behavior. It has been observed in testing under laboratory calibration conditions that there is a finite time of failure of the gage frame at loads which may be as low as 1500 lbs. The slotted hole section deforms relatively slowly; thus, this gage configuration has a certain time-dependency of life and load. If the loads are applied quickly and relieved quickly, the gage is capable of measurements significantly in excess of 1500 lbs. The gage frame capacity under relatively rapid loads has been measured to at least 2400 lbs without frame failure or severe distortion. The maximum load measured with frame failure under particular testing conditions was 2700 lbs. This value, however, should not be taken as a meaningful upper bound in that the load application rate was neither rigorously controlled nor excessively high. Under sustained loads, the gage can be observed to fail quite slowly, in the order of a few seconds. Finally, it should be noted that these effects are not perfectly reproducable. The capacity of the gage is critically dependent on the frame geometry and manufacturing tolerances, because the effective lever system of the gage puts approximately 90 percent of the applied force on the slotted hole. Force on the target is not geometry-dependent.

Gage measurement tabulations have shown that some units indicated loads in excess of the 1500-lb

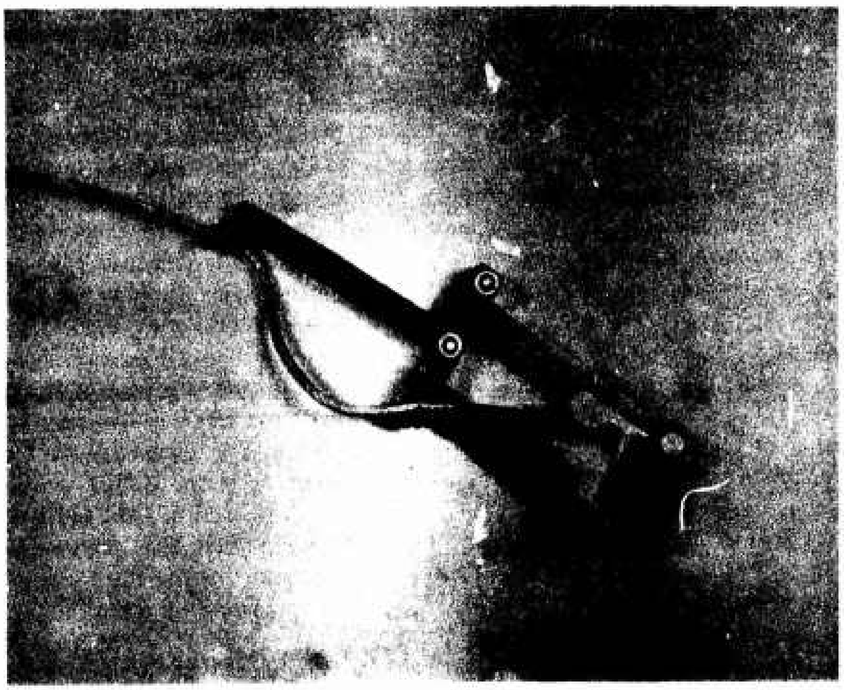

Figure B1. Longitudinal wire gage.

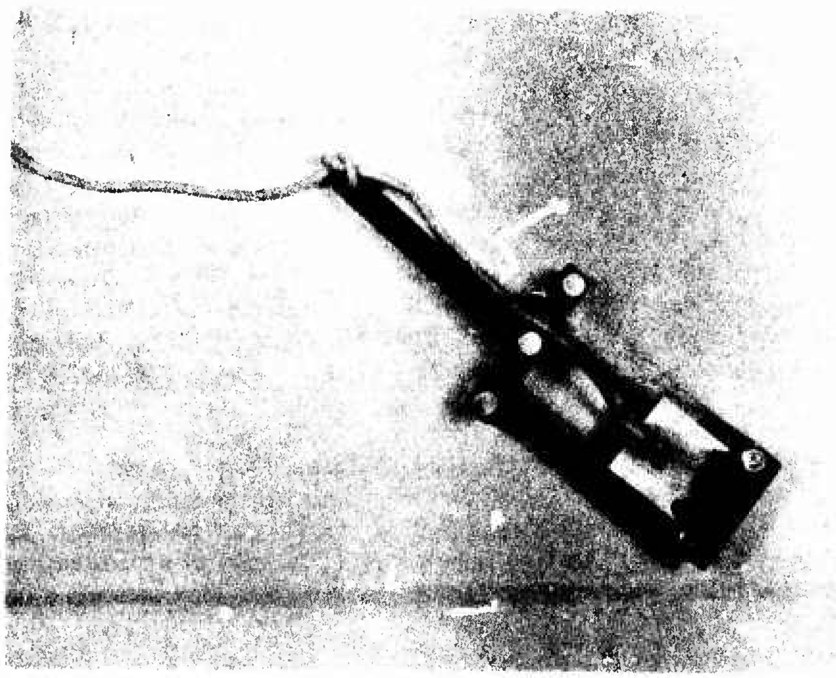

Figure B2. Bracket wire gage.

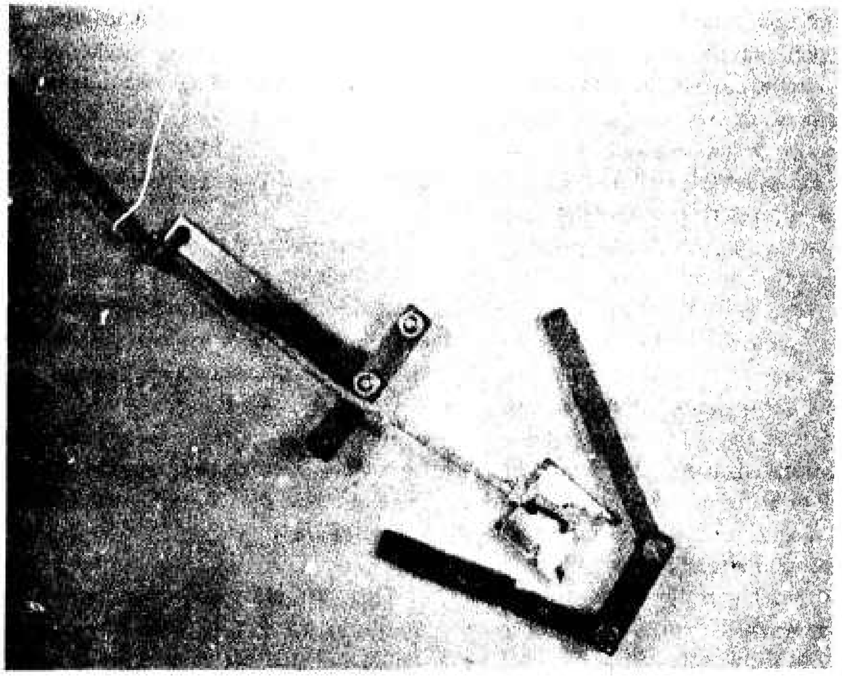

Figure B3. Gage in retrieval mode.

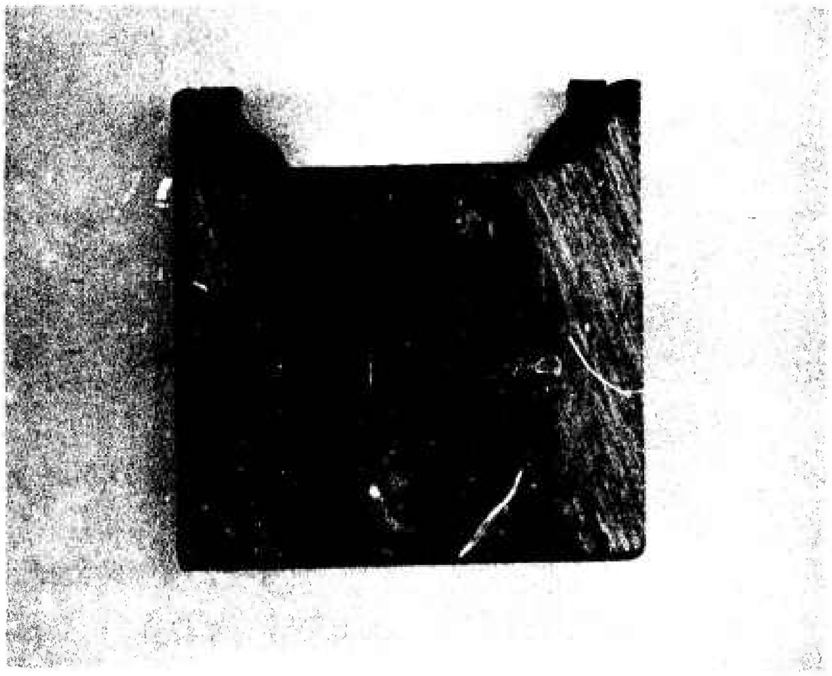

Figure B4. Typical target showin , indentations corresponding to a 2200-lb force.

value—which, if sustained, would have produced gage failure. To better evaluate these readings, the target indentations were read and each target was inspected for deformation of the general shape. Such deformation was observed, primarily in the extremities of the target legs. If the frame fails or is in the process of failing, separation of the target tips or leg ends must occur. As the target tip deforms, the indentations lose their precise calibration because of sheering action and rotational effects of the wire and the change in geometry of the effective target area for the wire.

Since the indentations obtained in field testing were larger than desirable for precise calibration, all targets were inspected for gross deformation of one or both target tip ends. All targets in the 1973 series were also inspected for gross physical distortion of the target, and to determine if one or both tips were deformed. If a single side of the target was deformed and the second side retained its original geometry (Figure B8) it was assumed that the gage at least partially failed, but that during this time the load was still being carried properly by the tip which did not show distortion or bending. The straight tip retained its proper back support and, therefore, the load values determined from it should be valid. If gross gage failure occurred, due either to extremely high or sustained loads, then both tips would be significantly distorted upon total failure of the frame, since both would lose their back support. These effects have been verified in the laboratory. As described earlier, the target condition after recovery indicated the validity of the load values.

In summary, one can reasonably accept those values shown where at least one leg of the target remained straight or was deformed minimally. When both legs were severely bent and/or the target was badly deformed, the results are questionable.

In cases where only one leg was deformed while the other remained straight, one can conclude that the indicated loads did, indeed, exist long enough to cause frame failure.

There are also cases where loads of significant magnitude (3 to 4 kips) were measured, but gage frame failure did not occur. It must be assumed that these were short-duration loads.

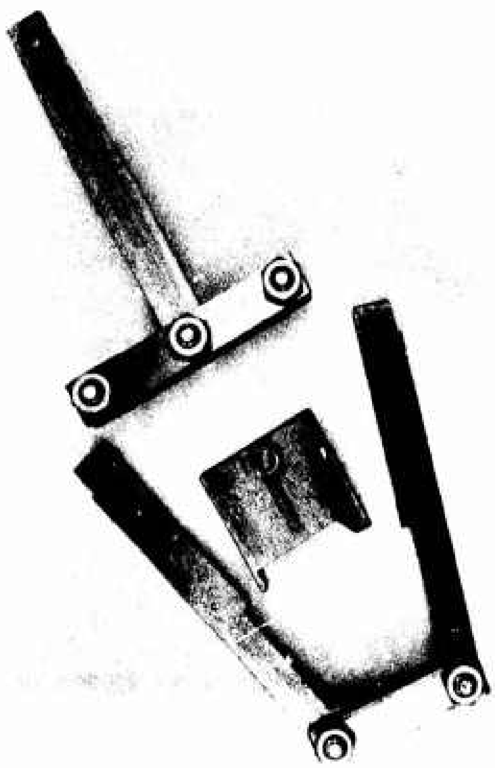

Figure B5. Original gage frame.

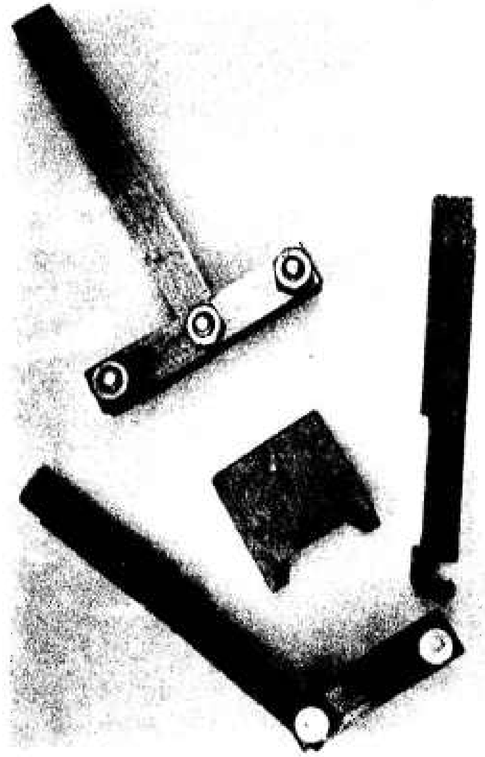

Figure B6. Modified gage frame slotted frame member.

Figure B7. Gage frame failure at slotted section.

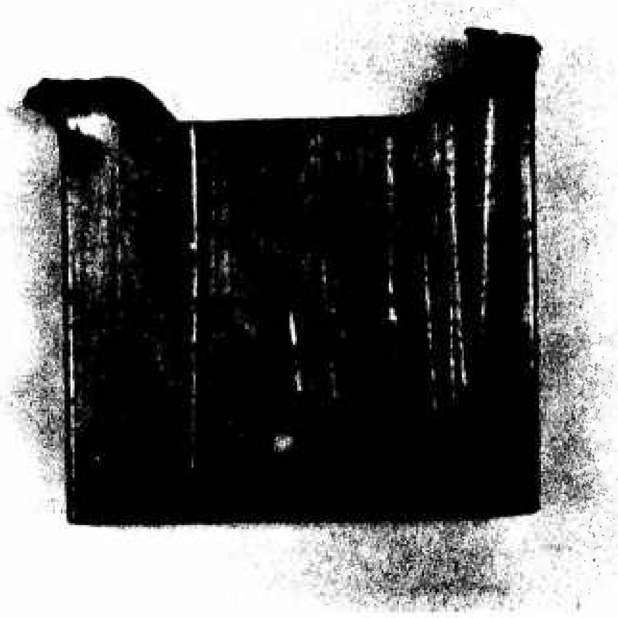

Figure B8. Target from failed gage frame–indentation on the right side acceptable.

APPENDIX C: MATTRESS INSTRUMENT LOCATION CHARTS

Location: BURNSIDE, LA. Date: 19 OCT 73

Remarks: MAT #20
BRACKET WIRE GAGES

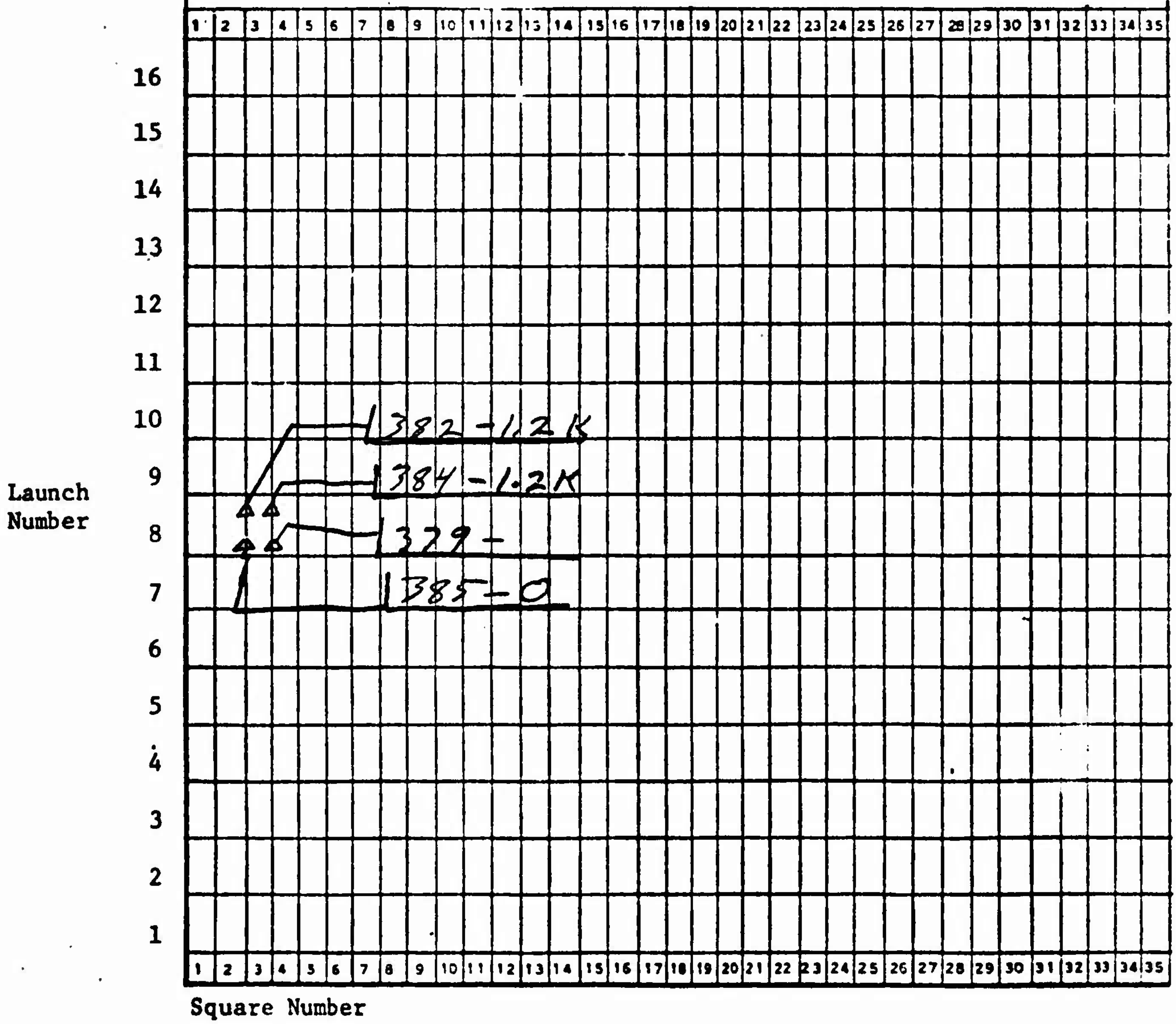

MATTRESS INSTRUMENT LOCATION CHART

Location: *BURNSIDE, LA.* Date: *19 OCT 73*

Remarks: *MAT # 23*

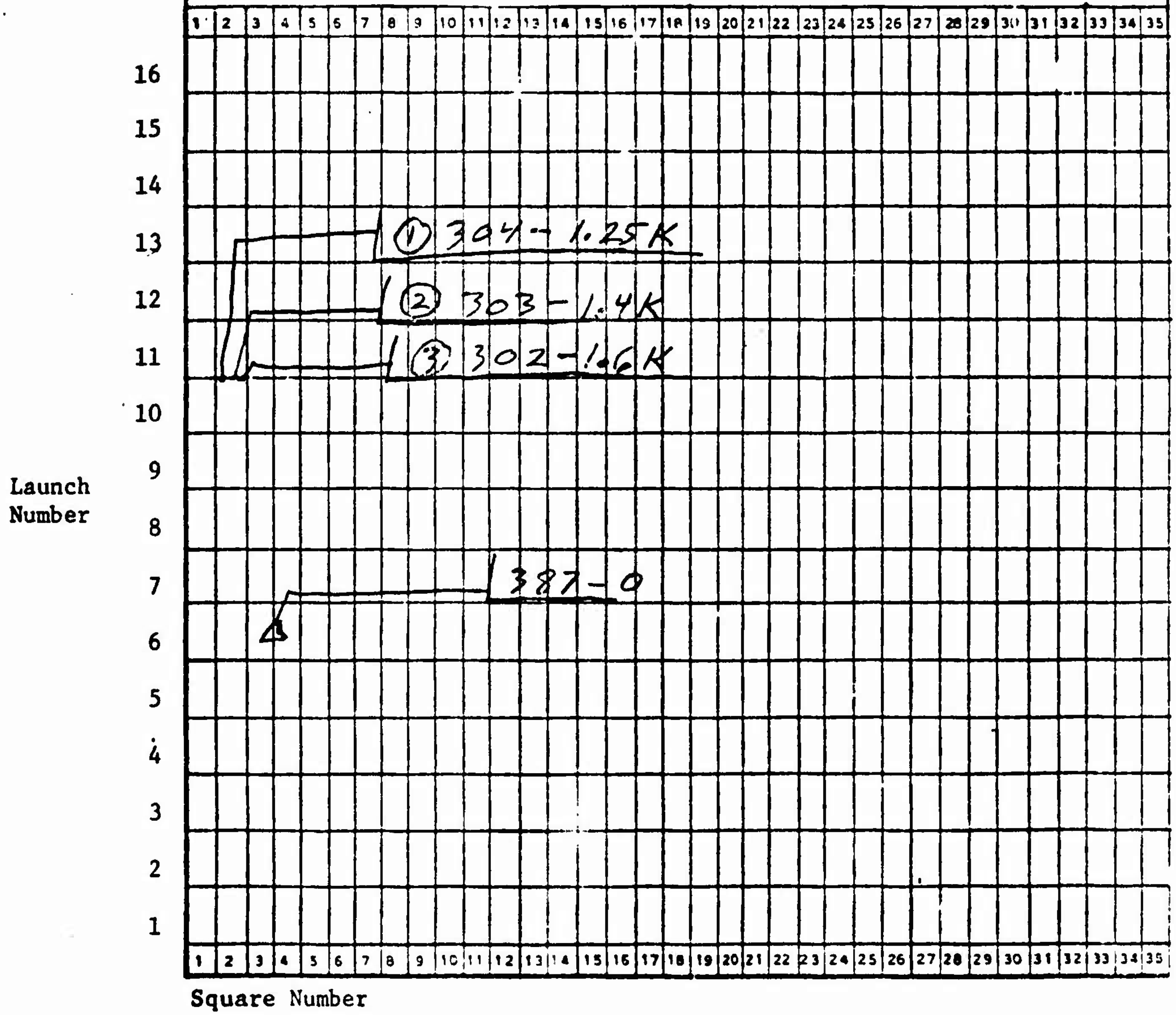

MATTRESS INSTRUMENT LOCATION CHART

Location: MARCHANT, LA.   Date: 22 OCT 73

Remarks: MAT #15

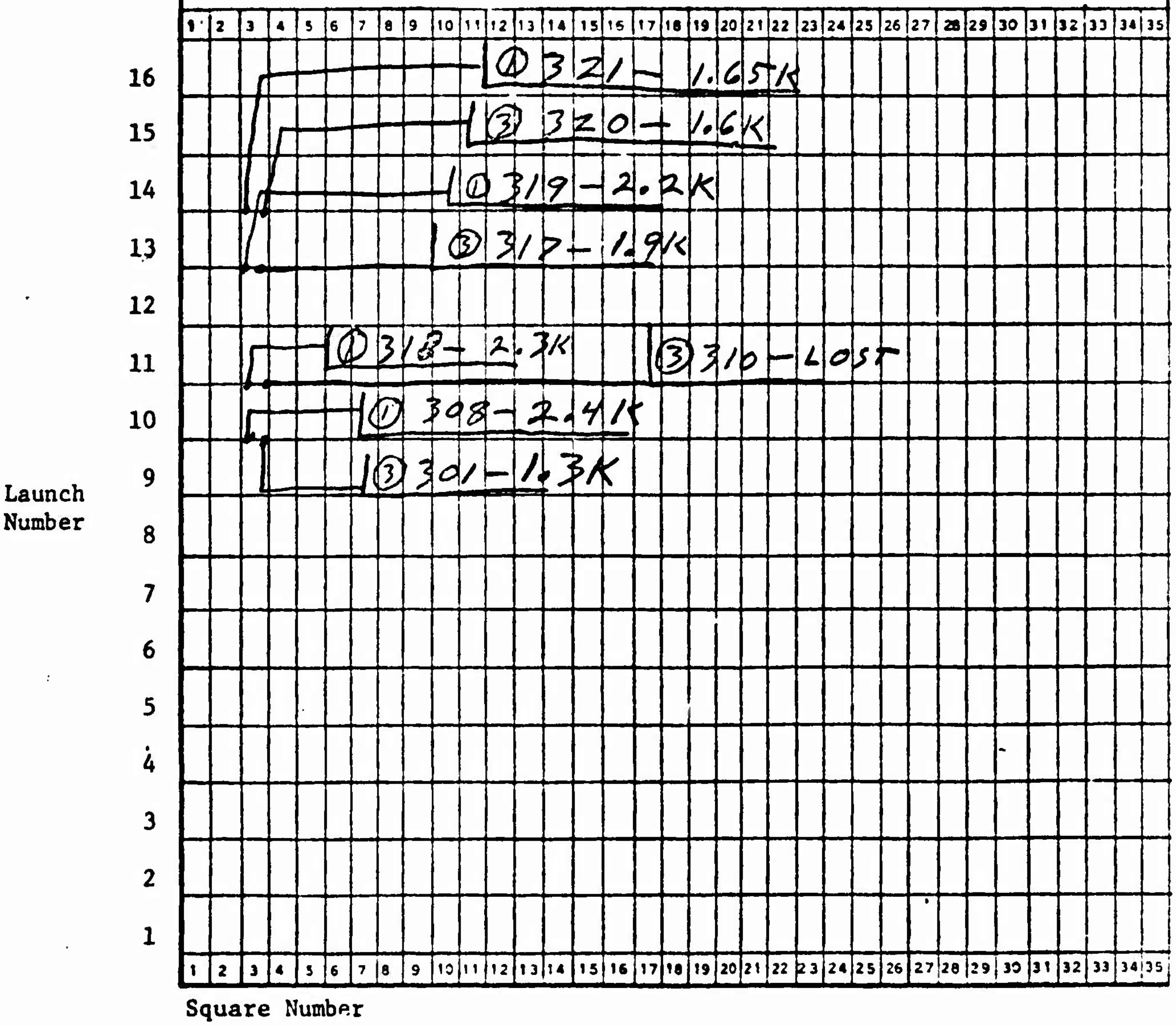

MATTRESS INSTRUMENT LOCATION CHART

Location: MARCHANT, LA.

Date: 22 OCT 73

Remarks: MAT #16

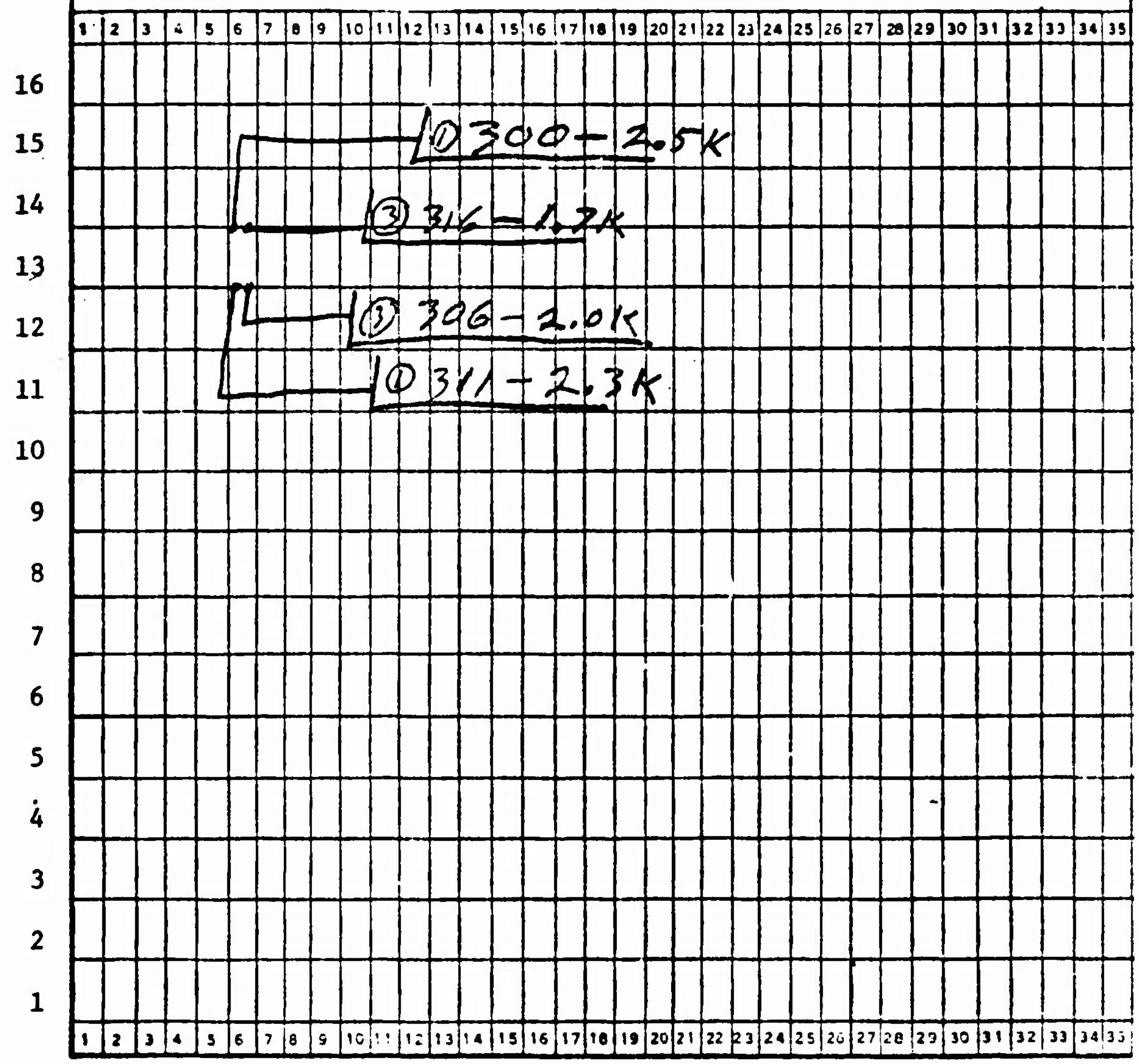

Launch Number

Square Number

MATTRESS INSTRUMENT LOCATION CHART

Location: MARCHANT, LA. Date: 22 OCT 73

Remarks: MAT # 17

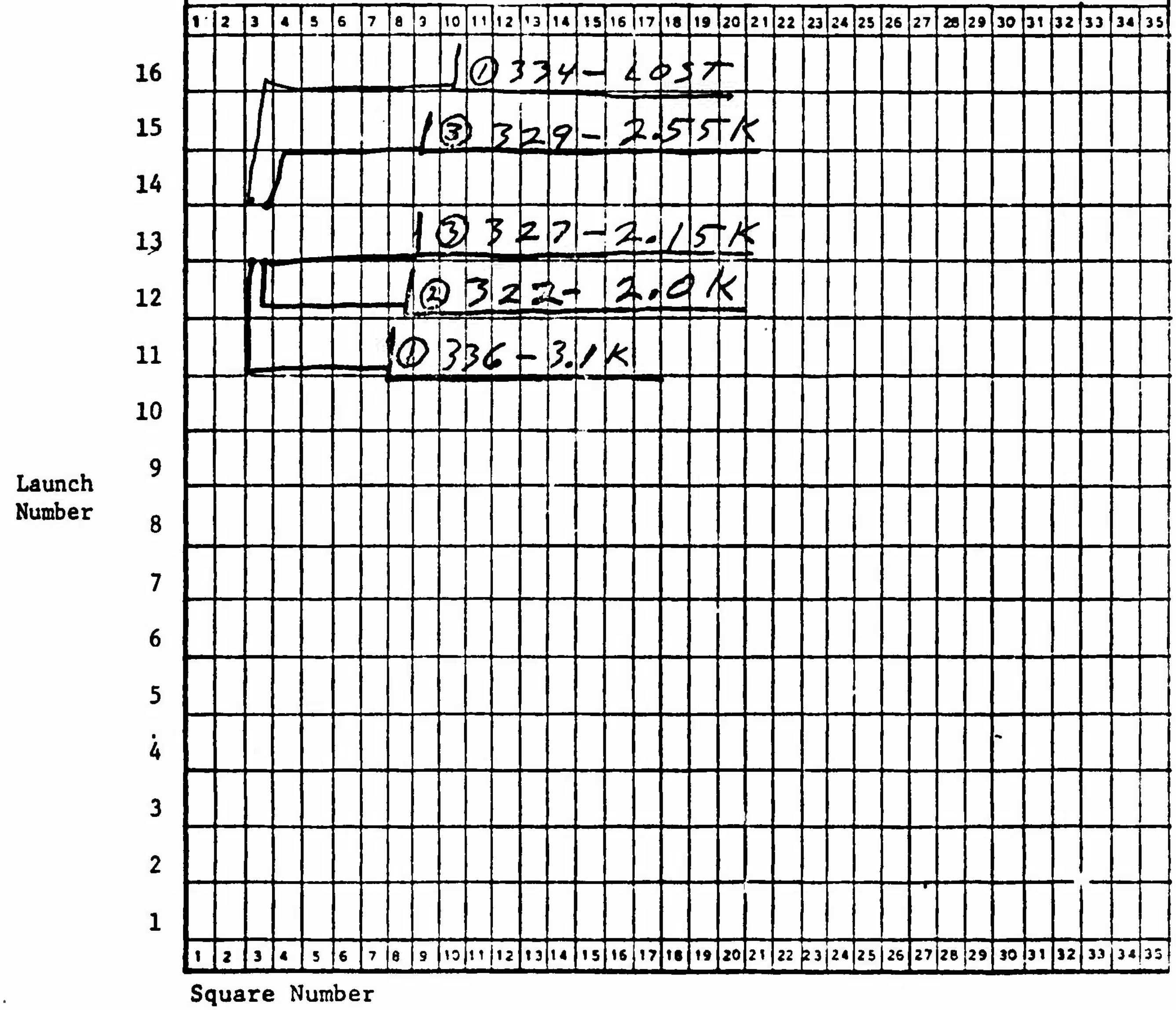

MATTRESS INSTRUMENT LOCATION CHART

Location: MARCHANT, LA. Date: 21 OCT 73

Remarks: MAT #9

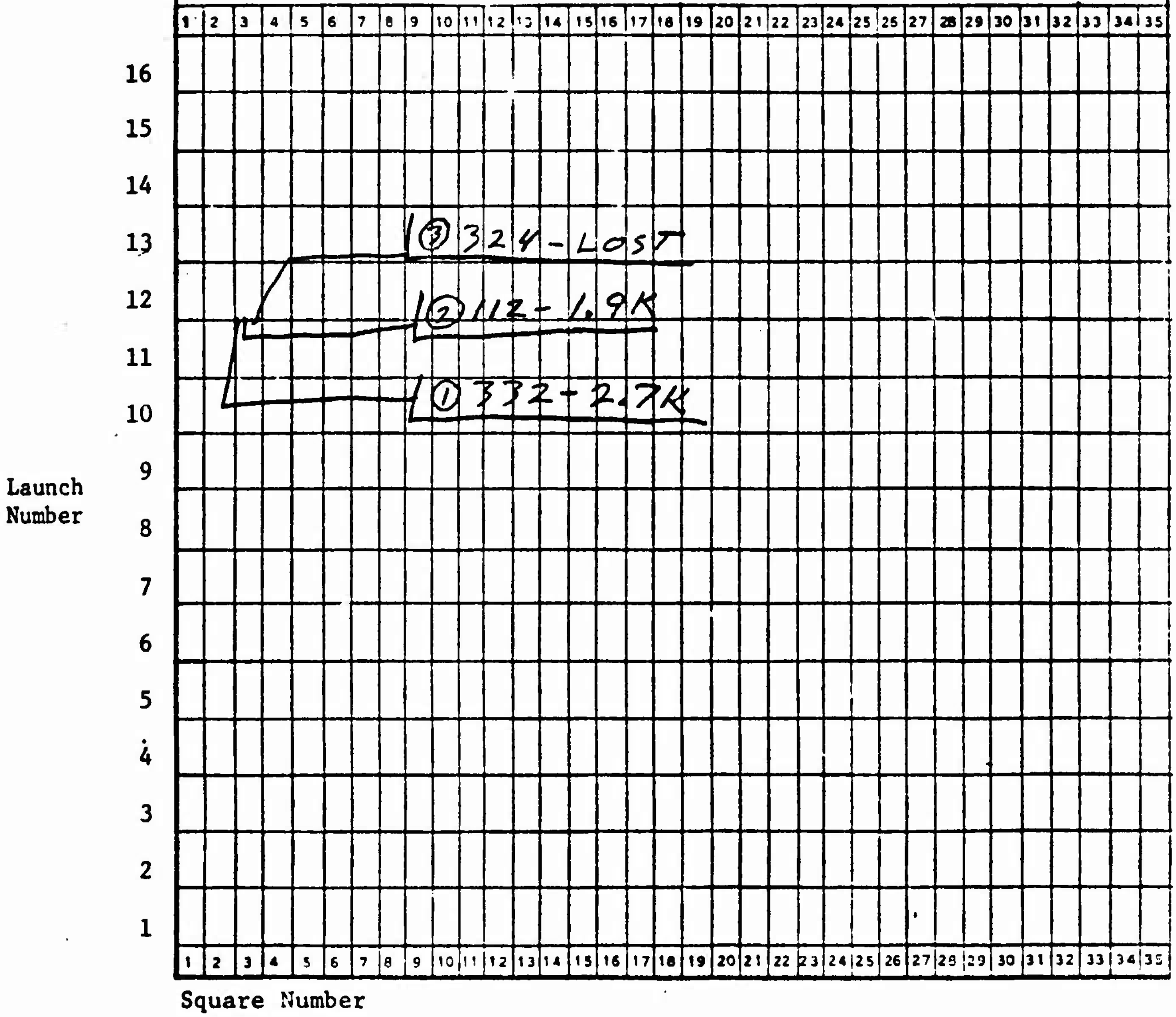

MATTRESS INSTRUMENT LOCATION CHART

Location: PLAQUEMINE, LA. Date: 24 OCT 73

Remarks: MAT #10

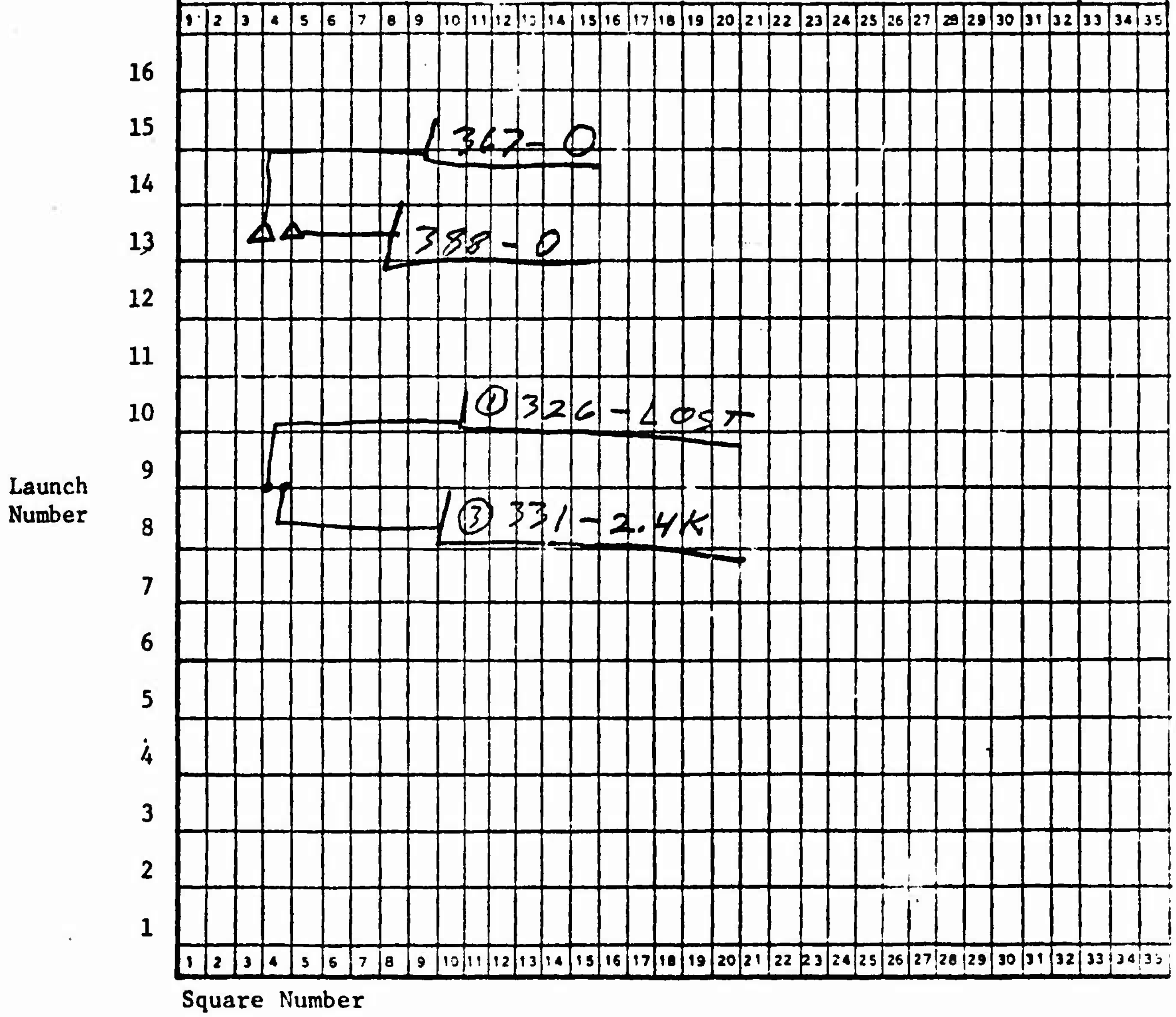

MATTRESS INSTRUMENT LOCATION CHART

Location: ALLENDALE, LA.   Date: 25 OCT 73

Remarks: MAT #1; WATER 130 FT. DEEP
LAUNCH CABLES 4 & 5 BROKE
WHILE THESE GAGES WERE
IN PLACE

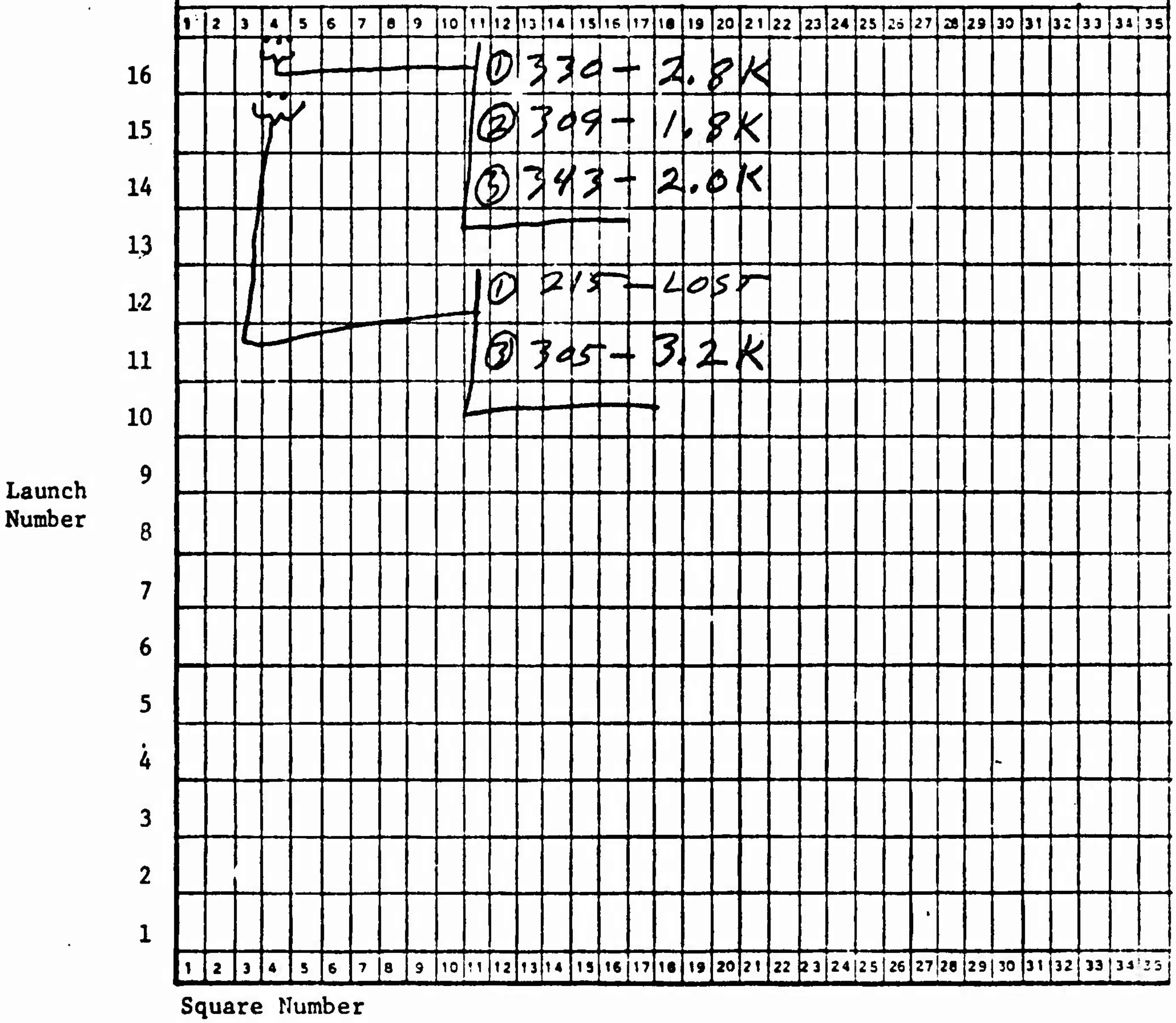

MATTRESS INSTRUMENT LOCATION CHART

Location: ALLENDALE, LA. Date: 26 OCT 73

Remarks: MAT #7, WATER 150 FT. DEEP
18 LAUNCHES, TWO SHORE TIE OFF
CABLES BROKE DURING LAUNCH OF THIS
MAT, ALSO, HAD AN "AUTOMATIC CUT-OFF".
GAGE #241 WAS ACCIDENTALY KICKED
AND FELL APART AT EDGE OF PLANT.
CENTER LOGITUDINAL WIRE CUT BETWEEN BLOCK
19&20 OF LAUNCH 16 SQUARE 8

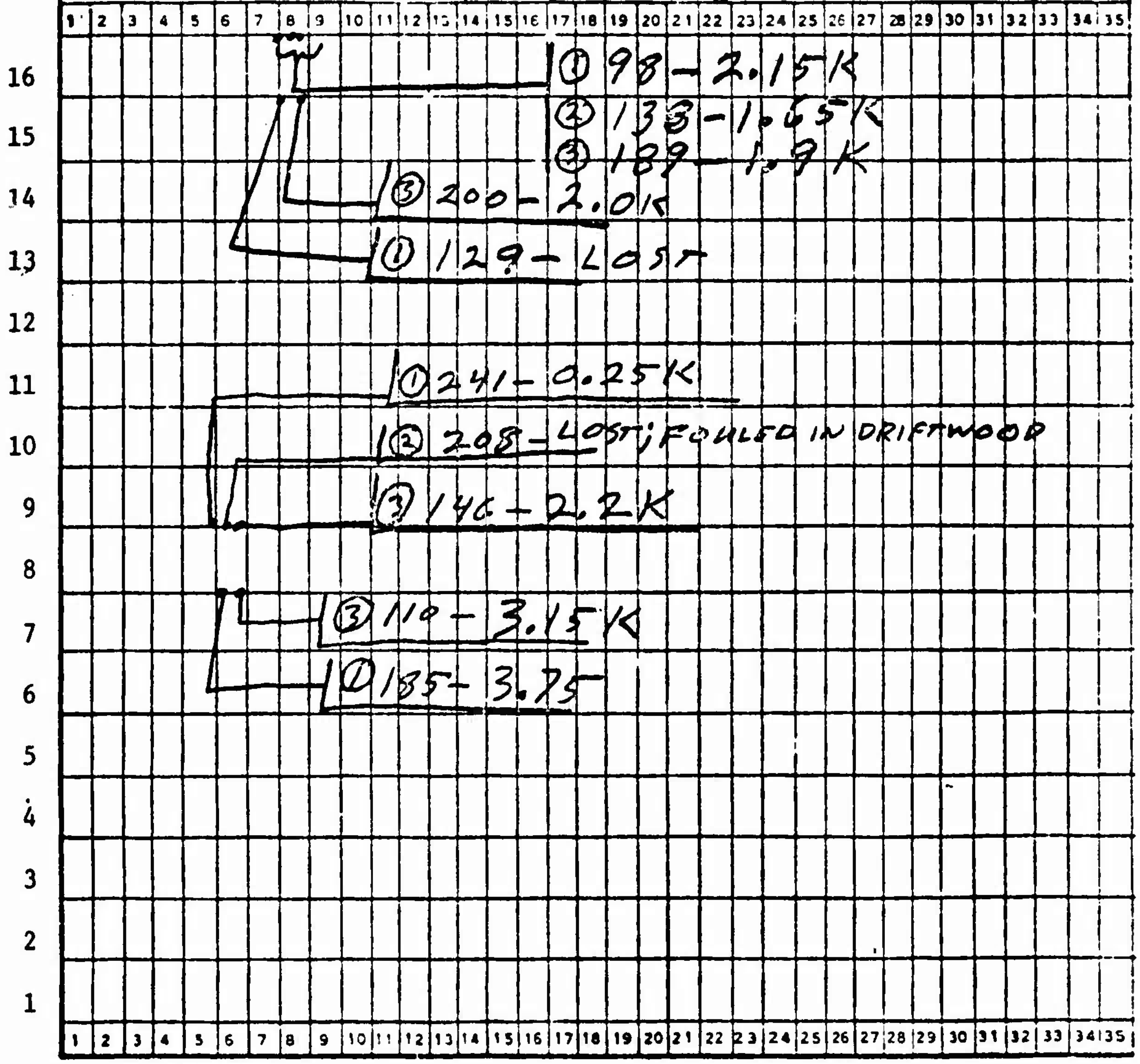

MATTRESS INSTRUMENT LOCATION CHART

Location: ALLENDALE, LA.   Date: 26 OCT 73

Remarks: MAT #8

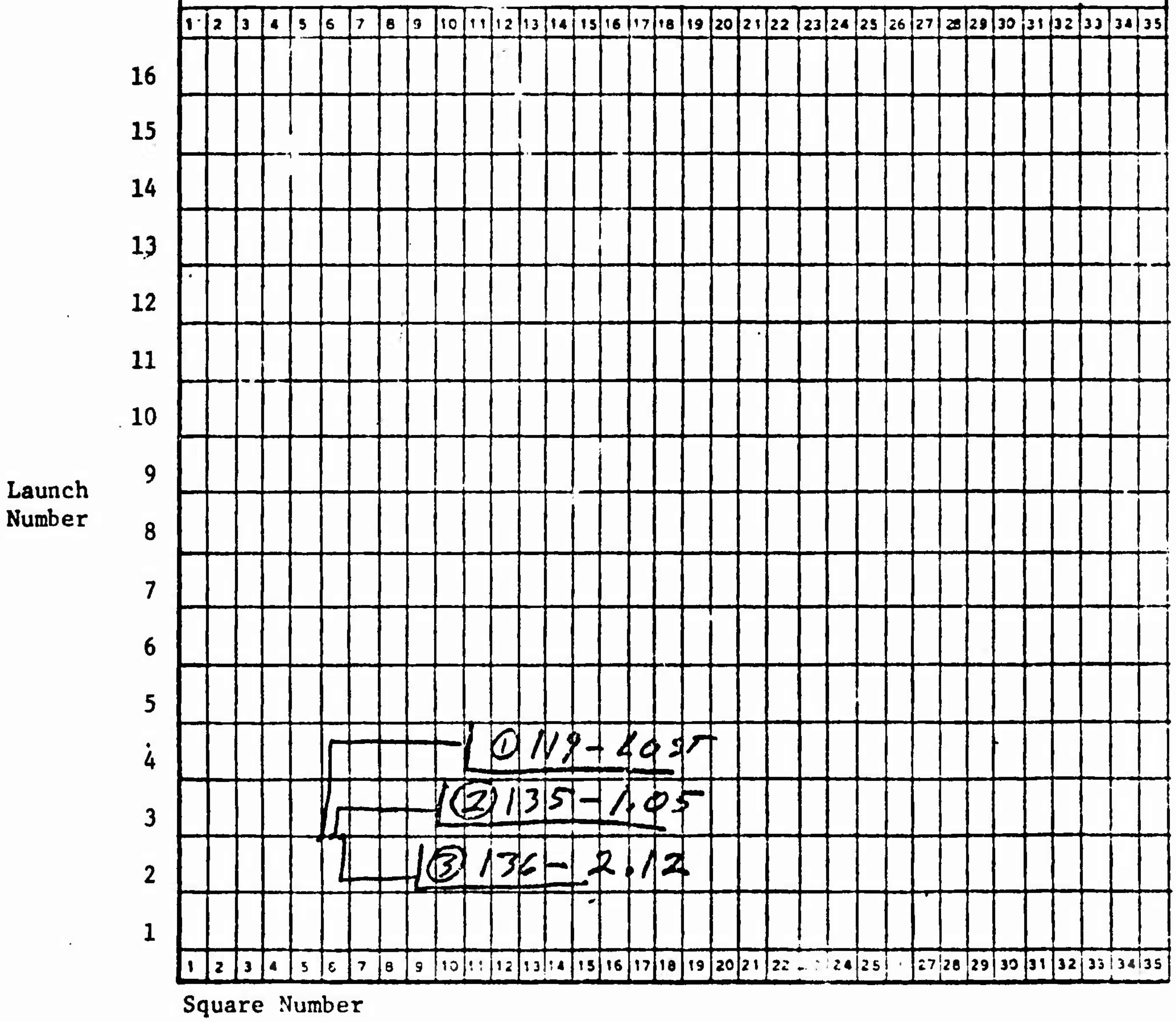

MATTRESS INSTRUMENT LOCATION CHART

Location: MARCHANT, LA.

Date: 21 OCT 73

Remarks: MAT #9

BRACKET WIRE GAGE

Launch Number	1	2	3	4	5	6	7	8	9	10	11	12	13	14	15	16	17	18	19	20	21	22	23	24	25	26	27	28	29	30	31	32	33	34	35
16																																			
15																																			
14																																			
13																																			
12																																			
11																																			
10																																			
9																																			
8																																			
7	△						370-0																												
6																																			
5																																			
4																																			
3																																			
2																																			
1																																			

Square Number

MATTRESS INSTRUMENT LOCATION CHART

Location: BALESHED, MS. Date: 7NOV73

Remarks: MAT #5

ALL LONGITUDINAL WIRES WERE CUT AT THE END BLOCKS BETWEEN LAUNCH 8 & 9

ONLY THE CENTER LONGITUDINAL WIRE WAS CUT AT THE END BLOCKS BETWEEN LAUNCH 10 & 11

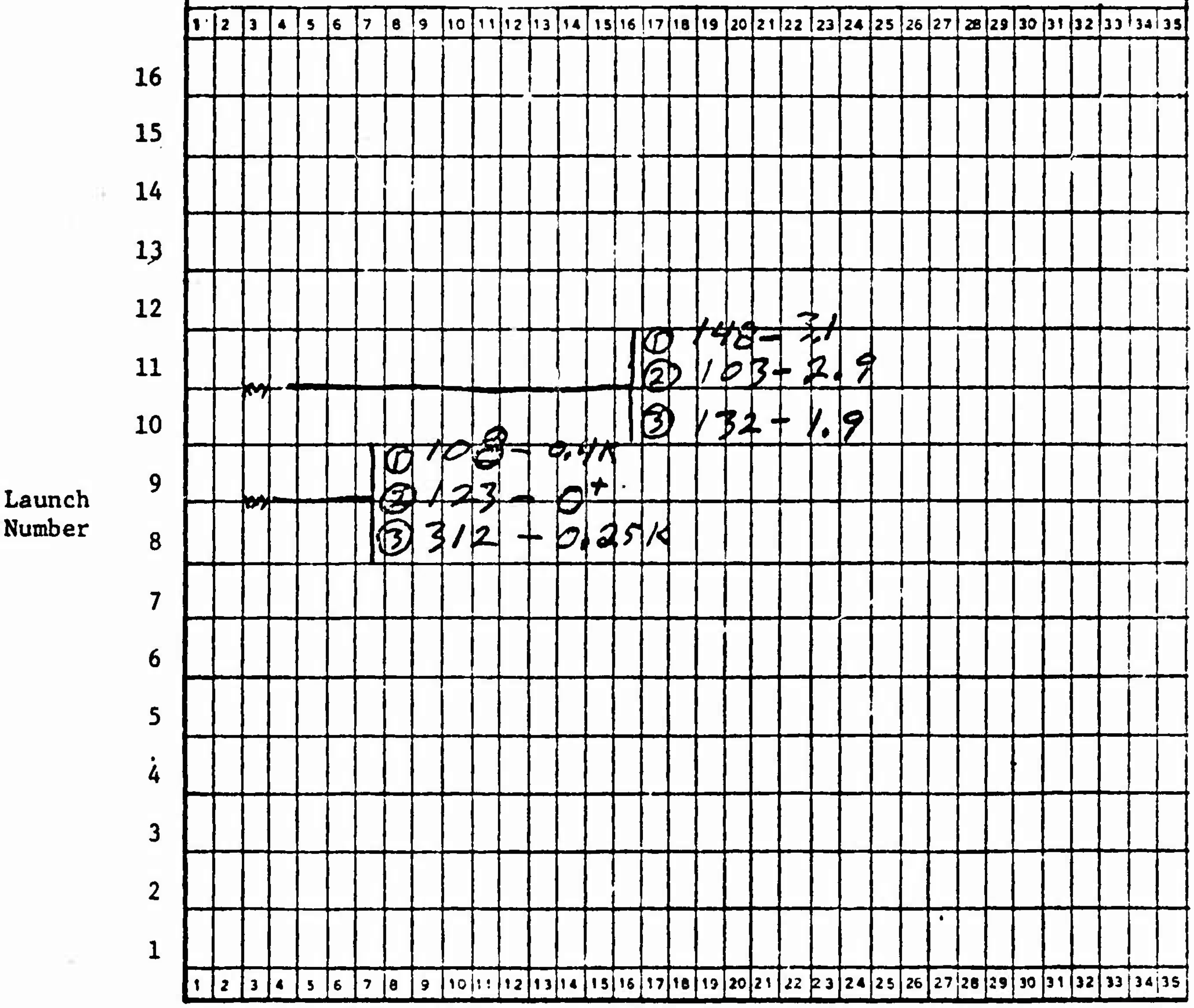

Square Number

MATTRESS INSTRUMENT LOCATION CHART

Location: BALESHED, MS Date: 7NOV73

Remarks: MAT #6

ONLY THE CENTER LONGITUDINAL WIRE WAS CUT AT THE END BLOCKS BETWEEN LAUNCH 4 & 5

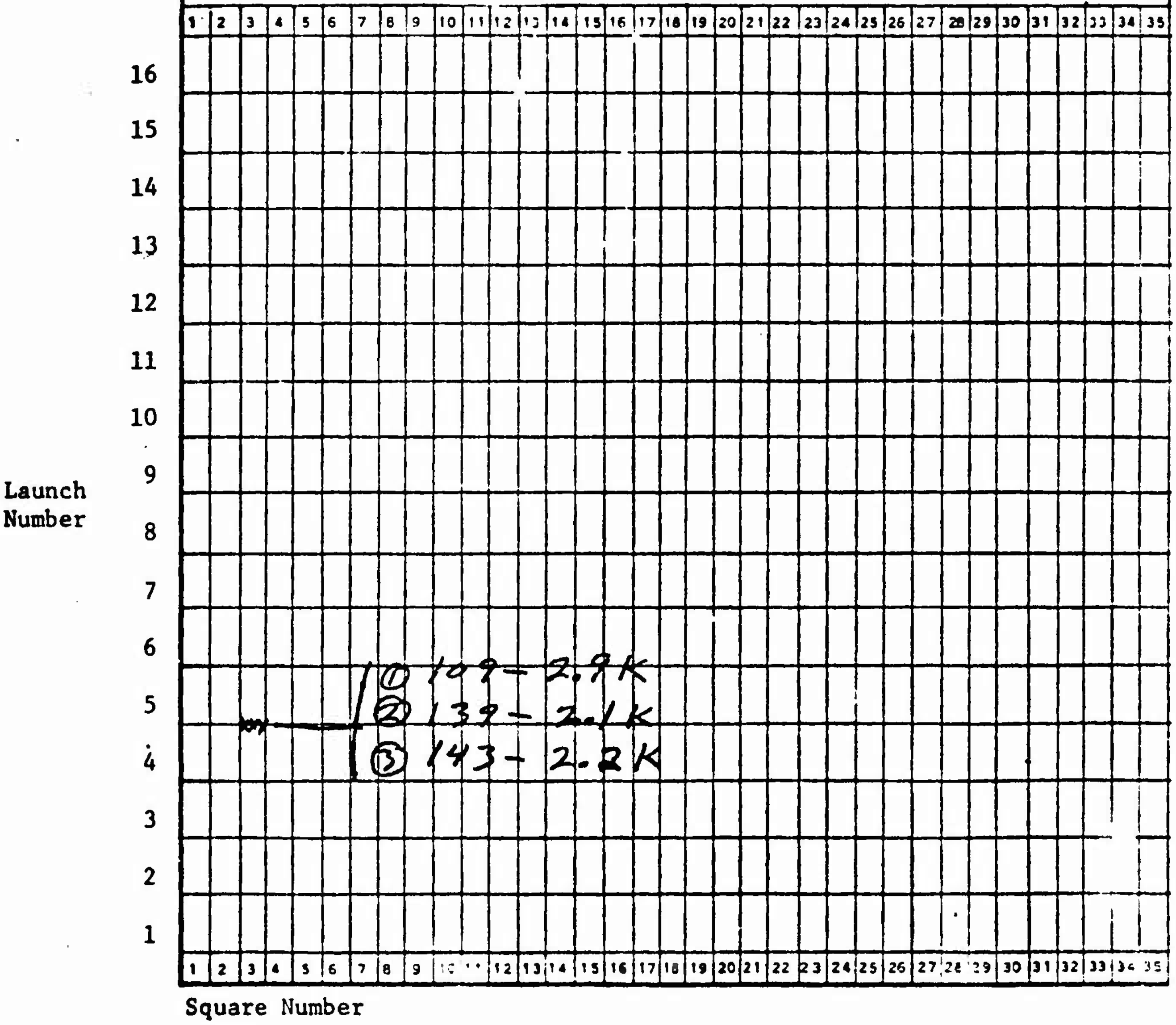

MATTRESS INSTRUMENT LOCATION CHART

Location: COOCHIE, LA. Date: 12 NOV 73

Remarks: MAT #12

Launch Number

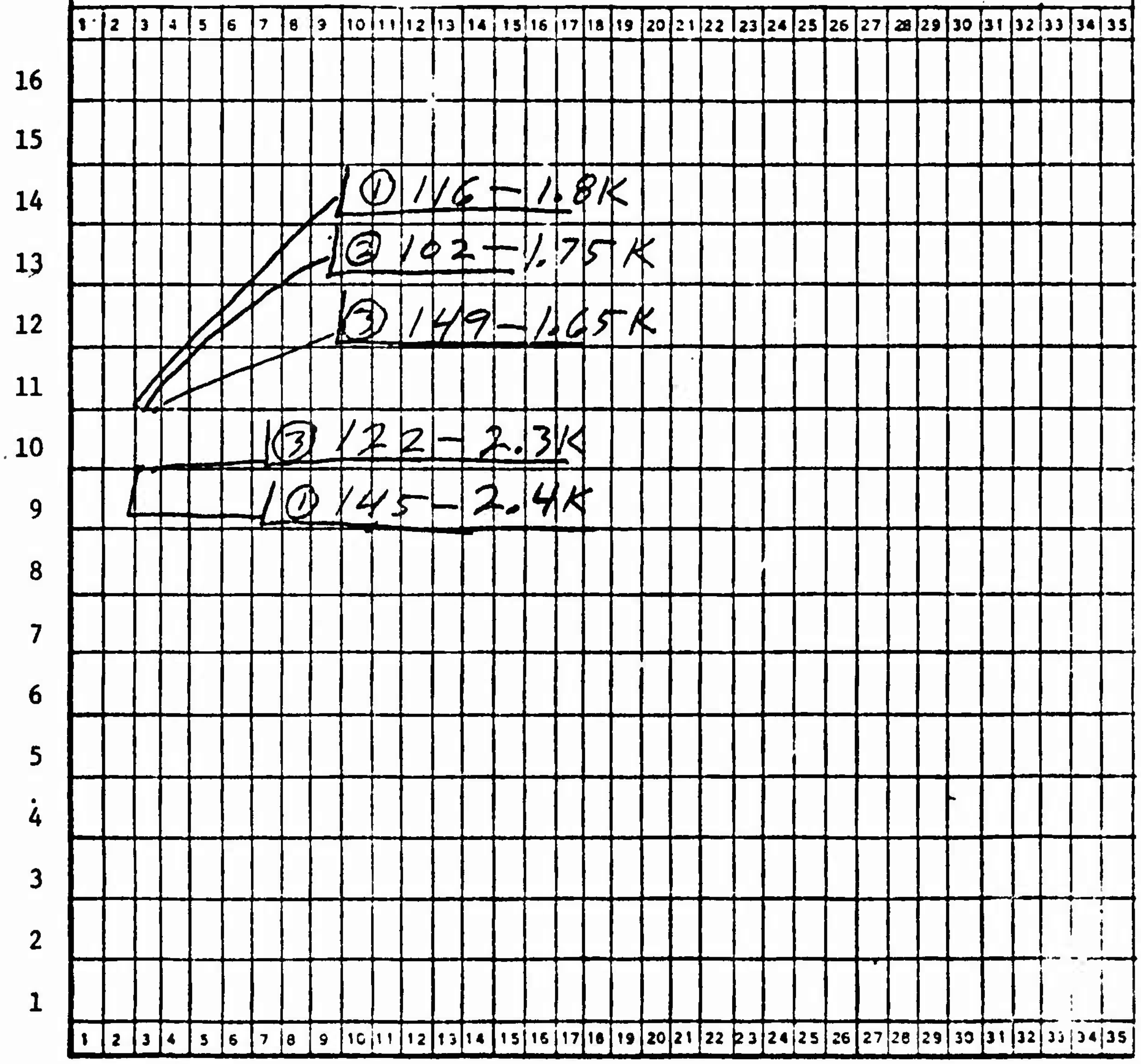

Square Number

MATTRESS INSTRUMENT LOCATION CHART

Location: COOCHIE, LA. Date: 13NOV73

Remarks: MAT #19; WATER 80FT DEEP

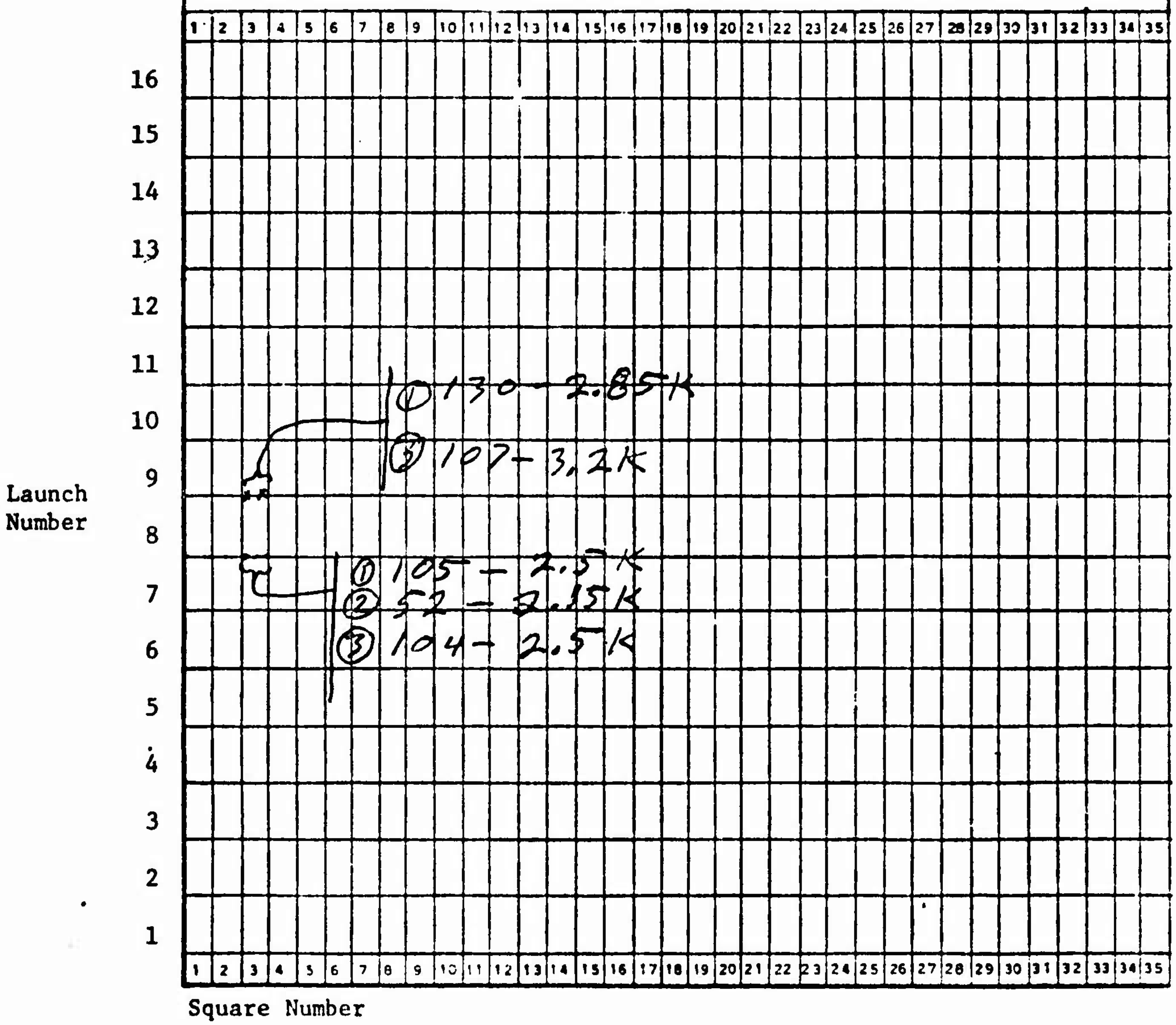

MATTRESS INSTRUMENT LOCATION CHART

Location: PT. BREEZE, LA.   Date: 15 NOV 73

Remarks: MAT #18; WATER 70 FT. DEEP

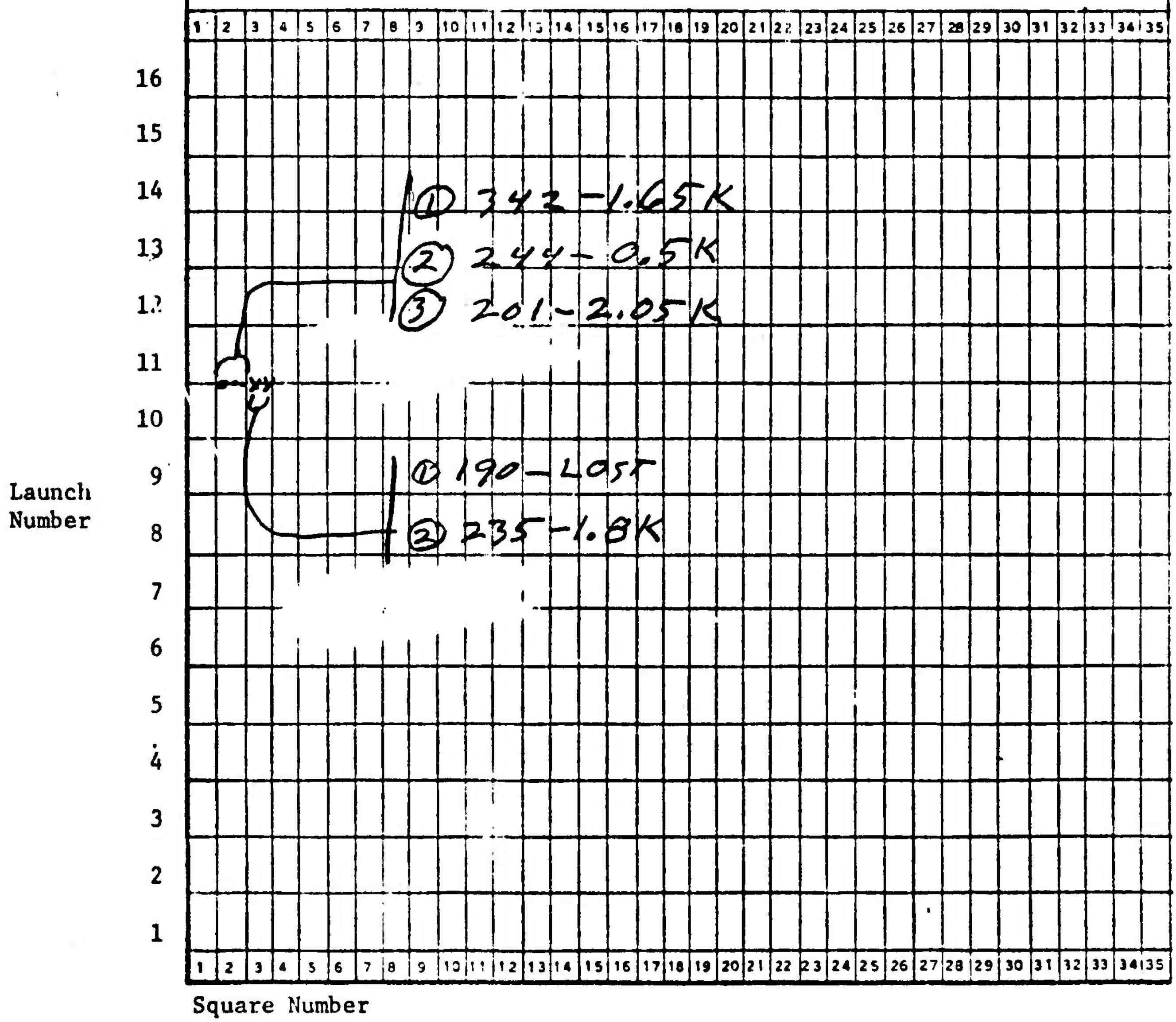

MATTRESS INSTRUMENT LOCATION CHART

Location: PT. BREEZE, LA. Date: 15 NOV 73

Remarks: MAT #19

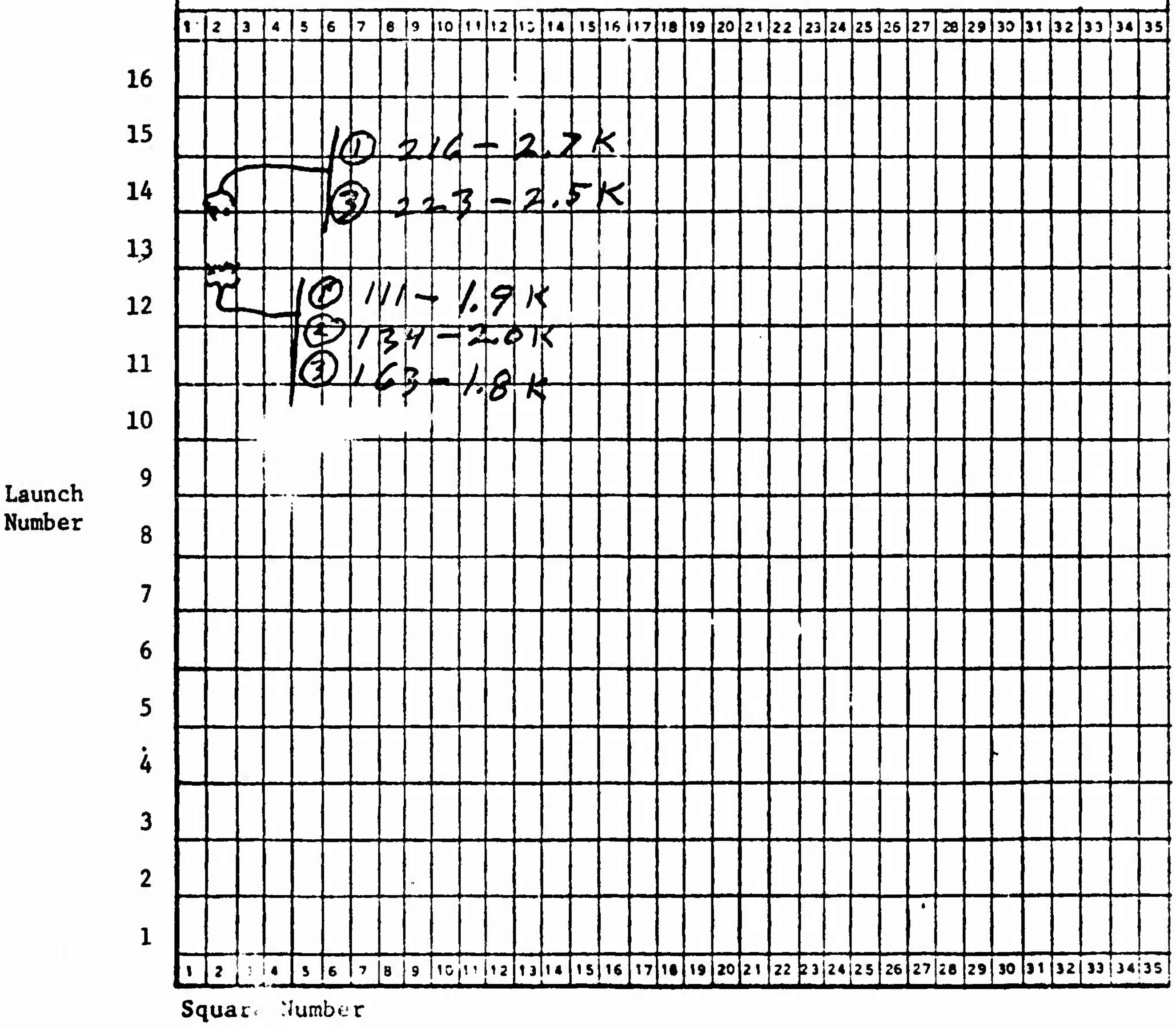

MATTRESS INSTRUMENT LOCATION CHART

Location: PT. BREEZE, LA. Date: 15 NOV 73

Remarks: MAT # 20

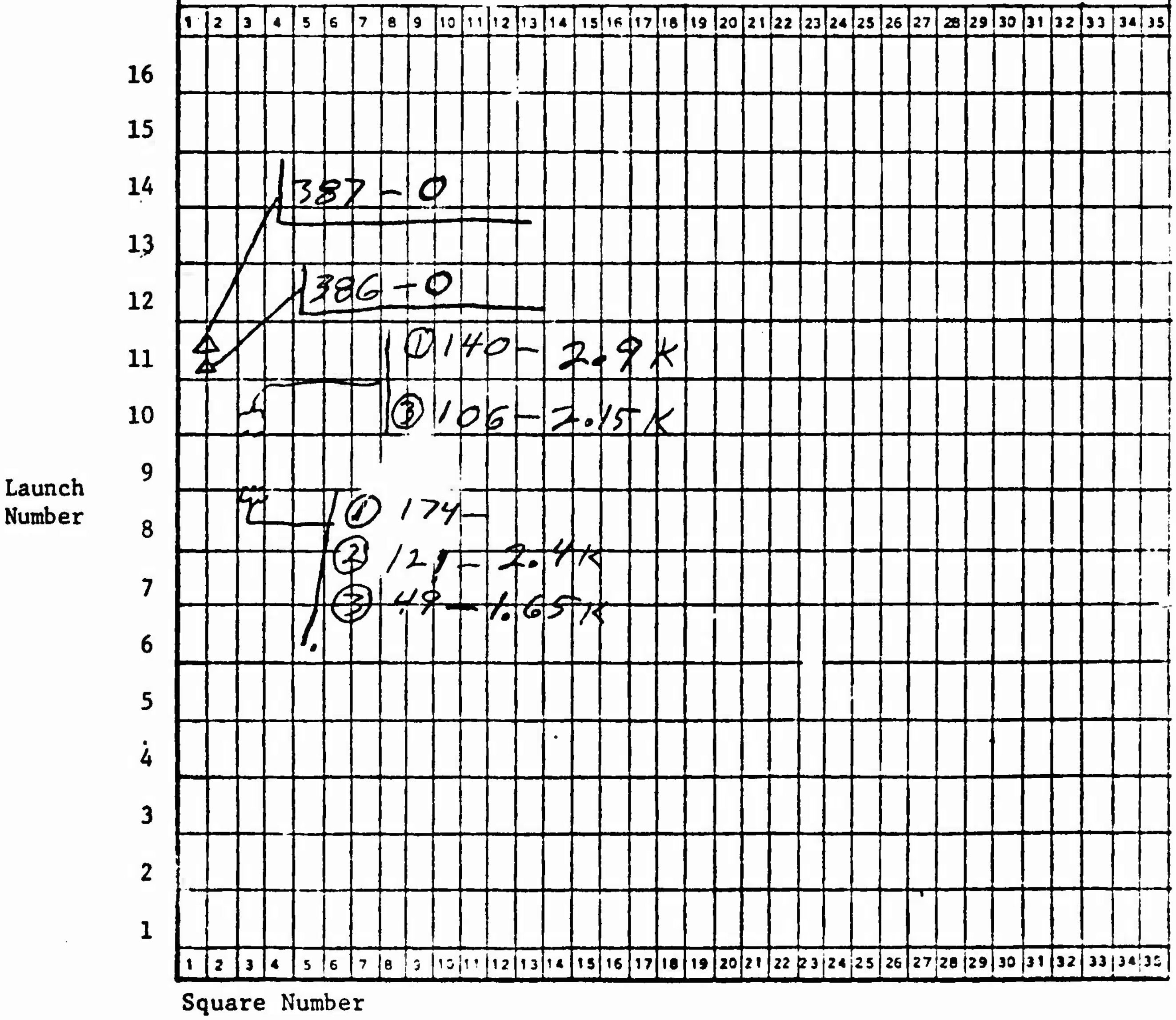

MATTRESS INSTRUMENT LOCATION CHART

Location: PT. BREEZE, LA. Date: 15 NOV 73

Remarks: MAT #21

GAGES 219, 158 & 218 DID NOT GO OVER BOTTOM LIP BECAUSE MAT PULLER HELD MAT UP. GAGES 58 & 210 DID NOT GO OVER BOTTOM LIP DUE TO HIGH LAUNCH RATE.

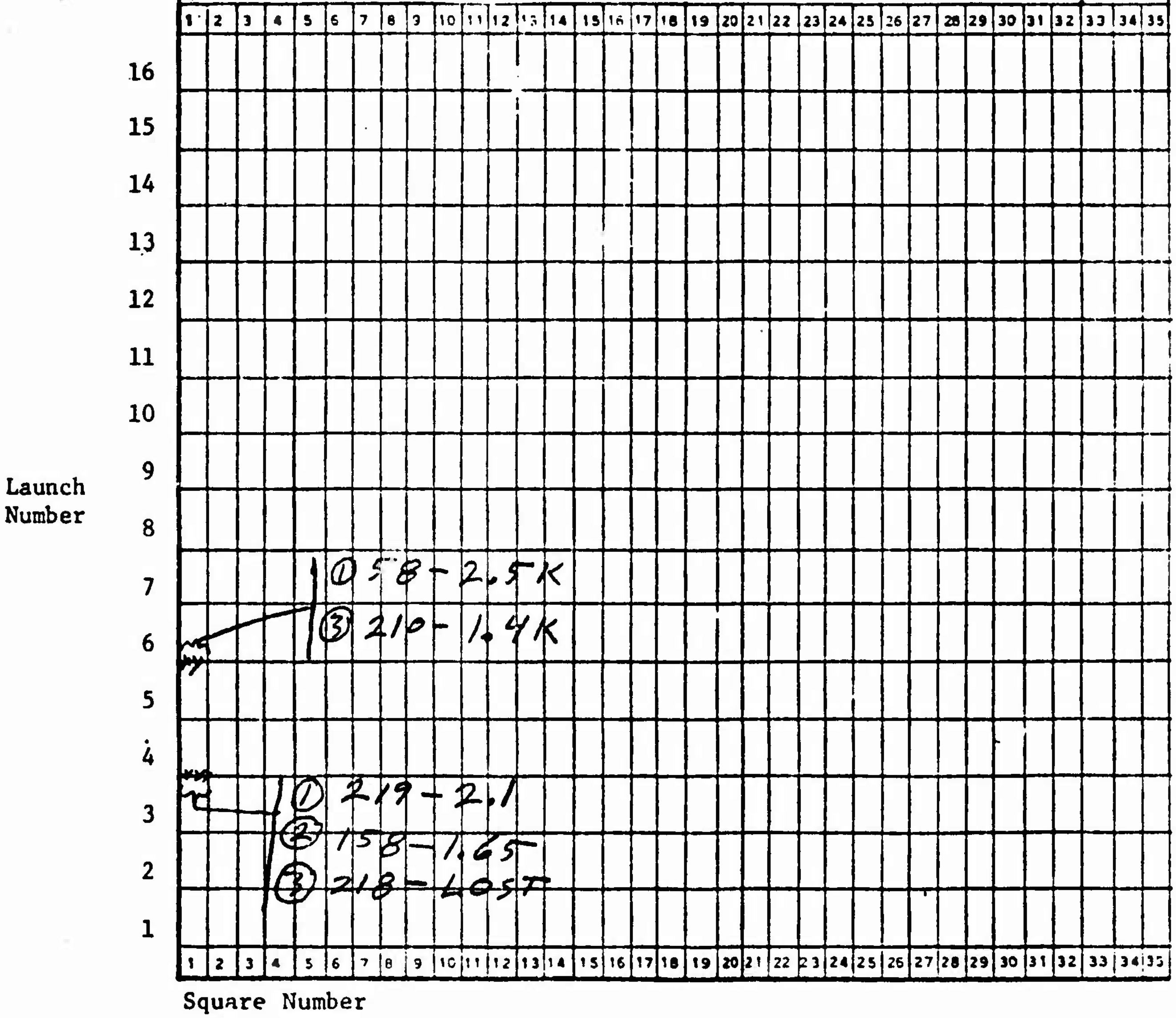

MATTRESS INSTRUMENT LOCATION CHART

Location: PT. PLEASANT, LA. Date: 4 DEC 73

Remarks: MAT #4; WATER 100 FT. DEEP
GAGE 341 FELL APART AT LIP
GAGE 406 "SELF RETRIEVED" 3 FT. IN WATER
GAGE 396 " " AT LIP

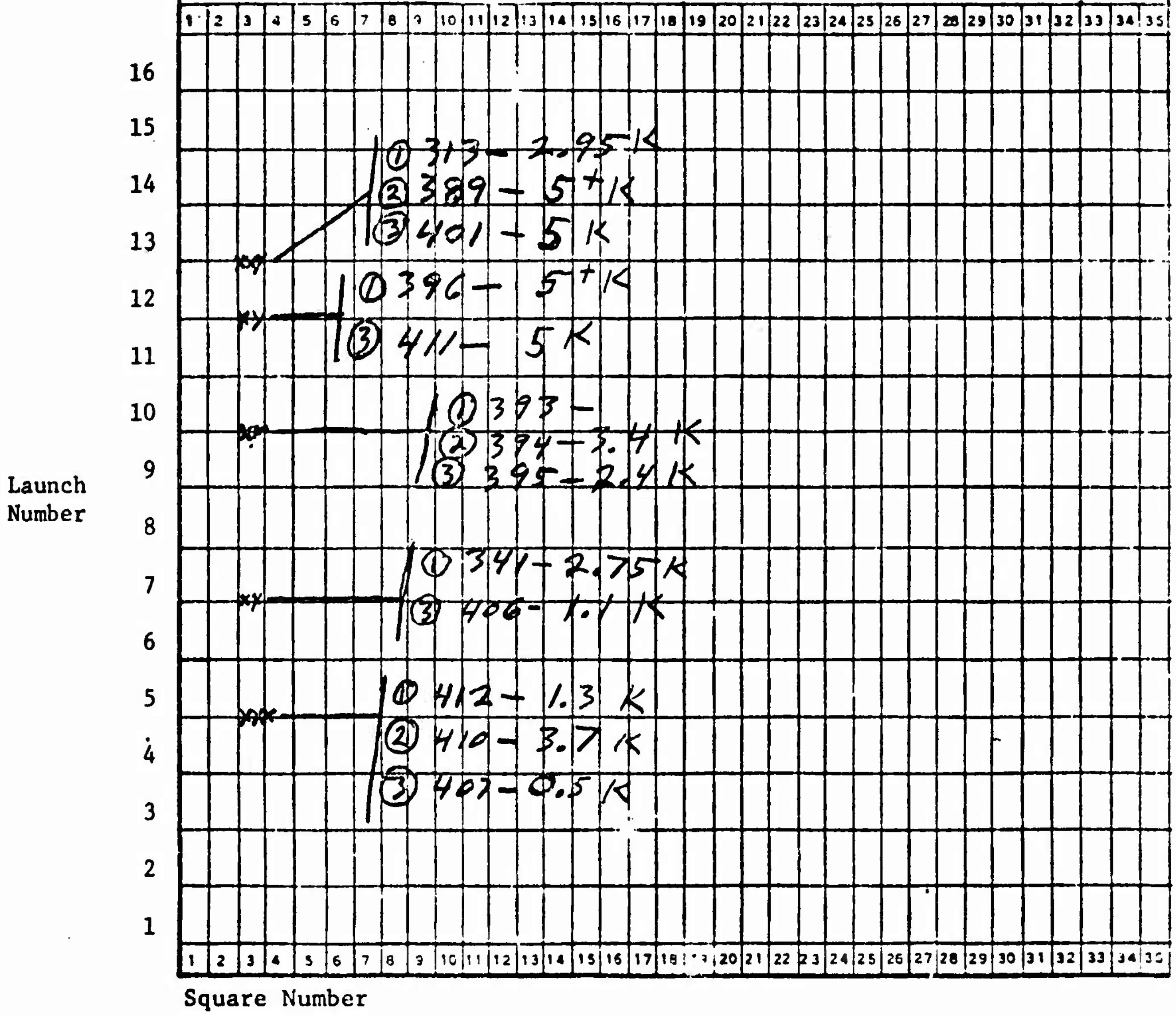

MATTRESS INSTRUMENT LOCATION CHART

Location: PT. PLEASANT, LA. Date: 4 DEC 73

Remarks: MAT #4; WATER 100 FT. DEEP
GAGE 341 FELL APART AT LIP
GAGE 406 "SELF RETRIEVED" 3 FT. IN WATER
GAGE 396 " " AT LIP

Launch Number

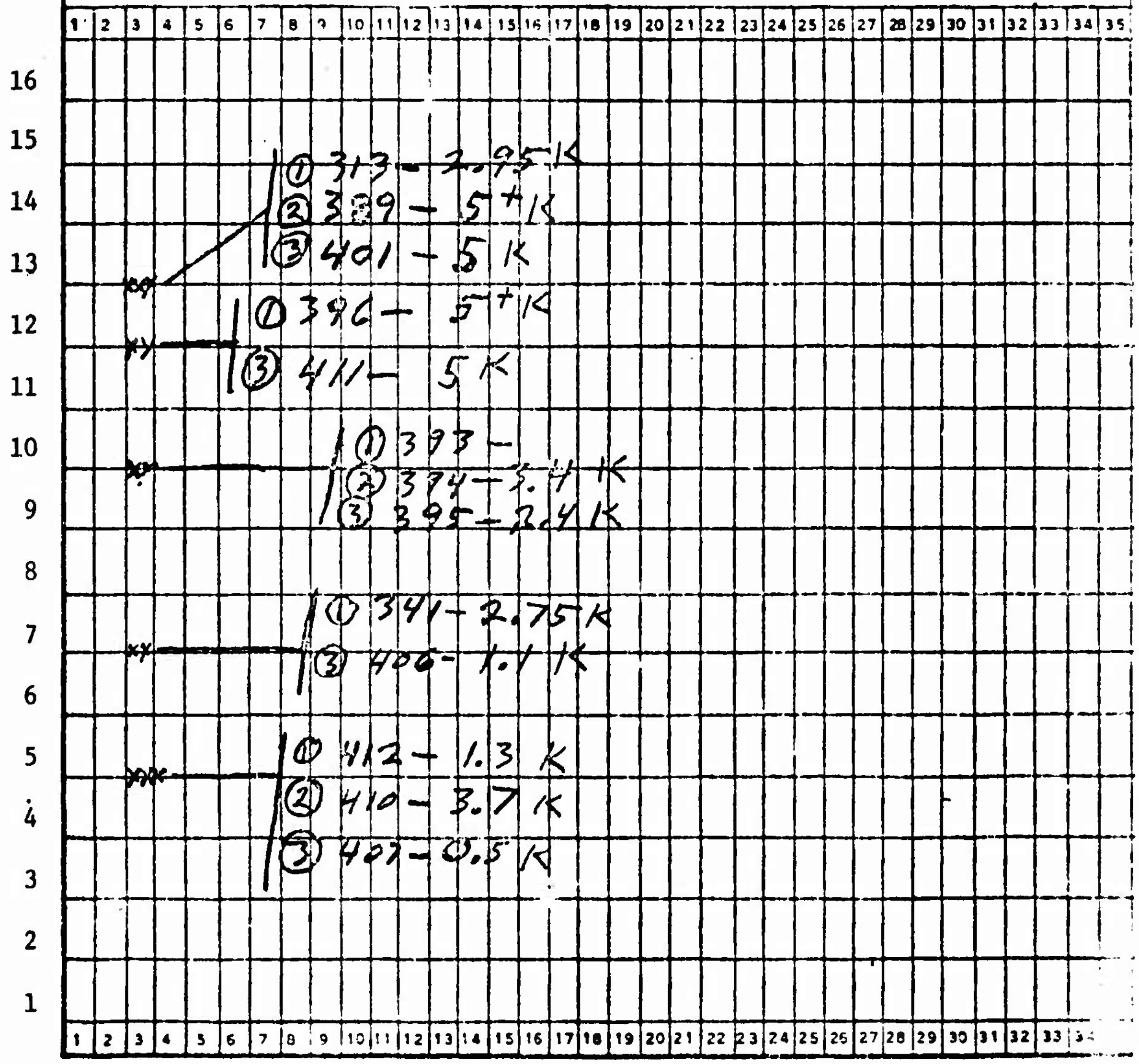

Square Number

MATTRESS INSTRUMENT LOCATION CHART

Location: PT. PLEASANT, LA. Date: 4 DEC 73

Remarks: MAT #5

GAGE 402 FELL APART ON DECK

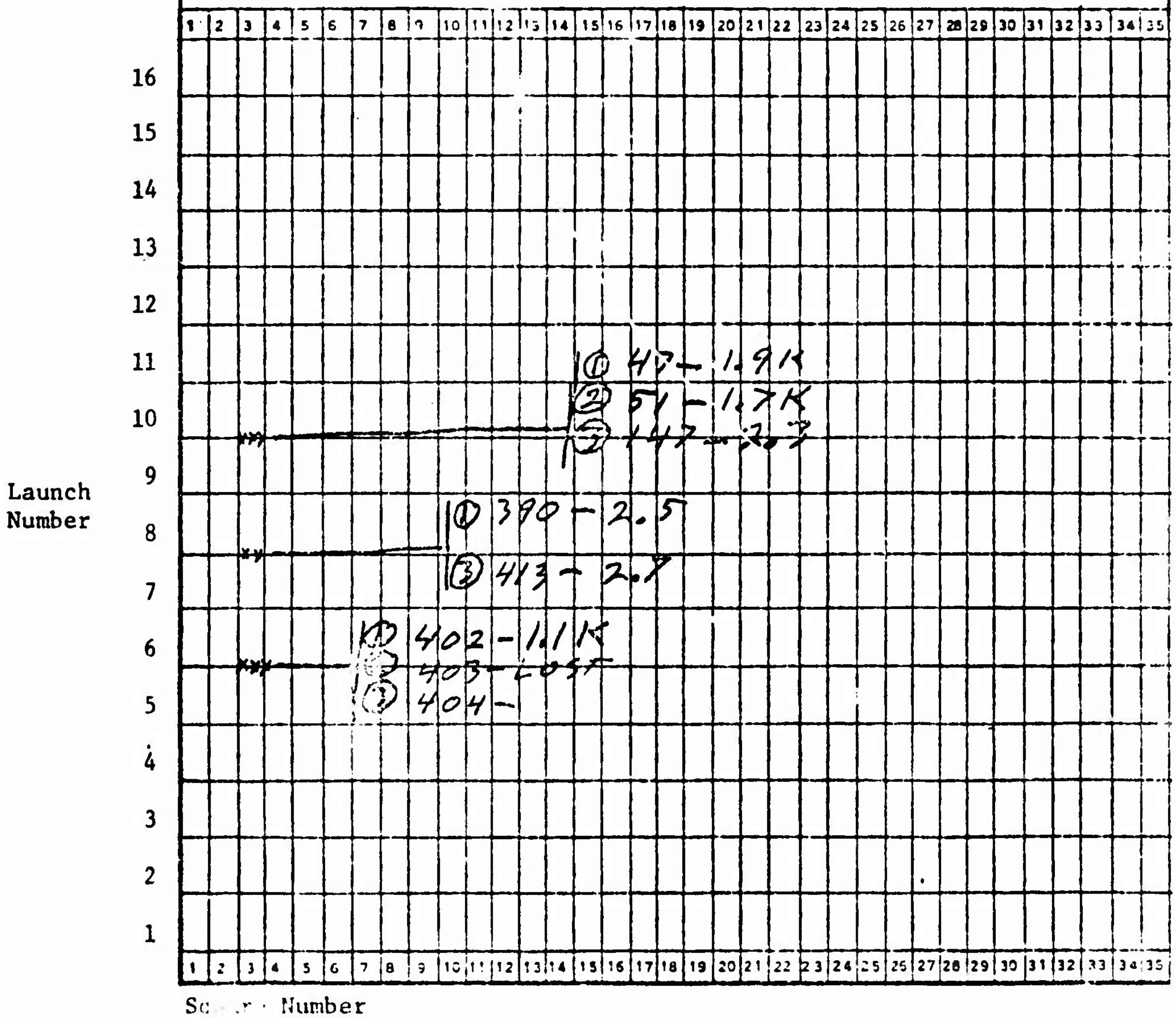

MATTRESS INSTRUMENT LOCATION CHART

Location: PT. PLEASANT, LA. Date: 5 DEC 73

Remarks: MAT #11; WATER 100 FT. DEEP

Launch Number

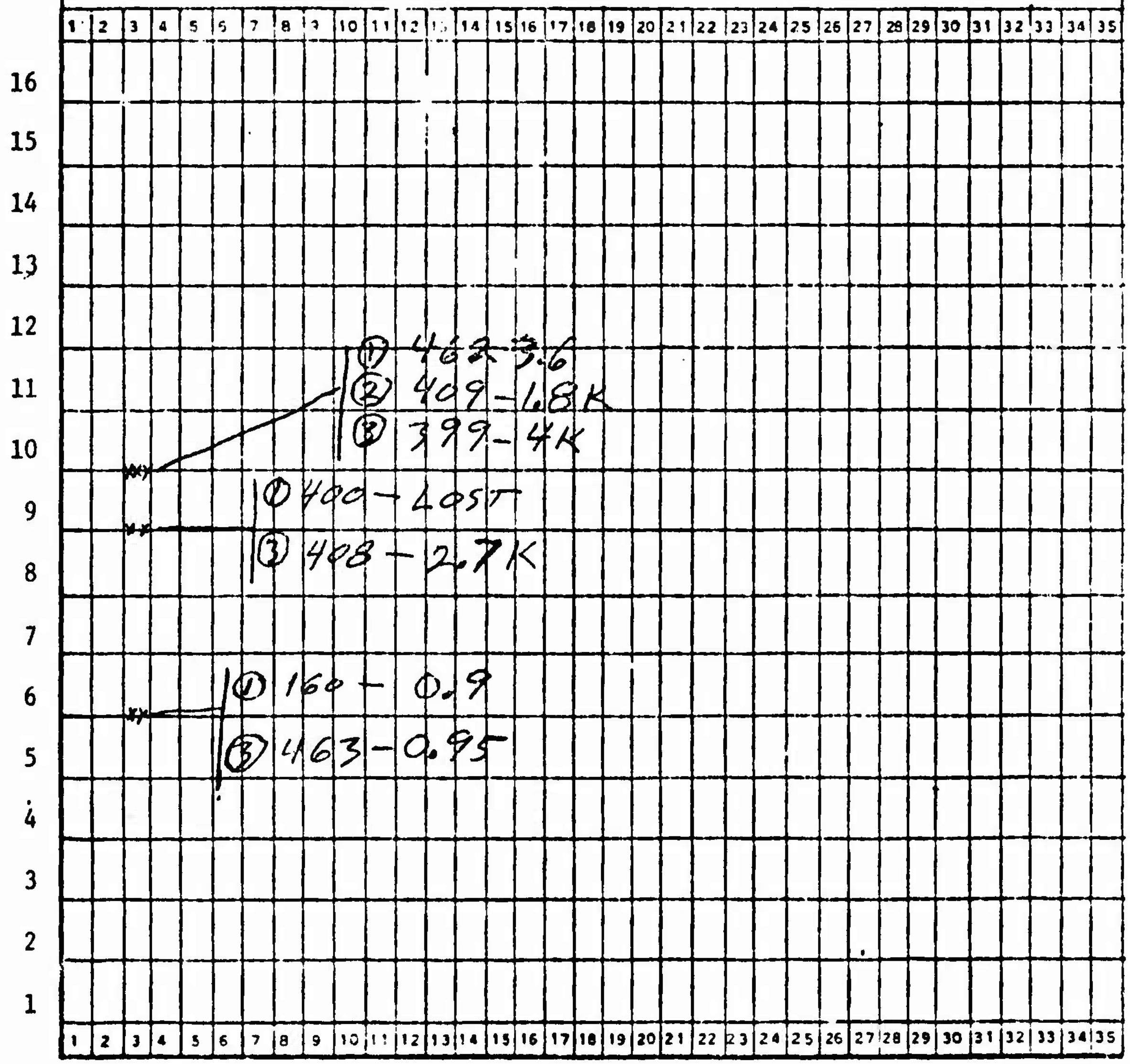

Square Number

MATTRESS INSTRUMENT LOCATION CHART

Location: PT. PLEASANT, LA. Date: 5 DEC 73

Remarks: MAT #12

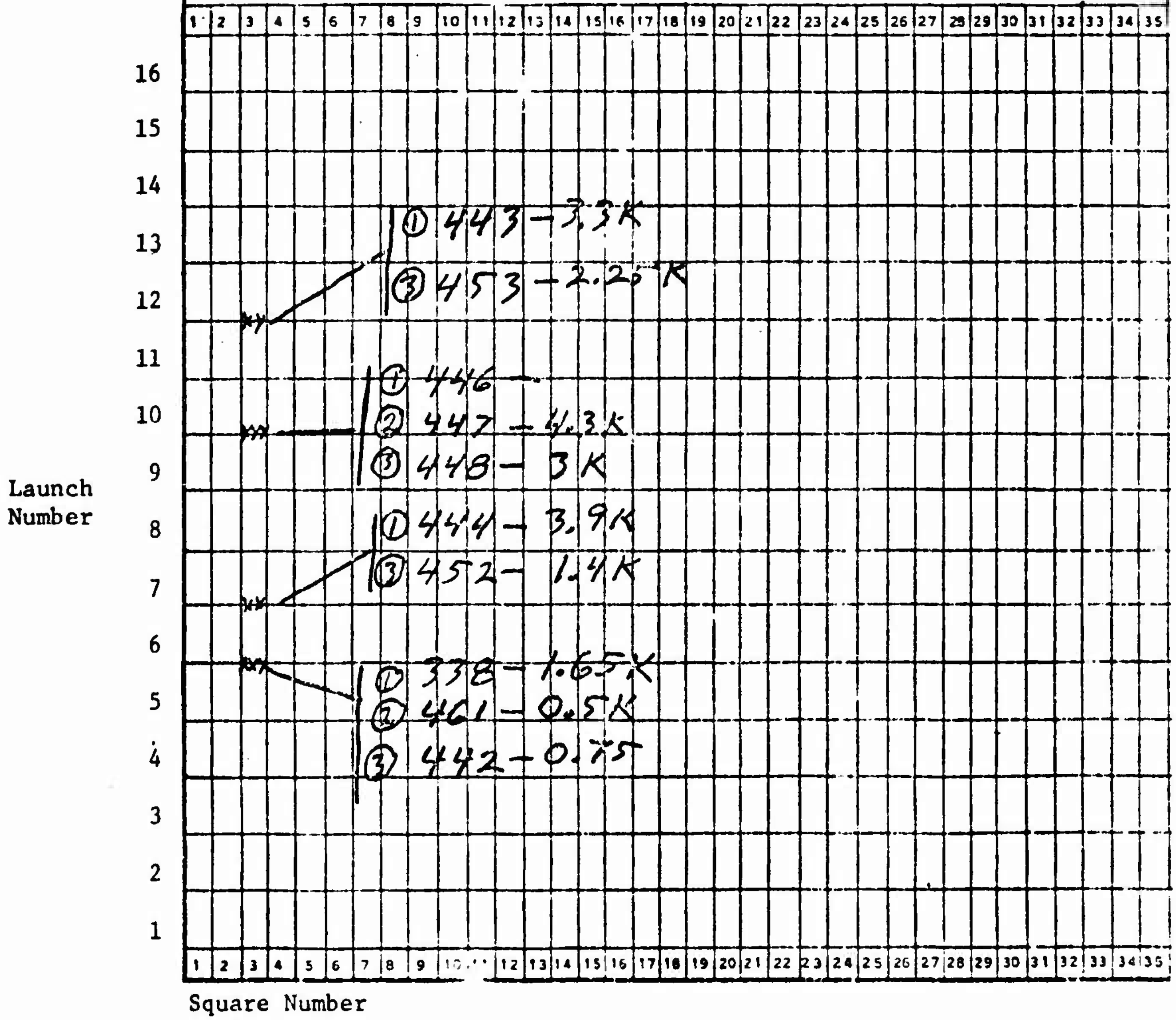

MATTRESS INSTRUMENT LOCATION CHART

Location: PT. PLEASANT, LA. Date: 5 DEC 73

Remarks: MAT #13

GAGES 454, 455 & 457 WERE 25 FT. IN THE RIVER WHEN MAT "FLOATED" UP; THESE GAGES "SELF RETRIEVED" DURING THIS FLOATATION.

Launch Number

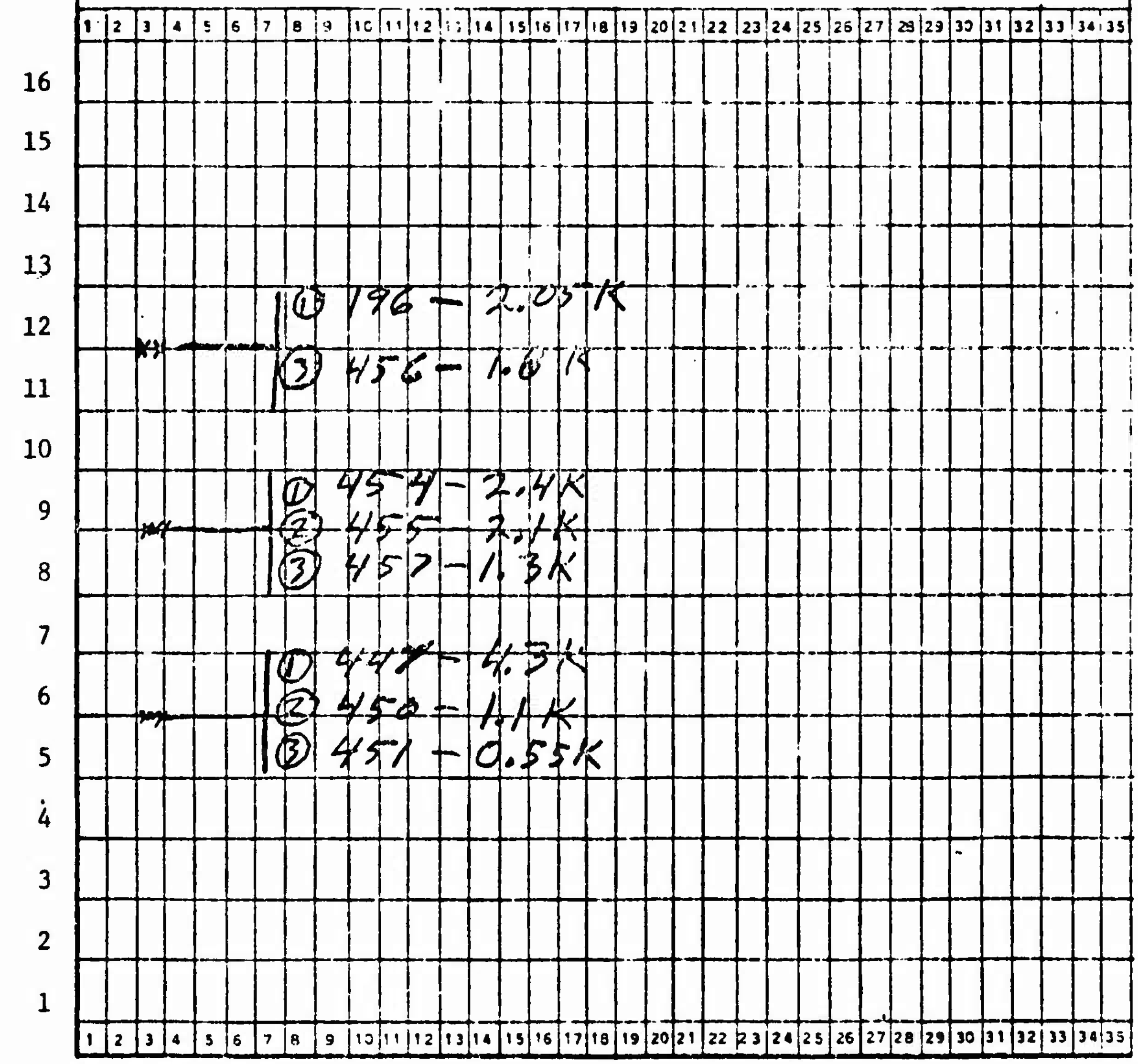

Square Number

MATTRESS INSTRUMENT LOCATION CHART

Location: PT. PLEASANT, LA. Date: 5 DEC 73

Remarks: MAT #14

Square Number: 1 2 3 4 5 6 7 8 9 10 11 12 13 14 15 16 17 18 19 20 21 22 23 24 25 26 27 28 29 30 31 32 33 34 35

Launch Number: 16 15 14 13 12 11 10 9 8 7 6 5 4 3 2 1

① 157 – 3.5K
② 445 – 5.1K
③ 459 – 3K

① 333 – 3.2K
③ 441 – LOST

① 122 – 2.3
② 307 – 0.95
③ 337 – 2.4

① 375 – 0.95K
③ 460 –

Square Number

MATTRESS INSTRUMENT LOCATION CHART

Location: PT. PLEASANT, LA. Date: 6 DEC 73

Remarks: MAT #17

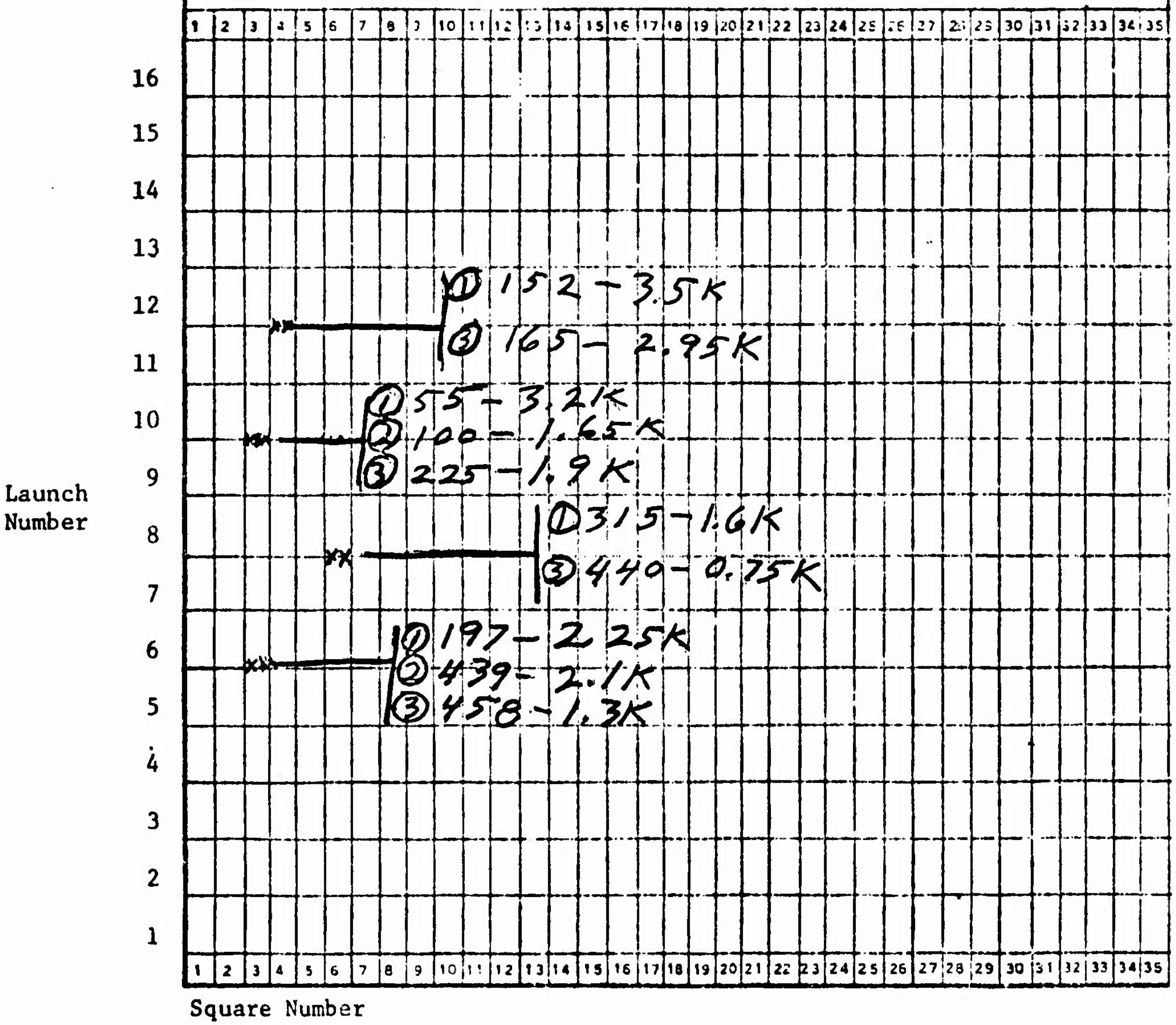

CERL DISTRIBUTION

Chief of Engineers
ATTN: DAEN-MCZ-S (2)
ATTN: DAEN-ASI-L
ATTN: DAEN-FEE-A
ATTN: DAEN-FE
ATTN: DAEN-RD
ATTN: DAEN-CWZ-R (3)
ATTN: DAEN-CWR-R (2)
Dept of the Army
WASH DC 20314

U.S. Military Academy
ATTN: Dept of Mechanics
ATTN: Library
West Point, NY 10996

The Engineering School
Technical Information Br.
Archives Section (Bldg 270)
Ft Belvoir, VA 22060

USA Engineering School
ATTN: ATSEN-DT-LD (2)
Ft Belvoir, VA 22060

Director
USA Cold Regions Research
Engineering Laboratory
PO Box 282
Hanover, NH 03755

Director, USA-WES
ATTN: Concrete Div
ATTN: Soils Div
ATTN: Library
PO Box 631
Vicksburg, MS 39181

Deputy Chief of Staff
for Logistics
US Army, The Pentagon
WASH DC 20310

The Army Library (ANRAL-R)
ATTN: Army Studies Section
Room 1A534, The Pentagon
WASH DC 20310

HQDA (SGRD/Chief),
Sanitary Engr Br
WASH DC 20314

Dept of the Army
ATTN: EACICT-P
HQ I Corps (Group)
APO San Francisco 96358

Commander-in-Chief
US Army, Europe
ATTN: AEAEN
APO New York, NY 09403

Commander, Naval Facilities
Engineering Command
ATTN: Dep Ass't Commander
for Design & Spec (04D)
200 Stovall Street
Alexandria, VA 22332

Chief, Naval Operations
ATTN: The Library
Dept of the Navy
WASH DC 20360

Chief, Hydrographic Office
ATTN: The Library
Dept of the Navy
WASH DC 20360

Chief
Naval Air Systems Command
ATTN: The Library
Dept of the Navy
WASH DC 20360

Naval Civil Engineering Lab
Technical Library Code L31
Port Hueneme, CA 93043

Officer in Charge
Naval Civil Engineering Lab
Port Hueneme, CA 93043

AF Civil Engr Center/PG
Tyndall AFB, FL 32401

AFWL/Civil Engr Div
Kirtland AFB, NM 87117

AF/PREE
Bolling AFB, DC 20332

AF/RDPQ
WASH DC 20330

Each Division Engineer
US Army Engr Div
ATTN: Library
ATTN: Chief, Engr Div

Each District Engineer
US Army Engr District
ATTN: Library
ATTN: Chief, Engr Div

Defense Documentation
Center
ATTN: TCA (12)
Cameron Station
Alexandria, VA 22314

Chief, Airports Standard
Div-AS58
Federal Aviation Administration
800 Independence Ave SW
WASH DC 20553

Office of Management Svc,
MS 110 - FAA
800 Independence Ave SW
WASH DC 20553

Transportation Research Board
National Research Council (3)
2101 Constitution Ave
WASH DC 20418

Dept of Trans Library
Acquisitions Section (SR)
TAD-491.1
400 7th Street SW
WASH DC 20590

Engineering Societies Library
345 East 47th Street
New York, NY 10017

Library of Congress (2)
Exchange and Gift Div
ATTN: American & British
WASH DC 20540

Superintendent of Documents
Div of Public Documents
ATTN: Library (2)
US Govt Printing Office
WASH DC 20402

Commanding General
USA Engr Command, Europe
APO New York, NY 09403

Engineer
US Army, Alaska
APO Seattle, WA 98749

Commander, TRADOC
Office of the Engineer
ATTN: ATEN
Ft Monroe, VA 23651

Bldg Research Advisory Board
National Academy of Sciences
2101 Constitution Avenue
WASH DC 20418

Air Force Weapons Lab
Technical Library (DOUL)
Kirtland AFB, NM 87117

Commanding General
US Army Forces Command
ATTN: AFEN-FEB
Ft. McPherson, GA 30330

Commanding General, 5th USA
ATTN: Engineer
Ft Sam Houston, TX 78234

Commanding General, 6th USA
ATTN: Engineer
Presidio of San Francisco, CA
94129

Plastics Technical Evaluation
Center
ATTN: SMUPA-VP3
Picatinny Arsenal
Dover, NY 07801

Institute of Defense Analysis
400 Army-Navy Drive
Arlington, VA 22202

Defense Logistics Studies Infor-
mation Exchange (2)
U.S. Army Logistics Management
Center
ATTN: AMXMC-D
Ft. Lee, VA 23801

Chief, Civil Engineering Research
Division
Air Force Weapons Lab AFWL/DE
Kirtland AFB, NM 87117

DEPARTMENT OF THE ARMY
CONSTRUCTION ENGINEERING RESEARCH LABORATORY
P.O. BOX 4005
CHAMPAIGN, ILLINOIS 61820

OFFICIAL BUSINESS
PENALTY FOR PRIVATE USE $300

POSTAGE AND FEES PAID
DEPARTMENT OF THE ARMY
DOD-314

U.S.MAIL

THIRD CLASS